

RAMAN-DYE-LABELED NANOPARTICLE PROBES FOR DNA STUDIES

A THESIS SUBMITTED TO
THE GRADUATE SCHOOL OF NATURAL AND APPLIED SCIENCES
OF
MIDDLE EAST TECHNICAL UNIVERSITY

BY

CEREN UZUN

IN PARTIAL FULFILLMENT OF THE REQUIREMENTS
FOR
THE DEGREE OF MASTER OF SCIENCE
IN
CHEMISTRY

SEPTEMBER 2012

Approval of the thesis:

**RAMAN-DYE-LABELED NANOPARTICLE PROBES FOR DNA
STUDIES**

Submitted by **CEREN UZUN** in partial fulfillment of the requirements for the degree of
Master of Science in Chemistry Department, Middle East Technical University by,

Prof. Dr. Canan Özgen
Dean, Graduate School of **Natural and Applied Sciences**

Prof. Dr. İlker Özkan
Head of Department, **Chemistry Dept.**

Prof. Dr. Mürvet Volkan
Supervisor, **Chemistry Dept., METU**

Examining Committee Members:

Prof. Dr. Ali Gökmen
Chemistry Dept., METU

Prof. Dr. Mürvet Volkan
Chemistry Dept., METU

Prof. Dr. Necati Özkan
Polymer Science and Technology Dept., METU

Prof. Dr. Semra Kocabıyık
Biology Dept., METU

Prof. Dr. Ceyhan Kayran
Chemistry Dept., METU

Date:

14 / 09 / 2012

I hereby declare that all information in this document has been obtained and presented in accordance with academic rules and ethical conduct. I also declare that, as required by these rules and conduct, I have fully cited and referenced all material and results that are not original to this work.

Name, Last Name : Ceren UZUN

Signature :

ABSTRACT

RAMAN-DYE-LABELED NANOPARTICLE PROBES FOR DNA STUDIES

UZUN, Ceren

M.Sc., Department of Chemistry

Supervisor: Prof. Dr. Mürvet VOLKAN

September 2012, 94 pages

The interaction between nanoscience and biomedicine is one of the important developing areas of modern science. The usage of functional nanoparticles with biological molecules provides sensitive and selective detection, labeling and sensing of biomolecules. Until today, several novel types of tagging materials have been used in bioassays, such as plasmon-resonant particles, quantum dots (QDs), and metal nanoshells. However, nowadays, Surface enhanced raman scattering (SERS) tags have been attracting considerable attention as a tagging system. SERS-tags provide high signal enhancement, and they enable multiplex detection of biomolecules due to high specificity.

This thesis is focused on the designing proper SERS nanotags for DNA studies. SERS nano-tags are nanostructures consisting of core nanoparticle generally silver, Raman reporter molecule for labeling, and shell to make surface modifications and to prevent deterioration arising from environmental impact. Based on this information, silver core synthesized by thermal decomposition and chemical reduction methods. Thermal decomposition method provides synthesis of silver nanoparticles in hydrophobic medium, resulting in proper silica coating

by reverse microemulsion method. On the other hand, silver nanoparticles synthesized by chemical reduction method exhibit hydrophilic property. Due to capping reagents, negatively charged silver nanoparticles could easily attach with positively charged Raman dye which is brilliant cresyl blue (BCB). After addition of Raman active molecule, silica coating process was done by using modified Stöber method. The resulting particles were characterized by Scanning Electron Microscopy (SEM), Energy-dispersive X-ray spectroscopy (EDX), UV-vis Spectrometry (UV-vis) and Surface-Enhanced Raman Spectroscopy (SERS).

In recent years, DNA detection has gained importance for cancer and disease diagnosis and the detection of harmful microorganisms in food and drink. In this study, gene sequences were detected via SERS. For this, probe sequences were labelled with Raman reporter molecule, BCB, and SERS nano-tags and were called as SERGen probes. Then, after hybridization of DNA targets to complementary probe sequences onto gold substrate, SERS peak was followed.

Keywords: Surface Enhanced Raman Spectroscopy, SERS nanotag, SERGen probes, multiplex analysis, DNA, hybridization.

ÖZ

DNA ÇALIŞMALARI İÇİN RAMAN BOYA İLE ETİKETLENMİŞ NANOPARÇACIK SONDALARI

UZUN, Ceren

Yüksek Lisans, Kimya Bölümü

Tez Yöneticisi: Prof. Dr. Mürvet VOLKAN

Eylül 2012, 94 sayfa

Nanobilim ve biyomedikal arasındaki etkileşim modern bilimin gelişmekte olan en önemli alanlarından birini oluşturmaktadır. Fonksiyonel nanoparçacıklarının biyolojik moleküllerle kullanılması, hassas ve seçici bir tayinle beraber, biyomoleküllerin etiketlenerek analiz edilmesini sağlar. Bu zamana kadar, örnek olarak plazmon rezonans parçacıkları, kuantum noktacıkları ve metal nanokabuklar olmak üzere, pek çok etiketleme malzemeleri, biyoanalizlerde kullanılmıştır. Ancak, son zamanlarda, Yüzeyce Güçlendirilmiş Raman Spektroskopisi (YGRS) nano-etiketleri, etiketleme sistemleri olarak dikkat çekmektedir. YGRS-etiketleri sinyal şiddetini arttırmasının yanı sıra, özgül olması sayesinde biyolojik moleküllerin çoklu analizini mümkün kılar.

Bu tez, DNA çalışmaları için uygun YGRS nano etiketlerinin hazırlanması üzerine odaklanmıştır. YGRS nano etiketleri, genellikle gümüş olmak üzere çekirdek nanoparçacıkları, etiketleme için Raman aktif molekül ve yüzey modifikasyonlarının yapılabildiği ve çevresel etkenleri önleyen kabuktan oluşur. Bu bilgiler ışığında, gümüş çekirdek nanoparçacığı yüksek sıcaklıkla parçalanma ve kimyasal indirgeme metotları ile sentezlenmiştir. Yüksek sıcaklıkla

parçalanma yöntemi gümüş nanoparçacıklarının hidrofobik bir ortamda sentezlenmesini mümkün kılar, dolayısıyla silika kabuk ile kaplanması ters mikroemülsiyon yöntemi ile gerçekleştirilmiştir. Öte yandan, kimyasal indirgeme yöntemi ile sentezlenen gümüş nanoparçacıkları hidrofilik özellik gösterirler. Tutucu reaktantlar nedeniyle yüzeyi negatif yük ile yüklenmiş olan gümüş nanoparçacıkları, kolay bir şekilde pozitif yüklü Raman boya olan brilliant cresyl blue (BCB) ile tutturulabilir. Raman aktif boyanın eklenmesinden sonra, silika kaplama prosesi geliştirilmiş Stöber yöntemi ile yapılmıştır. Sentezlenen parçacıklarının karakterizasyonu Taramalı Elektron Mikroskobu (SEM), Geçirimli Elektron Mikroskobu (TEM), Enerji Dağılım X-ray Spektroskopisi (EDX), UV-vis Spektrometri (UV-vis) ve Yüzeyde Güçlendirilmiş Raman Spektroskopisi (YGRS).

Son zamanlarda, DNA tayini kanser ve hastalık tanısında ve aynı zamanda besin ve içeceklerdeki zararlı mikroorganizma analizlerinin yapılması hususunda önem taşır. Bu çalışmada, insan proteazom gen dizilimleri YGRS yardımıyla tayin edilmiştir. Bunun için, prob dizilimler Raman tanıyıcı molekül olan BCB ve SERS nano-problarla etiketlenip, SERGen prob adını almıştır. Daha sonra, altın tabaka üzerinde DNA hedeflerinin eşlenik prob dizilimleri ile hibridizasyonu yapıp, YGRS sinyali takip edilmiştir.

Anahtar Kelimeler: Yüzeyde Güçlendirilmiş Raman Spektroskopisi, YGRS nano etiketleme, YGRS gen prob, çoklu analiz, DNA, hibridizasyon

To my Parents

ACKNOWLEDGEMENTS

I am heartily thankful to my supervisor, Prof. Dr. Mürvet Volkan for her trust and great encouragement along this study. Whenever I am on the horns of a dilemma about not only my studies but also life, she enlightened me with her experiences.

I also wish to express my deepful thanks to Prof.Dr. Semra Kocabıyık and her laboratory team for their help throughout DNA hybridization experiments and other biological experiments.

I would like to thank Dr. Murat Kaya for his guidance and valuable suggestions during this study. I learnt many things from him about academic world and real world.

My special thanks go to C-50 lab team, Yeliz Akpınar, Dilek Ünal, Tuğba Nur Aslan, Elif Kanbertay and Ufuk Özgen for their continuous help during my study and their great and warm friendship. Thanks to them I never felt lonely myself inside and outside the laboratory. You are my second family.

I would like to thank Enis Doko for his help and support throughout my study.

I would like to thank Seçkin Öztürk. He helped me so much during SEM and TEM measurements in Central Laboratory. Thanks for his comments about the measurements, and understanding personality before NanoTR congress.

Endless thank to my family, Bergüzar Uzun, Feridun Uzun and Şebnem Uzun for their love, trust and patience. They gave me endless love, believe me and support me every situation.

TABLE OF CONTENTS

ABSTRACT	iv
ÖZ	vi
ACKNOWLEDGEMENTS	ix
TABLE OF CONTENTS	x
LIST OF TABLES	xiii
LIST OF FIGURES	xiv
LIST OF ABBREVIATIONS.....	xviii
CHAPTERS.....	1
1.INTRODUCTION.....	1
1.1.Nanoscience and Nanotechnology	1
1.1.1 Nanoscale: Relation between Physical and Biological Sciences	1
1.1.2 Approaches for Synthesis of Nanoparticles	3
1.1.2.1 Top-down and Bottom-Up Approach	3
1.2 Functionalization of Nanoparticles with Biological Molecules	4
1.2.1 Tagging Materials	6
1.2.1.1 Plasmon resonant particles (PRP's)	6
1.2.1.2 Quantum Dots (QD's)	9
1.2.1.3 Metal Nanoshells	10
1.2.1.4 Surface Enhanced Raman Scattering Tags (SERS- tags)	11
1.3 Raman Scattering	13
1.3.1 Raman with Improved Sensitivity	16
1.4 Surface Enhanced Raman Scattering (SERS)	16
1.4.1 Electromagnetic Enhancement	17
1.4.2 Chemical Enhancement	19
1.4.3 SERS vs Fluorescence Spectroscopy	20
1.5 Applications of SERS	21
1.6 Synthesis of Silver Nanoparticles	23

1.7 Synthesis of SERS nano-tags	24
1.7.1 Sol-gel Methods for Silica Coating	24
1.8 Aim of The Study	26
2. EXPERIMENTAL	28
2.1 Chemicals and Reagents	28
2.1.1 Synthesis of Silver Nanoparticles.....	28
2.1.1.1 By Thermal Decomposition Method	28
2.1.1.2 By Chemical Reduction Method	28
2.1.2 Preparation of SERS Nano-Tags	29
2.1.2.1 By Reverse Microemulsion Method.....	29
2.1.2.2 By Stöbe Method	29
2.1.3 DNA Oligonucleotides and Chemicals used for DNA Hybridization.....	29
2.1.3.1 DNA Oligonucleotides.....	29
2.1.3.2 Chemicals used for DNA Hybridization	30
2.2 Instrumentation	30
2.2.1 Centrifugation	30
2.2.2 UV-VIS Spectrometer	30
2.2.3 Raman Spectrometer	30
2.2.4 Field Emission Scanning Electron Microscopy(FE-SEM)....	31
2.2.5 Transmission Electron Microscopy (TEM)	31
2.2.6 Energy Dispersive X-Ray Spectroscopy (EDX)	32
2.3 Procedures	32
2.3.1 Synthesis of Silver Nanoparticles by Thermal Decomposition Method	32
2.3.2 Synthesis of Silver Nanoparticles by Chemical Reduction Method	32
2.3.3 Preparation of Silica Coated Silver Nanoparticles by Reverse Microemulsion Method	34
2.3.4 Preparation of Silica Coated Silver Nanoparticles by Stöber Method.....	36

2.3.5. Preparation of A Raman-Dye- Labeled Nanoparticle Probes	37
2.3.6 Preparation of SerGEN Probe	38
2.3.6.1 Non-covalent Labelling of Oligonucleotide Primers with BCB	38
2.3.7 Immobilization of SERGen Probes onto Gold Surface Under Hybridization Conditions	39
3.RESULTS AND DISCUSSIONS	42
3.1 Synthesis of Silver Nanoparticles by Thermal Decomposition Method	42
3.2 Synthesis of Silver Nanoparticles by Chemical Reduction Method	45
3.3 Preparation of Silica Coated Silver Nanoparticles by Reverse Microemulsion Method	50
3.4 Preparation of Silica Coated Silver Nanoparticles by Stöber Method	63
3.5 Preparation of A Raman-Dye- Labeled Nanoparticle Probes	65
3.6 Preparation of SerGEN Probe	76
3.7 Immobilization of SERGen Probes onto Gold Surface Under Hybridization Conditions	77
4.CONCLUSION	84
REFERENCES	86

LIST OF TABLES

TABLES

Table 1: Size of silver nanoparticles by thermal decomposition	45
Table 2: Usage of ammonia solution with different concentration in reverse microemulsion method as catalyst	53
Table 3: Changing of surfactant concentration during reverse microemulsion method.....	54
Table 4: Concentration of DBU used throughout reverse microemulsion method	58
Table 5: Effect of pH change onto colour of silver nanoparticles	67
Table 6: Stability Behaviour of the colloid depending on zeta potential ranging from 0 to ± 61 mV	68
Table 7: Zeta Potential measurements using silver nanoparticles at different pH ranges	68

LIST OF FIGURES

FIGURES

Figure 1. Scale of biomolecular interactions	2
Figure 2: Top-down and bottom-up strategies	4
Figure 3: Representation of (a) nucleic acid and (b) double helix structure of DNA molecule	5
Figure 4: Absorption Spectra of Silver Nanoparticles with diameters ranging from 10-100 nm	7
Figure 5: Gold Colloids for Detection of DNA Sequences	8
Figure 6: Schematic illustration of ZnS capped CdSe QD covalently attached to a protein.	9
Figure 7: a) Absorbance spectrum of SiO ₂ -Au core-shell nanoparticles. b) TEM image of gold colloid growing on a silica core	11
Figure 8: Direct Attachment of Raman reporter molecule onto gold nanoparticle	12
Figure 9: Schematic illustration of designing core-shell SERS tags	13
Figure 10: Differences in mechanism of Raman and IR.....	14
Figure 11: Rayleigh and Raman Spectra of carbon tetrachloride	15
Figure 12: Electromagnetic (EM) enhancement of SERS	18
Figure 13: Charge-transfer mechanism in SERS cross-section	19
Figure 14: Schematic diagrams of SERS vs fluorescence	20
Figure 15: Scheme for the synthesis of silver nanoparticles by TD	33
Figure 16: The experimental setup used for the synthesis of silver nanoparticles by thermal decomposition method	33
Figure 17: Scheme for the synthesis of silver nanoparticles by chemical reduction method.....	34

Figure 18: Scheme for the silica coated silver nanoparticles by reverse microemulsion method	35
Figure 19: Ag NP's in cyclohexane before silica coating and Ag@SiO ₂ Nanostructures in water	36
Figure 20: Scheme for the silica coated silver nanoparticles by Stöber method ..	37
Figure 21: Scheme for the preparation of SERS nano-tags	38
Figure 22: Schematic representation of noncovalent labeling of DNA with BCB.	39
Figure 23: Schematic representation of rupture of disulfide bonds	40
Figure 24: Schematic representation of immobilization of SERGen probes onto gold surface under hybridization conditions	41
Figure 25: Absorption spectra of nanoparticles (a) before thermal decomposition method (b) after thermal decomposition	45
Figure 26: TEM images of silver nanoparticles	45
Figure 27: FE-SEM image of silver nanoparticles synthesized by chemical reduction method.....	46
Figure 28: Effect of temperature on the appearance of silver nanoparticles	47
Figure 29: Effect of addition rate of silver perchlorate	48
Figure 30: Peak Positions of Plasmon Absorptions of Silver Nanoparticles Prepared by Thermal Decomposition and Chemical Reduction Methods.....	48
Figure 31: EDX image of silver colloids synthesized by chemical reduction method.....	50
Figure 32: Chemical structure of Igepal CO-520.....	51
Figure 33: Synthesis of Silica Coated Silver Nanoparticles	51
Figure 34: Reference Solution prepared Using 500 µl Ag NP's in cyclohexane ..	52
Figure 35: Silver Nanoparticles Following Silica Coating Process of Sample A, B, C, D and ref	54
Figure 36: Silver Nanoparticles Following Silica Coating Process of Sample E, F, G and H.....	55
Figure 37: TEM image of Sample G.....	56

Figure 38: TEM image of sample H	56
Figure 39: Silver Nanoparticles following silica coating process of S1, S2, ref., S3 and S4.....	59
Figure 40: TEM image of silica coating using low amount of catalyst, DBU (sample S1)	60
Figure 41: The whole TEM micrograph of silica coated silver nanoparticles prepared in this study (Sample S2)	61
Figure 42: Comparison of TEM micrograph of silica coated silver nanoparticles prepared by Ying et al and in our laboratory	62
Figure 43: Absorption spectra of silica coated silver nanoparticles via reverse microemulsion method.....	63
Figure 44: FE-SEM image of resulting silica coated silver nanoparticles by Stöber method	64
Figure 45: Absorption spectra of silica coated silver nanoparticles via Stöber method.....	65
Figure 46: SERS spectrum and chemical structure of BCB	66
Figure 47: Colour change of silver nanoparticles when the pH changed from 6.0 to 9.0.....	67
Figure 48: Decrease in signal intensity of silver nanoparticles after 30 minutes reaction period.....	69
Figure 49: Decrease in signal intensity of silver nanoparticles after 30 minutes reaction period.....	70
Figure 50: SERS spectrum of BCB adsorbed onto silver nanoparticles surface with high concentration (10^{-3} M)	71
Figure 51: Absorption spectra of BCB adsorbed onto silver nanoparticles surface with low concentration (10^{-4} M)	72
Figure 52: Raman spectra of SERS nanotags prepared using 10^{-4} M BCB	72
Figure 53: Absorption spectrum of gold nanoparticles when different amount of BCB was added by titration.	73
Figure 54: FT-IR spectrum of silica coated silver nanoparticles	74

Figure 55: FT-IR spectrum of BCB.	75
Figure 56: FT-IR spectrum of SERS nano-tags.	75
Figure 57: Chemical structure of BCB	76
Figure 58: Schematic representation of rupture of disulfide bonds by using DTT	78
Figure 59: Possible interactions between oligonucleotides and gold surface without spacer	78
Figure 60: SERS spectra of BCB-labeled DNA after hybridization onto gold surface with silver colloid.	80
Figure 61: Future Work.....	81
Figure 62: SERS spectra of nano-tags after functionalized with amine groups..	82
Figure 63: SERS spectra of electrostatic attachment of SERS nanotags to the probe DNA.....	83
Figure 64: SERS spectra of covalent attachment of SERS nanotags to the probe DNA	83

LIST OF ABBREVIATIONS

A	Adenine
AOT	Sodium di-2-ethylhexyl Sulfosuccinate
APTES	(3-Aminopropyl)triethoxysilane
BCB	Brilliant Cresyl Blue
C	Cytosine
CTAB	Cetyltrimethylammonium Bromide
DBU	1,8- Diazabicycloundec-7-ene
DMA	Dimethylamine
DNA	Deoxyribonucleic Acid
DTT	Dithiothreitol
EDX	Energy Dispersive X-ray Spectrometry
FE-SEM	Field Emission Scanning Electron Microscopy
G	Guanine
Igepal CO-520	Polyoxyethylene (5) Nonylphenylether
NIR	Near-Infrared
PTC	Phosphatidylcholine
PRP's	Plasmon Resonant Particles
QD's	Quantum Dots

RNA

Ribonucleic Acid

SPR

Surface Plasmon Resonance

CHAPTER 1

INTRODUCTION

1.1. Nanoscience and Nanotechnology

In science and technology, the prefix 'nano' refers to one billionth of a unit. One nanometer (nm) is one billionth (10^{-9}) of a meter. Nanoscience and nanotechnology deal with the materials at the nanometer scale. While nanoscience searches the functions of objects at atomic, molecular and macromolecular scales, nanotechnology is interested in the design, synthesis and application of devices by changing the shapes and sizes of the objects.

1.1.1 Nanoscale: Relation between Physical and Biological Sciences

In literature, nanoscale is defined as the size of atoms ranging from 1 nm to 100 nanometers and nanomaterial is generally defined as a material which has dimension less than 100 nanometers. That is to say, nanomaterials consist of all the structures and systems at nanoscale. Significant point in this respect is that nanoscale materials have specific and different properties compared to the bulk materials. These variances arise from mainly two reasons. One reason is that the surface areas of nanomaterials are larger than the materials having the same mass but in a larger size. Larger surface area not only affects the mechanical and electrical properties of materials, but also increases the chemical reactivity of materials. Second reason is that the size of the particle moves into the region where quantum effects predominate. In other words, once particles become smaller and smaller they exhibit quantum mechanical behaviour.

As indicated in Figure 1, many biological entities such as viruses, bacteria, proteins and antibodies are known as biological nanomaterials and they have sizes within the range of nanoscale. Due to proper sizes of nanomaterials, many scientists show great concern for the design of nanomaterials to manipulate biological nanomaterials. In order to provide incorporation of nanomaterials into cell easily, the sizes of them should be less than 50 nm. On the other hand, nanoscale materials smaller than 20 nm can circulate through the body after moving out of the blood vessels. It should be noted that after special treatments, nanostructures become proper for drug delivery systems to carry large doses of chemotherapeutic agents or therapeutic genes into tumor-cells that are capable of invading and growing into nearby tissues and organs while saving healthy cells.

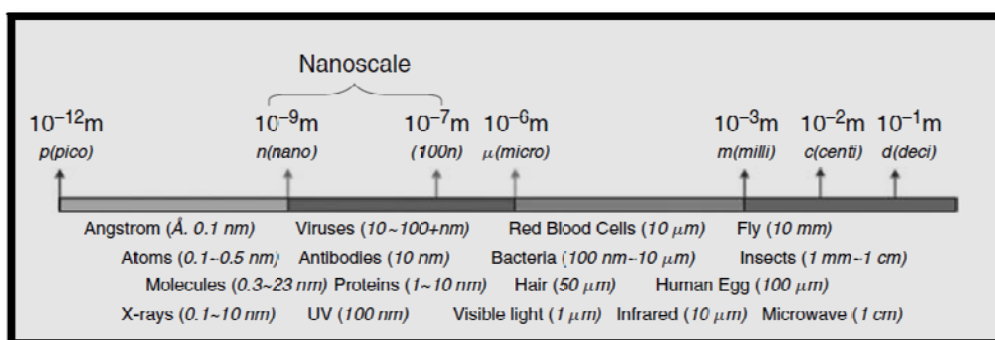


Figure 1. Scale of biomolecular interactions [1]

Nanomaterials designed should carry on several conditions in order to apply these structures in biology and medicine. These conditions incorporate that synthesized nanomaterials firstly should be biocompatible and non-toxic, in other words, nanomaterials should not prevent biological activities of the proteins and cells, and secondly nanomaterials should keep on the chemical and physical properties after chemical surface modifications.

1.1.2. Approaches for Synthesis of Nanoparticles

The synthesis of nanostructures is mainly categorized into two processes which are known as 'top-down' or 'bottom-up' processes.

1.1.2.1. Top-down and Bottom-Up Approach

Top-down approaches start with bulk material and break down the microstructure into a nanostructure until the desired structure is obtained. Most microfabrication techniques such as lithography and milling techniques for inorganic materials describe this definition. However, top-down techniques may result in the crystallographic damage and contamination problems. As the surface area of nanomaterials is very large, such defects may affect mechanical properties and surface modification of nanostructures severely. On the other hand, bottom-up approaches start with smaller components to arrange the nanostructures atom by atom and layer by layer to obtain more complex assemblies. Due to reduction of Gibbs free energy, nanostructures produced with this approach are closer to a thermodynamic equilibrium state. Nanomaterials synthesized by bottom-up approach have generally fewer defects, better regularity of arrangement of particles and more homogeneous chemical composition compared to nanomaterials synthesized by top-down approach.

Figure 2 indicates the process of "top down" as compared to "bottom up" self-assembly.

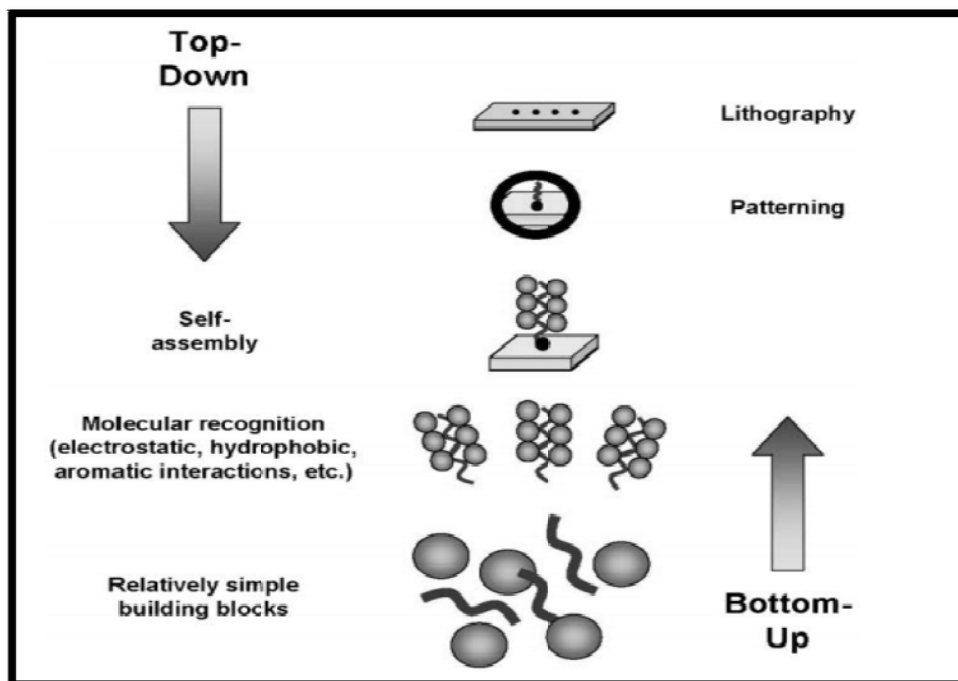


Figure 2: Top-down and bottom-up strategies [2]

1.2. Functionalization of Nanoparticles with Biological Molecules

In order to functionalize nanomaterials with biomolecules, different interdisciplinary knowledge consisting of molecular biology, bioorganic and bioinorganic chemistry and surface chemistry can be employed. In literature, there are several methods for the synthesis of nanoparticles, however, functionalization of nanoparticles with biomolecules should be performed in controlled conditions such as specific salt concentration, pH and temperature. The functionalization of nanoparticles with biomolecules can be carried out via mainly three methods. First method is to direct attachment of nanoparticles and biomolecules by electrostatic interactions. Second method is to make surface modifications by using organic linker molecules, and finally, the third method is to take advantage of affinity of

biotin-avidin linkage where avidin is adsorbed onto the surface of nanoparticles.

Many biological molecules can be used to recognize and bind other molecules with high selectivity. With this respect, molecular recognition is an important ability of biological molecules [3, 4] Antibodies and oligonucleotides are the most known receptors used as applications of molecular recognition. In short, antibodies are special proteins produced by the body's immune system that can recognize and bind specific antigen or a virus, and in this manner, infectious parts of immune system can be destroyed. On the other hand, oligonucleotides are single stranded deoxyribonucleic acid (DNA) and linear chains of nucleotides which are made up of a phosphate group, a pentose sugar and one of several kinds of organic molecules called bases. DNA comprise the bases Adenine (A), Cytosine (C), Guanine (G), and thymine (T) [5] as shown in Figure 3. The molecular recognition capability arises from the fact that the base A only binds to T and C only binds to G. This shows that using of oligonucleotides as molecular recognition application provides really high selectivity and specificity.

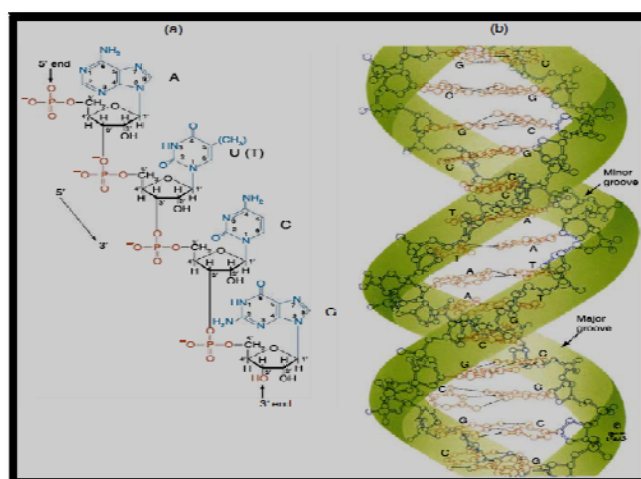


Figure 3: Representation of (a) nucleic acid and (b) double helix structure of DNA molecule [5]

1.2.1. Tagging Materials

In recent years, scientists are focused on nonradioactive tagging systems for the increase usage of biomolecules in nanotechnology in order to provide improved safety and specificity. In bioassays, upto date, several types of tagging materials have been used such as plasmon-resonant particles [6], quantum dots (QDs) [7], metal nanoshells [8], and Raman tags [9]. Recently, the design of Surface Enhanced Raman Scattering tags (SERS-tags) have gained considerable interest due to several advantages compared to other tagging systems.

1.2.1.1. Plasmon resonant particles (PRP's)

Nanometer-sized silver or gold colloids are known as plasmon resonant particles, and these colloids are one of the important nanostructures used as labelling and detection of biomolecules in bio-analysis [6]. Plasmon resonant particles have generally 10-120 nm diameter in size and they are advantageous, namely: they are inert, non-toxic, stable in different environmental conditions and they have convenient optical and electronic properties, and besides synthesis of these nanostructures in different size and shape does not need so long procedures. Plasmon resonant particles have unique surface plasmon resonance band (SPR) in the visible range [10]. The surface plasmon oscillation of metal free electrons results in a strong enhancement of absorption and scattering of electromagnetic radiation with the SPR frequency of the metal nanoparticles, giving them not only intense colors but also interesting optical properties. The formation of nanoparticle can easily monitored by recording of UV-vis spectra of the reaction solution. That is, the absorption spectra of plasmon resonant particles are characterized by intense absorption peak that is absent in the bulk spectra. The SPR band depends on the particle size, shape, structure, dielectric properties of metal and surrounding medium. These factors influences the electron charge density on the particle surface.

The optical properties of silver nanoparticles highly depend on the particle size. Smaller nanoparticles absorb near 400 nm, while larger spheres due to increased scattering have peaks that broaden and absorb light at longer wavelengths called as red-shifting. Figure 4 shows the absorption spectra of silver nanoparticles ranging from 10-100 nm in diameters.

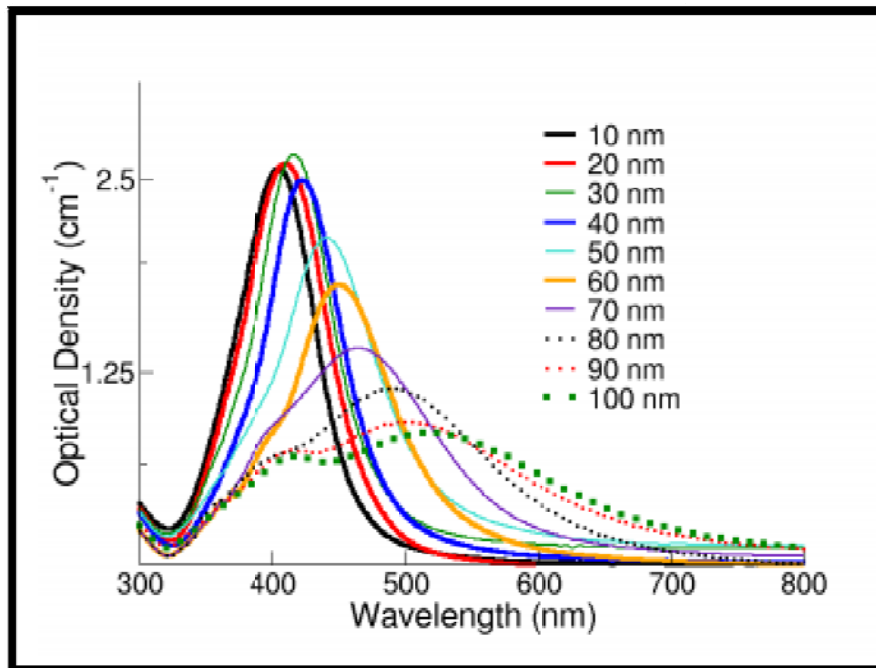


Figure 4: Absorption spectra of silver nanoparticles with diameters ranging from 10-100 nm [11]

For small nanoparticles, the EM field is uniform so that conduction electrons around nanoparticles produce only dipole type oscillations. This event leads to a single and narrow peak in the absorption spectrum. On the other hand, as the size of nanoparticle increases, electromagnetic field around nanoparticle becomes uniform resulting in the formation of several peaks and broadening of these peaks. Besides, small nanoparticles, smaller than 30 nm, exhibit only absorption, whereas large nanoparticles exhibit both absorption and resonant scattering which result in red-shifting in absorption spectra.

The relationship between the ratio of surface area to volume to the diameter of particles given as follows.

$$S_R = \frac{\text{Surface Area}}{\text{Volume}} = \frac{4\pi r^2}{\frac{4}{3}\pi r^3} = \frac{3}{r} = \frac{6}{D}$$

The equation shows that the surface area to volume ratio increases as the size of particles decreases.

Gold PRP's are advantageous in terms of functionalization of gold particles with alkylthiol-modified oligonucleotides is simple compared to silver PRP's as shown in Figure 5 [12]. In order to provide bioconjugation of silver PRP's, some surface modifications could be done by generating core-shell nanostructure.

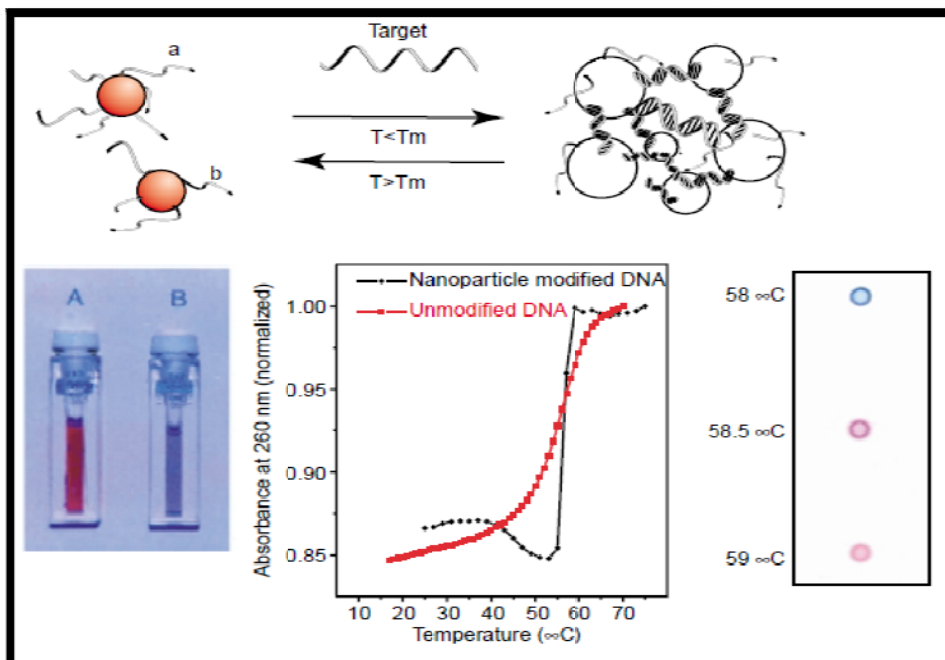


Figure 5: Gold Colloids for detection of DNA sequences [12]

Nevertheless, despite the benefits, it is necessary to prevent PRP's from aggregation, changing in shape and oxidation. Traditionally bioconjugation of PRP's is derived from electrostatic and hydrophobic interactions. However, it should be noted that non-covalent binding may cause desorption of biomolecules from the surface of PRP's, and may results in unwanted bindings with target sites. For this, more reproducible and effective methods that is emphasize on covalent surface attachment chemistry for the attachment of biomolecules to PRP's must be developed [13]

1.2.1.2. Quantum Dots (QD's)

In addition to PSP's, there is a great interest for the synthesis of semiconductive nanocrystals, in other word, quantum dots as tagging material. QD's is the nanocrystal of cadmium selenide coated with zinc sulfide is shown in Figure 6.

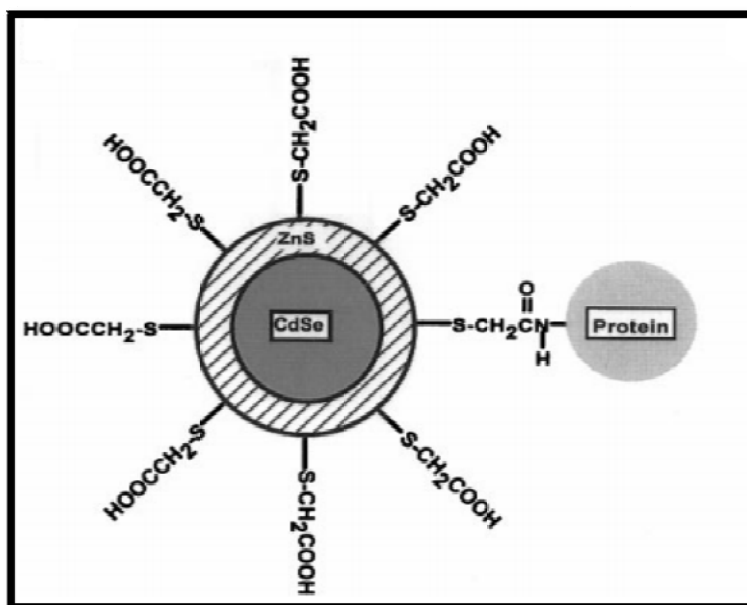


Figure 6: Schematic illustration of ZnS capped CdSe QD covalently attached to a protein [14]

They offer many advantages due to their special optical properties [14]. These properties arise from the size of QD's ranging from 1-10 nm in radius. For example, QD's offer narrow band emission and broad UV excitation, which enables multiplexed imaging of cells or tissue under a single light source [14-16]. Other applications consist of biosensing using QD-fluorescent resonance energy transfer based nanoprobe and cancer research. In literature, it was estimated that the molar extinction coefficients of CdSe QD's are changing from 10^5 to 10^6 $M^{-1} cm^{-1}$, depending of particle size. These values are 10-100 times greater than organic dyes. However, it should be noted that for biological applications, QD's need to be in water-soluble form by making functionalization of these nanostructures with different chemicals or encapsulation by block copolymers. The second disadvantage of quantum dots is the biotoxicity of these nanostructures. When exposed to UV-light excitation, surface oxidation of QDs and this leads to the release of cadmium ions which is really toxic even if concentration of QDs is in low amount.

1.2.1.3. Metal Nanoshells

An interesting alternative to tagging materials are metal nano-shells consisting of dielectric core and metallic shell. Nanoshells provide strong localized- surface- plasmon (LSP) resonances which could be used in plasmon-related spectroscopies. By controlling the thickness of metallic shells with respect to dielectric core, it is proper to achieve this enhancement.

Metal Nanoshells strongly absorb light in the near infrared region as shown in Figure 7, where optical transmission through tissues and cells is high.

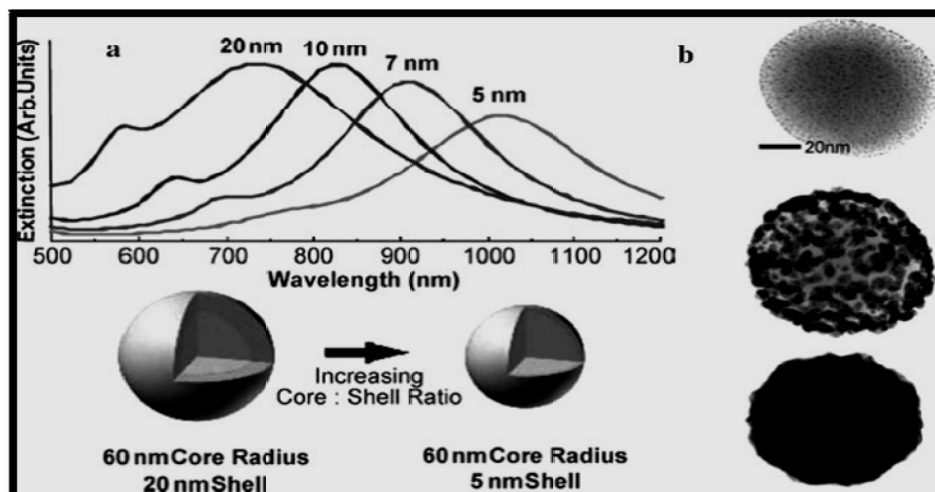


Figure 7: a) Absorbance spectrum of SiO₂-Au core-shell nanoparticles. b) TEM image of gold colloid growing on a silica core [17]

For this, metal nanoshells are proper to use as near-infrared (NIR) absorbers. In general, the usage of metal nanoshells consist of inhibition of photo-oxidation of conjugated polymer films [18], Raman sensors [19], substrates for blood biosensing [20] and drug delivery [21].

However, there are some problems arising from the corrections due to self-absorption. Yet, when compared with Mie theory and experimental results, the difference is quite negligible. On the other hand, these nanostructures are not enough to achieve single molecule detection. So that, higher enhancements between the nanoshells are required.

1.2.1.4. Surface Enhanced Raman Scattering Tags (SERS-tags)

Compared to other tagging materials mentioned before, Surface Enhanced Raman Scattering tags (SERS-tags) are highly specific making them sufficient for single detection systems. SERS tags are generally designed in

core-shell geometry, and they are labeled nanoparticle, generally consisting of gold or silver as a core. With the combination of Raman reporter molecule, SERS tags provide 10^6 - 10^{14} fold enhancement compared to Raman scattering intensity.

In literature, there are two principal approaches to develop SERS nano-tags. The first approach is to direct attachment of Raman reporter molecule which is Raman-active dye onto silver or gold nanoparticles [22] in Figure 8. The strategy provides high selectivity and sensitivity and results in multiplexed detection of DNA and RNA target molecules.

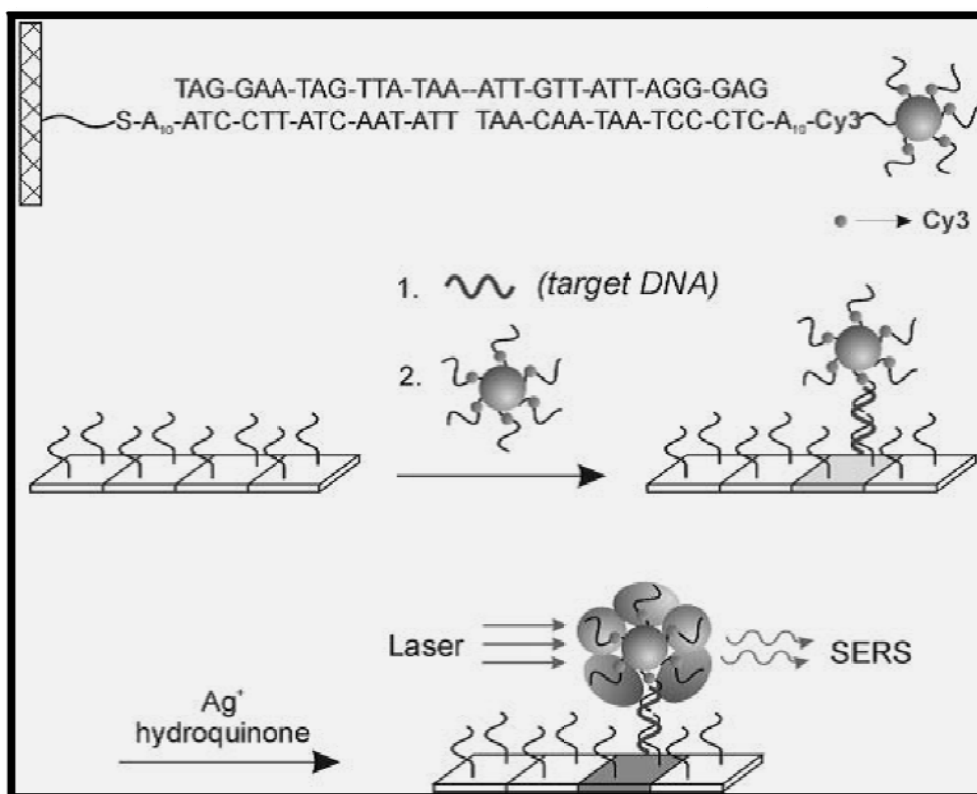


Figure 8: Direct attachment of Raman reporter molecule onto gold nanoparticle [22]

However, this approach has one restriction which is the instability of SERS tags caused by direct exposure of tag surface to environmental conditions

which generally decreasing the reliability of the assay. The second and improved approach is to design core-shell SERS tags in which the surface of nanoparticles was covered with a layer of silica or polymer. The function of silica shell is to protect SERS nanotags from agglomeration, to provide easy surface functionalization with amino or carboxylic groups, to increase the stability, and to enhance optical properties of SERS-tags. Figure 9 shows the schematic illustration of the preparation of raman dye embedded core-shell SERS nanotags.

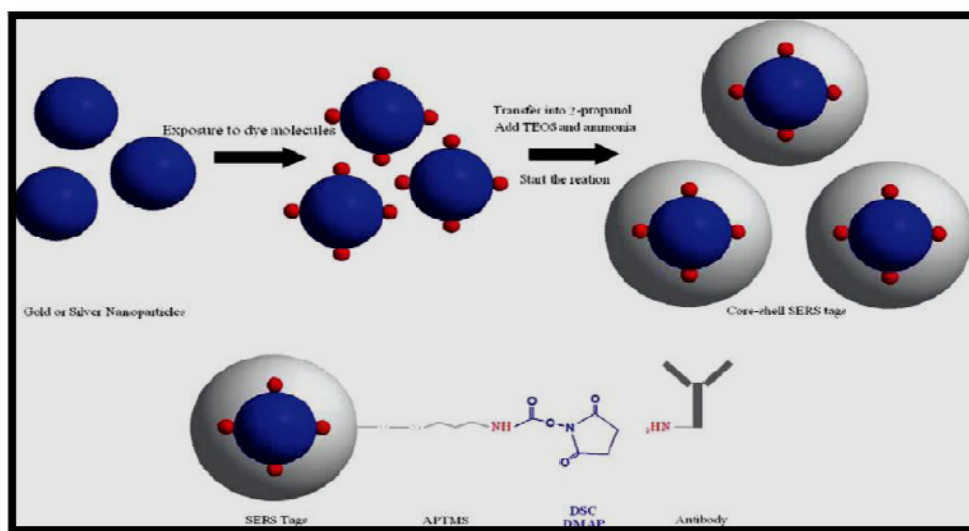


Figure 9: Schematic illustration of designing core-shell SERS tags [23]

It should be noted that in literature after adsorption of Raman reporter molecule onto silver or gold core, the encapsulation of core particles can be achieved with silica shell by sol-gel procedure or other alternative improved procedures.

1.3. Raman Scattering

Raman Scattering is a fundamental form of molecular spectroscopy. Likewise Infrared (IR) absorption, Raman Scattering provides information about the structure and properties of molecules depending on their vibrational transitions [24]. The theory of Raman scattering is more

complex compared to theory of IR absorption, but there are some similarities between two theories.

IR spectrum occurs from the rotational and vibrational motions of a molecule which is not electronically excited. For IR absorption, the molecule should show change in the dipole moment with respect to its vibrational motion. IR absorption is a one-photon event [25]. That is, IR photon collides with the molecule, the photon disappears, and the molecule is excited by the vibrational energy of the photon at the frequency of vibrational resonance. On the other hand, Raman scattering is a two-photon event. The change of polarizability of incoming radiation creates an induced dipole moment, and the radiation scattered by this induced dipole moment consists of Rayleigh scattering and Raman scattering. When incident photons are scattered from a molecule inelastically, it is called as Rayleigh scattering. In other words, Rayleigh scattering corresponds to the light scattered at the frequency of incident light. When elastically scattering is observed, it is called as Raman scattering. Figure 10 shows the differences in theory of these two methods.

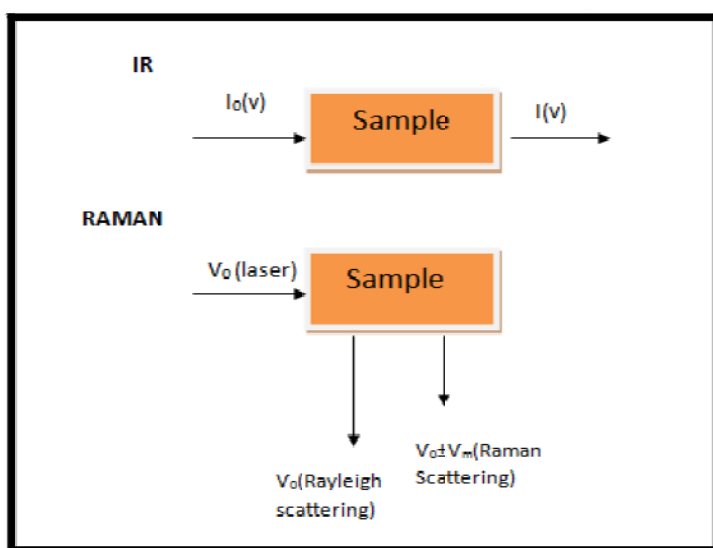


Figure 10: Differences in mechanism of Raman and IR.

The short history about Raman Scattering is the discovery of this phenomenon by Sir Chandrasekhra Venkata Raman in 1928. Sir Raman used very simple instruments which are sunlight as the light source, a telescope as the collector and his eyes as detector. Scattered photons could show a shifting in frequency and could have higher or lower energy compared to incoming photons. Losing energy by exciting a vibration decreases the frequency of scattered photon, known as Stokes scattering, and gaining energy from the molecular vibrations increases the frequency of scattered photon, known as anti-Stokes scattering. In Figure 11, Rayleigh and Raman spectra of carbon tetrachloride (liquid) is presented according to IUPAC recommendations.

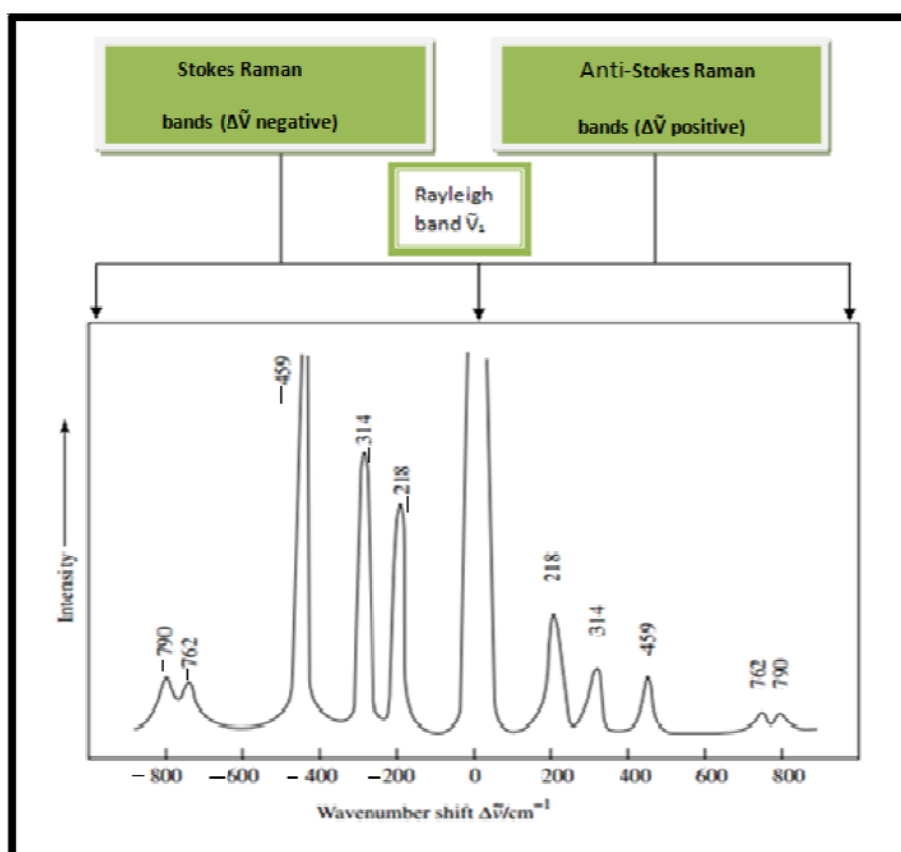


Figure 11: Rayleigh and Raman Spectra of carbon tetrachloride

1.3.1.Raman with Improved Sensitivity

General trend in Raman Spectroscopy is to increase sensitivity and to decrease detection limit by using SERS advantages. By this, it is likely to increase applications of Raman or even make Raman spectroscopy possible to apply some systems that could not be used before. With the help of SERS advantages, it is possible to increase applications of Raman spectroscopy in several systems. "Trace detection" is one of the important applications of SERS. For several methods, choosing the proper analyte to increase sensitivity of these methods is one of the important strategies that scientists use. However, for SERS applications, optimization of experimental conditions such as changing substrates or power of laser excitation is necessary to increase signals and lower the detection limits.

1.4. Surface Enhanced Raman Scattering (SERS)

Surface Enhanced Raman Spectroscopy (SERS) is a Raman Spectroscopic (RS) technique providing enhanced Raman signal from Raman -active molecules that adsorbed onto specially prepared metal surfaces. Generally, enhancement of intensity in Raman signal has been observed as 10^4 - 10^6 , and for some systems the values can be as high to 10^8 - 10^{14} . SERS provides surface selectivity and sensitivity that RS is lack of.

In the early 1970's, several groups were interested in observing vibrational spectra of molecules which covered onto solid surface as a monolayer coverage. It was known that such ability can be used in many fields such as electrochemistry, catalysis and surface sciences. Surface infrared spectroscopy was one of the optical techniques that was developing rapidly for this aim [26]

In 1974, which is also the first observation about SERS effect, Fleischmann et al [27] presented the results that they observed Raman signals from monolayer of pyridine covered onto electro-chemical roughened silver electrodes. According to Fleischmann, increase in surface area was responsible for the enhancement. However, on one side, Jeanmaire and Van Duyne, and on other side, Albrecht and Creighton demonstrated that enhancement of Raman signal could not be due to increase in surface area, but most probably due to different form of enhancement factors causing by the interaction between light and matter.

The reason of the dramatic enhancement in SERS is still controversial. However, intensity of Raman signal is directly proportional to induced dipole moment which is $\mu = \alpha E$. The formula exactly shows that the enhancement directly depends on the enhancement of polarizability α , and the enhancement of electrical field E. The enhancement factors are going to mention as **electromagnetic enhancement** and **chemical enhancement** in details.

1.4.1. Electromagnetic Enhancement

The widespread idea about the most effective enhancement factor of Raman scattering is the electromagnetic enhancement. In electromagnetic enhancement, when nanostructures on substrate are exposed to electromagnetic radiation with certain frequency, conduction electrons onto surface of nanostructures are driven into collective oscillation by this radiation, which is defined as surface plasmon resonance (SPR). Oscillating dipoles generated in nanostructure also radiates a secondary field as shown in Figure 12. The total oscillating field E at the surface is the sum of both incident and secondary fields. So that, generation of large electromagnetic fields onto surface of nanostructures results in enhancement of Raman intensity.

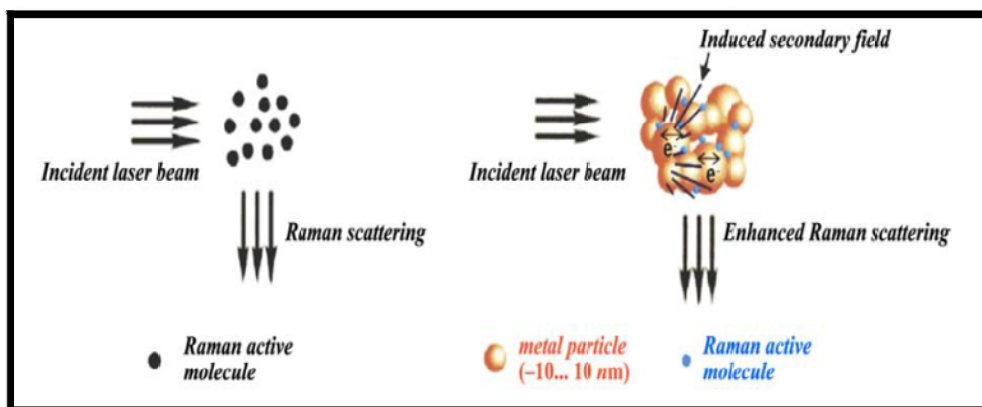


Figure 12: Electromagnetic (EM) enhancement of SERS [28]

The magnitude of enhancement depends on several factors, such as electric properties of metal, the distance between molecule and surface, position of the molecule with respect to surface, frequency of incident light, morphology of the surface and also surface roughness and this value can be calculated by Lorenz- Mie theory [29]. According to calculations made about the effect of surface roughness, it was observed that for smooth metal surface, the interaction between light and surface results in only six fold enhancement [30] on the other hand, roughened surfaces provide 10^4 to 10^7 enhancement of Raman signals. It should be noted that electromagnetic theory emphasizes on the importance of SERS substrate selection. Because, only rough electrodes and nanoparticles can be used to obtain desired enhancement in SERS. Ag, Au or Cu substrates are the most preferred substrates because of the proper dielectric constants, easy handling of these metals due to low chemical reactivity [31, 32]. In short, shape, size and composition of metallic nanostructures which are used as substrate play important role to obtain strong SERS signal and good signal reproducibility [33].

1.4.2 Chemical Enhancement

Existence of chemical enhancement is one of the controversial issue over the years in terms of effects on SERS enhancement. Adsorption or orientation of the molecule on surfaces may also cause chemical effects and such effects can increase or decrease SERS intensity. However, such effects should not be considered as SERS enhancement factor. For example, due to strong electrostatic repulsion, negatively charged dye cannot adsorp onto silver [34] nanoparticle, so that no SERS signal can be observed. The central idea about chemical enhancement is that molecular orbitals of adsorbate molecule are broadened into resonances due to interaction with the conduction electrons. While resonances lying near the Fermi energy level are filled partially, the others lying below this level are completely filled by conduction electrons. The chemical adsorption between molecule and metal surface introduce new possibilities for excitation of electrons in orbitals. The explanation of this theory is also known as charge transfer mechanism. In this mechanism, electrons can be excited from orbitals of adsorbate molecule to unfilled metal orbitals above Fermi level which is called as molecule-metal charge transfer, or electrons of metal can be excited to partially filled orbitals of adsorbate molecule which is called as metal-molecule charge transfer as can be seen in Figure 13.

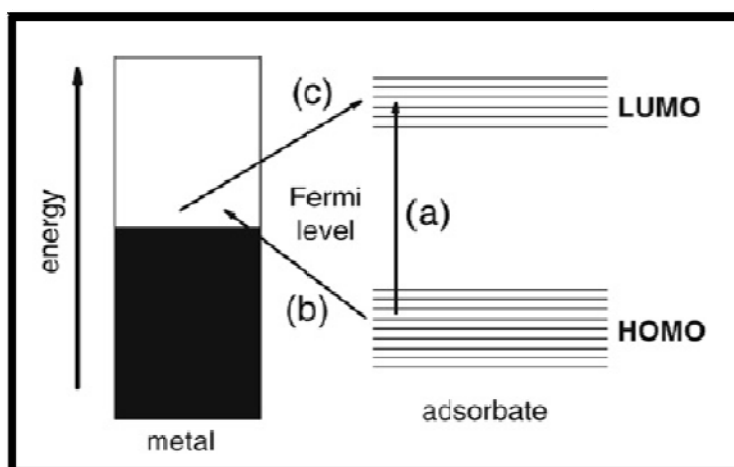


Figure 13. Charge-transfer mechanism in SERS cross-section [35]

Spectroelectrochemical experiments in which metal-molecule charge transfer excitations observed as red-shift and molecule-metal charge transfer excitations observed as blue-shift. Chemical enhancement can not be limited by chemically-bound molecules, however for charge transfer, there should be covalent bond between the molecules and metal surface.

1.4.3.SERS vs Fluorescence Spectroscopy

The weakness of Raman effect is the main reason why Raman spectroscopy could not be used in spite of its high specificity for detection of biological molecules for many years. However, today SERS can solve the problems arising from Raman effect. When applications are concerned, it is the fact that fluorescence spectroscopy is the other alternative for detection of biological molecules after SERS [36]. Fluorescence has some advantages over SERS, for example fluorescence makes single-molecule detection possible with an efficient fluorophore. This is also possible with SERS, however the need for using SERS substrate adds additional complication. On the other hand, compared to fluorescence, SERS offers many advantages. Firstly, SERS provides high specificity, that is SERS provides a structural 'fingerprint' of the biological molecules. Narrow band spectra of SERS allows simultaneous multiplex detection of biological molecules as can be seen in Figure 14.

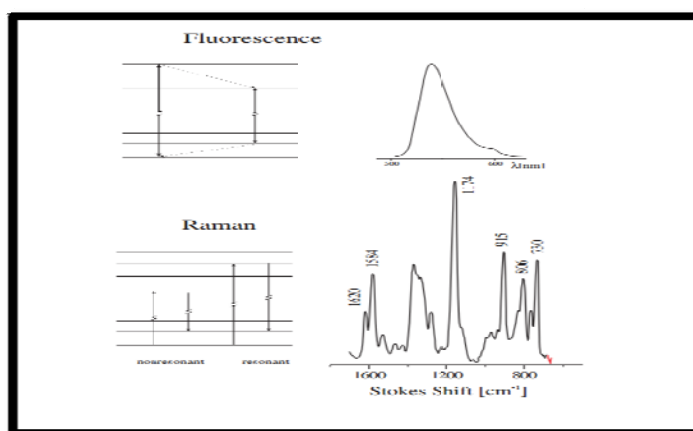


Figure 14: Schematic diagrams of SERS vs fluorescence [36]

However, fluorescence spectrum are relatively broad bands resulting in less structural information on the molecule [37]. Secondly, whereas fluorophore is needed for fluorescence spectroscopy, SERS can be directly used for any molecule. This difficulty for fluorescence can be prevented by providing attachment of fluorescent tags to molecules. This tagging system is also used to design good SERS probes, however avoiding this step is obviously attractive advantage of SERS. Thirdly, SERS can work at any excitation wavelength, whereas the working region of fluorescence is limited with the visible region. This limitation may be problem for living tissues of which optical absorption spectrum is in the visible region, causing difficulty in interpretation of signals. Finally, photobleaching of the fluorophore is the other disadvantage of fluorescence, whereas there is no such a complication under SERS conditions.

1.5. Applications of SERS

SERS provides rich spectroscopic information and high sensitivity so that it is an ideal tool for trace analysis and in situ investigations of several processes. The high intensity obtained from SERS spectrum makes it possible to observe vibrational spectrum of diluted solutions. According to Kneipp et al, it is possible to observe SERS spectrum with 4×10^{-12} mol/l concentration of rhodamine 6G on silver solutions [38] On the other hand, the method provides opportunity for the study of several molecules from diatomic to biological molecules.

Several investigations focus on the possibility of using SERS for the analysis of the samples separated by chromatography techniques such as thin-layer chromatography (TLC), high performance liquid chromatography (HPLC) and gas chromatography (GC). According to literature it was mentioned that Tran et al. made trace analysis of dyes on filter paper using SERS technique , whereas Freeman described the combination of SERS with HPLC and Roth and Kiefer described combination with GC. On the other hand, Ni et al. demonstrated that combination of SERS with flow

injection analysis (FIA), it is possible to obtain real-time spectra of RNA bases on silver solutions.

Besides trace analysis of some samples, surface analysis is the important area where SERS can be applied successfully. Due to large enhancement factors, it is possible to detect mono or submonolayers adsorbed on metal surfaces.

Discovery of SERS also provides an advantage of detection of glucose level in blood quantitatively. According to National Institutes of Health, there are 171 million people suffering from diabetes mellitus worldwide. This disease due to fluctuations in glucose level may result in kidney disease, heart disease, blindness, nerve damage and gangrene. Many methods have been used for detection of glucose level until today, however all these methods have difficulties depending on their usage, however, SERS has advantage of being faster, easier and less painful method for measuring glucose level [39]

It was demonstrated that SERS can be also used to design robust and sensitive optical probes for intracellular detection. These measurements have significance in order to obtain information from subcellular structures and compartments. Today, SERS-based nanosensors using for living cell provides high content of information about the molecules and high sensitivity. The ability of detecting such information will be beneficial in future as clinical diagnostic and therapeutic monitoring.

Other important potential application of SERS includes single molecule detection. Due to high enhancement factors known as chemical and electromagnetic effects, SERS enhancement is observed on the order of 10^{14} . Single-molecule detection capability provides new aspects to SERS in the field of biochemistry [38]. This ability is an advantage for monitoring proteins in their own environment and rapid detection of DNA and RNA sequencing. Recently, DNA-based diagnostic systems have gained importance, because such information is motivated by applications in many

fields such as DNA diagnostics, gene analysis, fast detection of biological warfare agents, and also detection of genetic mutations before any symptom of the disease appears. DNA detection systems based on the hybridization of single-stranded DNA target and its complementary probe in proper conditions for hybridization in solution or on a solid support. In conclusion, SERS is a technique for detecting and identifying a molecule without any labelling, because almost all molecules have Raman-active vibration modes that can be seen by the Raman effect, and it allows continuous, fast, sensitive and selective detection [40].

1.6. Synthesis of Silver Nanoparticles

The sizes of silver nanoparticles are generally found to be smaller than 100 nm and they contain 20-15000 silver atoms. Due to interesting properties, nanoparticles of silver are finding their way into several areas of science including medicine [41], chemical catalysis [42], textile engineering [43], biotechnology [44], water treatment [45], electronics [46], and optics [47].

Today, there is growing attention to develop environmentally friendly methods for synthesis of monodisperse silver nanoparticles. It is possible to synthesize silver nanoparticles both physical and chemical methods. However, chemical methods are preferred due to simple synthesis and low cost. Because such methods mostly consist of chemical reduction of silver ions to silver nanoparticles with stabilizing agents in aqueous solutions or thermal decomposition in organic solvents. In literature, the methods for synthesis of silver nanoparticles until today have been arranged as chemical reduction by sodium citrate, borohydride, hydroxylamine and hydrogen [48], by microwave plasma synthesis [49], by laser ablation [50], by microemulsion [51], by photochemical method [52], by thermal decomposition [53], by hydrothermal process [54], by sonoelectrochemical [55], and by electron irradiation [56].

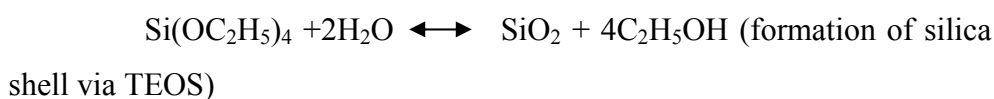
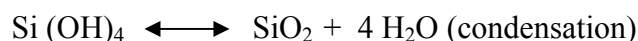
1.7. Synthesis of SERS nano-tags

Surface enhanced raman scattering tags in short, SERS-tags, include a Raman enhancing metal such as silver and gold core, a Raman active molecule (reporter molecule) attached to surface of metal core, and an encapsulant which can be rarely a polymer or usually SiO₂. The prepared nanostructure has a proper design to obtain SERS spectrum. Polymer encapsulant has some disadvantages including hydrophobicity which results in agglomeration in aqueous medium and swelling in organic solvents which results in leaking of the dye. However, the silica shell both protects the metal nanoparticle and the Raman active molecule. Except protecting ability, silica shell also provides further surface modification, good transparency (so that chemical reactions can be analyzed spectroscopically), biocompatibility.

1.7.1. Sol-gel Methods for Silica Coating

In literature, two synthetic approaches have been mentioned for silica coating. The first approach is the Stöber method and the second is the so-called reverse microemulsion (water-in-oil microemulsion)

In 1968, Stöber et al. pointed out the possible synthesis of silica particles by using tetraethoxysilane (TEOS) as silica precursor, water and ethanol as cosolvent, and ammonia as catalyst. The synthesis particles had sizes in the range of 500 nm to 2 μm [58]. The reaction proceeds as hydrolysis and condensation reactions of TEOS to synthesize silica particles. Later on, this chemistry has been used for silica encapsulation of noble metals such as gold and silver to increase their physical, chemical and biological properties. It was reported by Iler et al. [59], for silane precursor to crosslink onto the nanoparticle surfaces, the medium pH should be basic enough to achieve proper silica coating, but not too much basic to form silica nuclei. Stoichiometrically, the hydrolysis of TEOS in ethanol followed by condensation reactions are written as



The polymerization of silicic acid starts in acidic and basic medium in two ways. In acidic medium, condensation of silane groups produces chain-like or open-branched polymer, whereas in basic medium, internal condensation and crosslinking results in the attachment of siloxanes and hydroxyl groups of silicic acid onto the surface of nanoparticles [60, 61, 62].

In literature, it was reported that size distribution of silica shell on nanoparticles depends on concentration of TEOS, concentration of catalyst which is ammonia, concentration of water, alcohol used as the solvent and reaction temperature [63,64].

Optically, synthesized silica coated gold or silver nanoparticles show a significant red shift in absorption spectrum compared to the reactant silver and gold nanoparticles. This changing is arising from the change in dielectric constant around nanoparticles after silica coating.

In general, silica encapsulation process has based on Stöber sol-gel process, however this process is only proper for hydrophilic materials. Inapplicability of this process to hydrophobic material has accelerated the usage of reverse microemulsion systems for encapsulating nanoparticles. Reverse micelles are certain compositional range of water in oil microemulsions. Microemulsions are transparent, isotropic and thermodynamically stable systems formed by at least three components, two of which are nonmiscible water and nonpolar oil phase, and third component is surfactant which has an amphiphilic behaviour. The size of the micelles ranges from a few to tens of nanometers and depends on both molar ratio of water to surfactant, as well as concentrations of cosurfactants

and nonpolar solvent presented in the reaction medium. In this system, water droplets behave such as nanoreactors in which synthesis of nanoparticle is taking place and as water is added to system, a microemulsion is formed including nano-sized water droplets in oil phase. It should be noted that as the water amount increases, that is, as the molar ratio of water to surfactant increases, the size of the micelles also increases. During microemulsion formation, hydrophilic head of surfactant points to the polar aqueous phase, whereas hydrophobic tail of the surfactant points to the nonpolar oil phase. Commonly used surfactants include AOT (sodium di-2-ethylhexyl sulfosuccinate), CTAB(cetyltrimethylammonium bromide), phosphatidylcholine (PTC), Igepal CO-520 (Polyoxyethylene(5) nonylphenylether), and TritonX-100 . The advantages of employing reverse micelle system for the synthesis of core-shell nanostructure is to produce really monodisperse structures due to ability of dissolving reactants in the water core so that size of the nanostructures are limited by the size of the micelles and second advantage is to easy exchange of hydrophobic nanostructures to aqueous phase among micelles after silica coating and finally to provide synthesis of nanoparticles at a higher concentration (up to 1.5×10^{13} particles ml^{-1}) nearly three orders of magnitude higher in concentration compared to the concentration of synthesized particles via Stöber method.

1.8. Aim of The Study

The aim of this study is , firstly, to synthesize silver nanoparticles via thermal decomposition and chemical reduction, and synthesized nanoparticles were coated with silica layer via reverse microemulsion and Stöber methods respectively. Secondly, in this study, we designed raman-dye-labeled nanoparticle probes by embedding Raman reporter molecule, BCB, into silica shell for Surface Enhanced Raman Spectroscopic(SERS) measurements for the detection of biological molecules. Thirdly, SERGen probes were prepared by non-covalent binding with BCB and SERS nano-

tags and by covalent binding with SERS nano-tags, and finally, hybridization experiments were done.

CHAPTER 2

EXPERIMENTAL

2.1 Chemicals and Reagents

In this study, all the chemicals and reagents were analytical grade and used without further purification. All the glass and plastics were cleaned in the 10 % HNO₃ solution at least one day, and then splashed with distilled water. During preparation of SERS nano-tags de-ionized water obtained from Millipore water purification system was used. For DNA hybridization studies, all the equipments and buffer solutions were sterilized in autoclave before each experiments.

2.1.1. Synthesis of Silver Nanoparticles

2.1.1.1. By Thermal Decomposition Method

- **Silver Acetate;**
- **Oleic Acid, (9Z)- Octadecenoic acid;** analytical standard, Fluka
- **Oleylamine, 9-Octadecenylamine;** 70.0 %, Fluka
- **Diphenyl ether;** 99.0 %, Sigma-Aldrich
- **Toluene;** 99.0 %, Merck
- **Methanol;** 99.5 %, Sigma-Aldrich

2.1.1.2. By Chemical Reduction Method

- **Silver Perchlorate;**
- **Sodium Citrate Tribasic Dehydrate;**

- **Sodium Borohydride;**

2.1.2. Preparation of SERS Nano-Tags

- **Brilliant Cresyl Blue;** Sigma Aldrich. 10^{-4} M stock solution was prepared by using de-ionized water

2.1.2.1. By Reverse Microemulsion Method

- **Tetraethyl Orthosilicate, TEOS;** 98.0 %, Aldrich
- **Polyoxyethylene (5) nonphenylether, Igepal CO-520;** M_n 441, Sigma-Aldrich
- **1,8-Diazabicycloundec-7-ene, DBU;** 98 %, Aldrich
- **Cyclohexane;** 99.0 %, Sigma-Aldrich
- **Acetone;** 99.0 %, Sigma-Aldrich
- **1-Butanol;** 99.0 %, Sigma-Aldrich
- **1-Propanol;** 99.0 %, Merck
- **Ethanol;** 99.5 %, Sigma-Aldrich

2.1.2.2. By Stöber Method

- **Tetraethyl Orthosilicate, TEOS;** 98.0 %, Aldrich
- **Ethanol;** 99.5 %, Sigma-Aldrich
- **Dimethylamine, DMA;** 60.0 %,

2.1.3. DNA Oligonucleotides and Chemicals used for DNA Hybridization

2.1.3.1. DNA Oligonucleotides;

- **As complementary targets;**
5'- SH- TTTTTTTTTT GCA GTG GAT TCT CGG GCC
- **As probe sequence;**

5'- GGC CCG AGA ATC CAC

The nucleic acid probes and target DNA oligonucleotides were purchased from Alpha DNA (Canada) and used without any purification. Later on, during experimental process, due to purification steps, **mini quick spin oligo columns (Sephadex G-25, Roche Applied Science)** were used.

2.1.3.2. Chemicals used for DNA Hybridization

- **Dithiothreitol, DTT;**
- **11-mercapto-1-undecanol;**
- **Sodium Chloride**

2.2. Instrumentation

2.2.1. Centrifugation

To remove unreacted species in the reaction medium, Sigma 2-16 model laboratory centrifuge with maximum rotating speed capacity of 15000 rpm was used.

2.2.2. UV-VIS Spectrometer

The optical properties of oligonucleotides and silver nanoparticles were performed by using Varian Cary 100 UV-Visible Spectrophotometer. With this double beam instrument, the range between 300-800 nm were scanned and quartz cells were used in all experiments.

2.2.3. Raman Spectrometer

The SERS spectra of BCB labeled oligonucleotides and SERS nano-tags were performed with Jobin Yvon LabRam HR confocal microscopy Raman spectrometer with charge coupled device (CCD) detector and holographic notch filter. He-Ne laser with total power of 20 mW is used to provide

SERS excitation. The spectrometer has 1800 grooves/mm grating and 200 μm entrance slit. These values kept constant for all measurements.

2.2.4. Field Emission Scanning Electron Microscopy(FE-SEM)

Field Emission Scanning Electron Microscopy (FE-SEM) was used to characterize size and shape of nanoparticles. SEM allows the generation of complete 3D datasets of the nanostructures. The model of instrument is Quanta 400 FE-SEM from FEI. It was operated at 30 kV at high vacuum with the resolution of 1.2 nm. All FE-SEM analysis were done in METU Central Laboratory. Samples containing water and organic solvent were dropped on copper grids without gold coating. Carbon coated copper grids were not preferred due to embedding of such small particles to the carbon tape. The large aluminium peak comes from the SEM-grids. All sample, after dropping process, were left to dry for one day before operating SEM analysis. From the FE-SEM images, average particle diameter of nanostructures were determined.

2.2.5. Transmission Electron Microscopy (TEM)

The JEOL 2100F Transmission Emission Microscopy (TEM) was used to characterize size and shape of nanoparticles smaller than 20 nm in diameter. The instrument is an advanced field emission electron microscope with an accelerating voltage of maximum 200 kV. It uses Schottky type field emission gun as an electron source, and the instrument has 0.19 nm TEM point resolution. 200 mesh holey carbon coated grids and 200 mesh lacey carbon coated grids were used for analysis. Analysis were done after dilution of samples 1:10 ratio and all the experiments were performed in METU Central Laboratory.

2.2.6. Energy Dispersive X-Ray Spectroscopy (EDX)

Energy dispersive X-ray spectroscopy (EDX) is an analytical tool used for elemental analysis. It is one of the powerful attachments of SEM. The same samples were used in EDX prepared for SEM analysis.

2.3. Procedures

2.3.1. Synthesis of Silver Nanoparticles by Thermal Decomposition Method

Silver nanoparticles, firstly synthesized by thermal decomposition method. 235 μ l oleylamine and 160 μ l oleic acid were dissolved in 12.5 ml diphenyl ether (boiling point, 259 ° C), then 85 mg silver acetate (Ag-Ac) as silver precursor was added to this mixture. In this study, oleic acid was used as reducing agent and oleylamine as stabilizer (Figure 15).

Thermal decomposition method is a chemical decomposition caused by heat, that is, the growth stage takes place at higher reaction temperature, so that synthesis of silver nanoparticles were heated with diphenyl ether upto 120° C for 5 hours in hot plate with magnetic stirrer. Before thermal decomposition, the solution has light brown colour, and after thermal decomposition, colour of the solution turned to dark brown colour.

After the reaction, the contents were cooled down to room temperature. 15 ml methanol was added to the product in order to make separation by centrifuging for 30 min at 13500 rpm. After centrifuging step, the precipitate was redispersed in toluene. The precipitation by methanol, centrifugation and redispersion in toluene steps were done three times to wash silver nanoparticles. Synthesized nanoparticles can be dispersed in nonpolar solvents, in this case the solvent was cyclohexane (Figure 16).

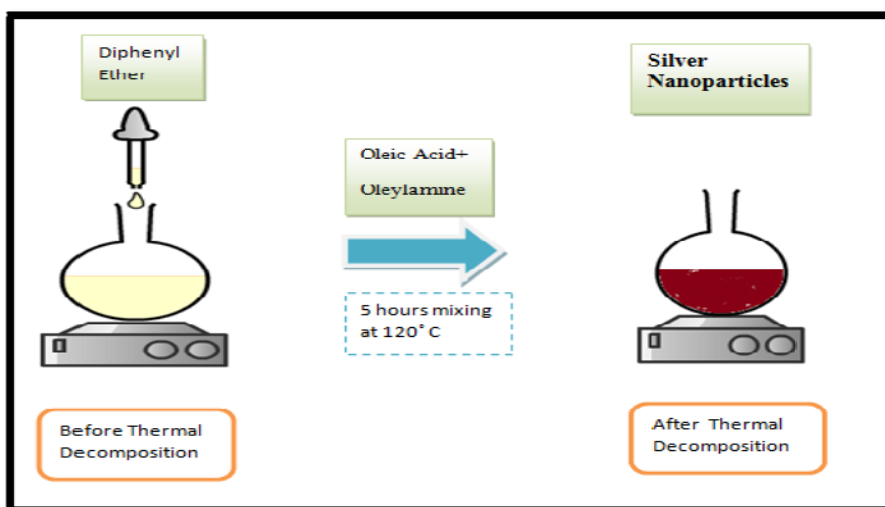


Figure 15: Scheme for the synthesis of silver nanoparticles by TD

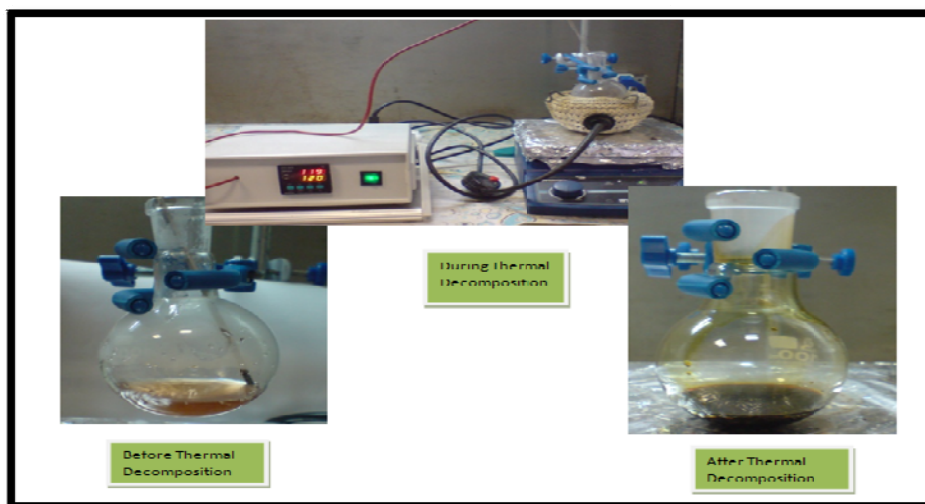


Figure 16: The experimental setup used for the synthesis of silver nanoparticles by thermal decomposition method

2.3.2. Synthesis of Silver Nanoparticles by Chemical Reduction Method

Silver nanoparticles, secondly synthesized by chemical reduction method. In a typical reaction, 4.0 mg NaBH_4 and 25.0 mg sodium citrate was dissolved in 198 ml of de-ionized water and left to cooling at 0°C . Afterwards, 2 ml

of 0.01 M AgClO_4 solution at 0°C was injected quickly to this solution under magnetic stirring. Mixing was continued for 20 minutes. During the reaction, the colour of the solution immediately turned light yellow and later on, deepened to bright yellow. Ag colloid solutions were stored at dark at room temperature for further experiments as shown in Figure 17.

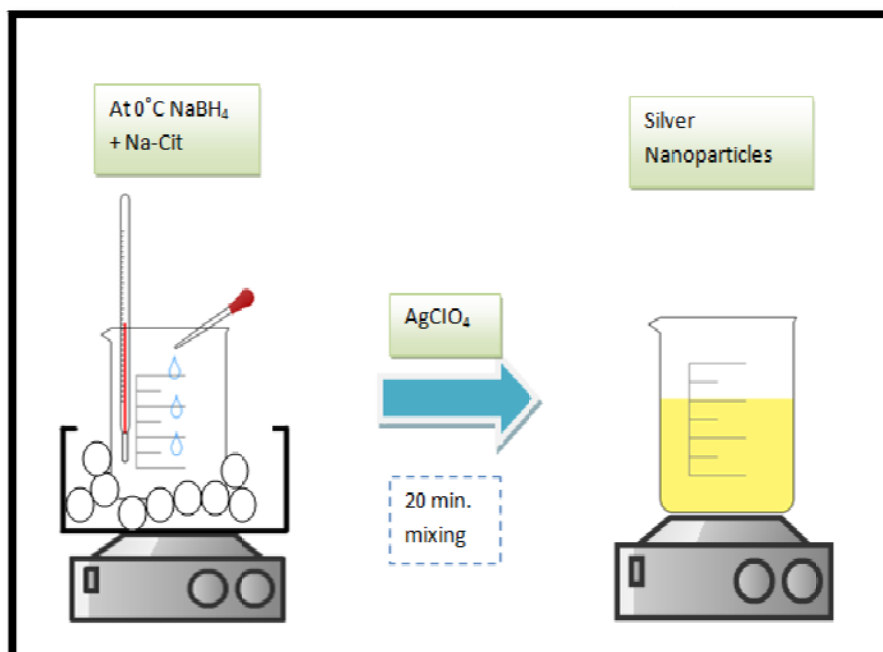


Figure 17: Scheme for the synthesis of silver nanoparticles by chemical reduction method

2.3.3. Preparation of Silica Coated Silver Nanoparticles by Reverse Microemulsion Method

Silver nanoparticles synthesized by thermal decomposition was used for silica coating by reverse microemulsion method. For this, 1000 μl of Igepal CO-520 was added to 6 ml of cyclohexane and dispersed by sonication for 20 minutes. Afterwards, 500 μl of silver nanoparticles were added to the solution, and left mixing for additional 30 minutes under magnetic stirring. Then 100 μl of TEOS was mixed with 20 μl of DBU in an eppendorf tube, and from this solution 40 μl was added to first solution (Figure 18).

In order to provide formation of micelles, extra 100 μl of de-ionized water was added to mixture. The mixture was left mixing for 24 hours at room temperature. In order to stop the reaction and isolate the nanoparticles from the medium, acetone was added to the solution, and centrifuged at 13500 rpm for 25 minutes.

Later on, washing steps were done by using 1-butanol, 1-propanol, ethanol and water respectively by using centrifuge to remove unwanted surfactants and reactant molecules. For washing steps sonication was used to provide redispersion of silica coated silver nanoparticles in the solvents and to prevent adsorption of nanoparticles onto centrifuge tubes. Finally, silica coated nanoparticles were dispersed in 10 ml de-ionized water (Figure 19).

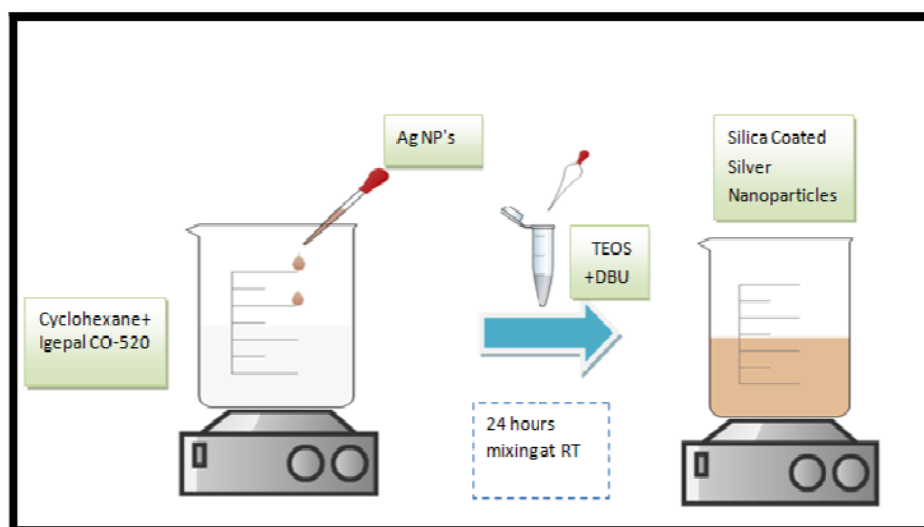


Figure 18: Scheme for the silica coated silver nanoparticles by reverse microemulsion method

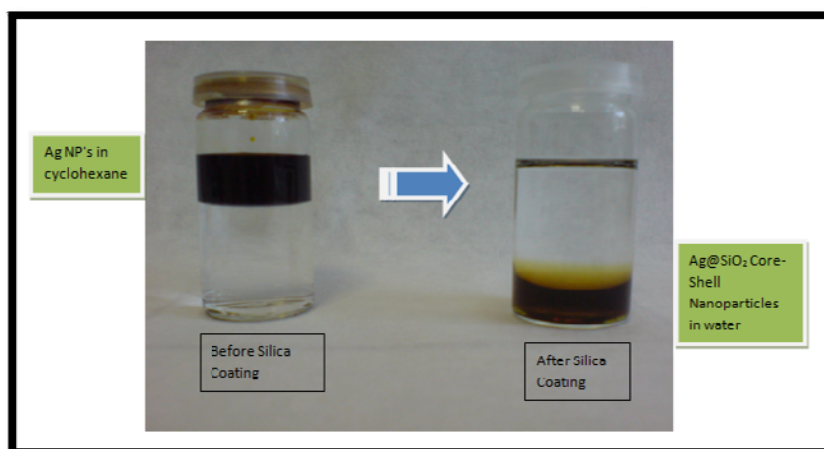


Figure 19: Ag NP's in cyclohexane before silica coating and Ag@SiO₂ Nanostructures in water

2.3.4. Preparation of Silica Coated Silver Nanoparticles by Stöber Method

Silver Nanoparticles synthesized by chemical reduction was used for silica coating by modified Stöber method. For this, 5 ml of silver colloid was added to 20 ml of ethanol. Later on, 6 μ l of TEOS was added to the solution, then silica coating was initiated by rapidly injecting of catalyst which is DMA. Then the solution left mixing for one day, and then washed with 3 times with ethanol-water solution (5:4) and one additional time with de-ionized water. Washing steps were done by using centrifuger for 10 min at 13500 rpm.

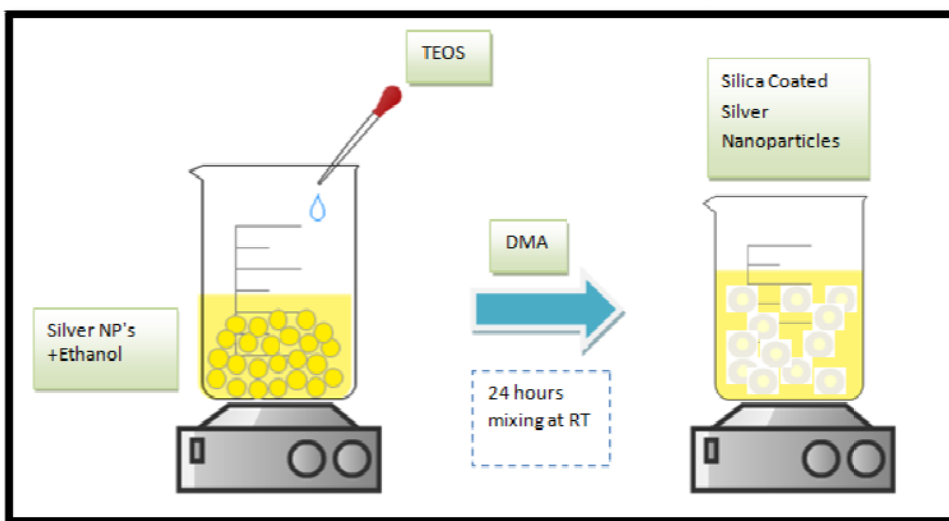


Figure 20: Scheme for the silica coated silver nanoparticles by Stöber method

2.3.5. Preparation of A Raman-Dye- Labeled Nanoparticle Probes

The pH of silver nanoparticles synthesized by chemical reduction method was adjusted to 7.0. The effect of pH change on the stability of silver nanoparticles was discussed in section 3.5. For encapsulation of Brilliant Cresyl Blue (BCB) in silica coating layer, firstly 5 ml of silver colloid synthesized was added to 20 ml of ethanol. Later on, 125 μl of 10^{-4} M BCB was added and solution was left mixing for 30 minutes under magnetic stirring at room temperature.

For silica coating step, different concentration of TEOS was added to the solution, then silica coating was initiated by rapidly injecting of DMA. The solution left to mixing for one day, and then washed with 3 times with ethanol-water solution (5:4) and one additional time with de-ionized water. Washing steps were done by using centrifuger for 5 min at 13500 rpm in

eppendorf tube and final product was diluted 2 ml with de-ionized water for FE-SEM and SERS analysis.

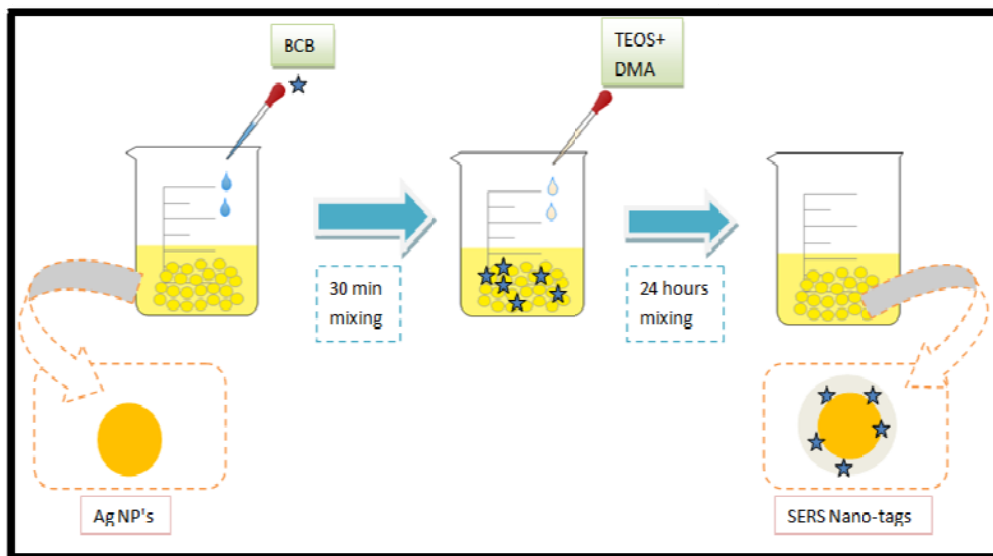


Figure 21: Scheme for the preparation of SERS nano-tags

2.3.6. Preparation of SerGEN Probe

Brilliant Cresyl Blue (BCB) was used as SERS-active label. The target DNA and probe DNA sequences used in hybridization experiments were 5'-SH- TTTTTTTTTT GCA GTG GAT TCT CGG GCC and 5'- GGC CCG AGA ATC CAC (the complementary sequence of the target) respectively.

2.3.6.1. Non-covalent Labelling of Oligonucleotide Primers with BCB

In the electrostatic attachment of cationic dye, BCB to the oligonucleotide, 10 μ l of dye solution was added to 1.5 μ l of (0.5 OD) probe DNA and incubated at 50 $^{\circ}$ C for 4 hours. In order to remove unreacted dye from the reaction mixture, gel filtration mini quick spin oligo columns were used. Figure 22 shows the process of noncovalent labelling of DNA with BCB.

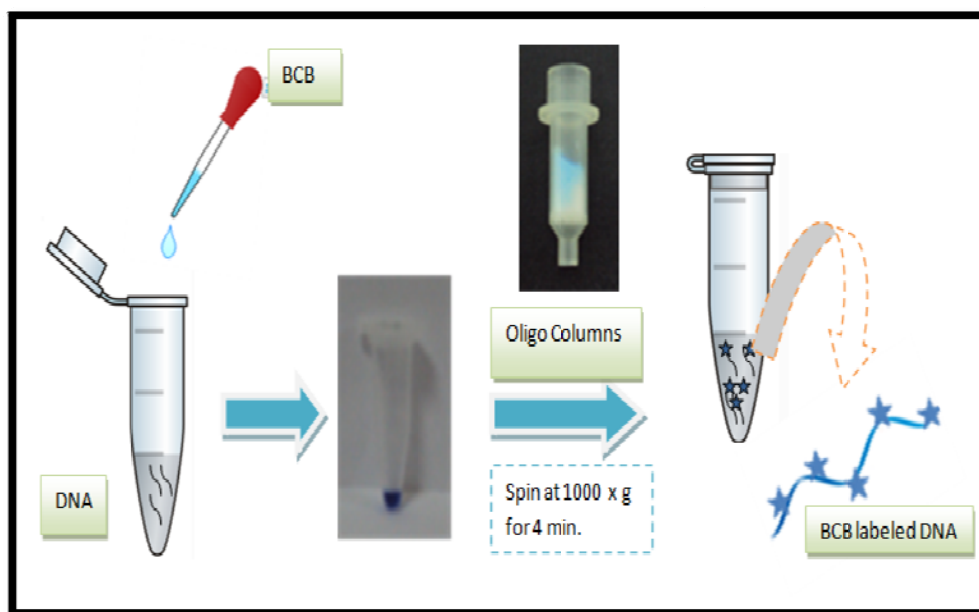


Figure 22: Schematic representation of noncovalent labeling of DNA with BCB

2.3.7. Immobilization of SERGen Probes onto Gold Surface Under Hybridization Conditions

For hybridization experiments, 0.911 μl of thiolated DNA targets were treated with 1.22 μl of dithiothreitol (DTT) in phosphate buffer (0.18 M, pH =8) for 1 hour at room temperature to cleave the possible formation of disulfide bonds between the oligonucleotides as shown in Figure 23.

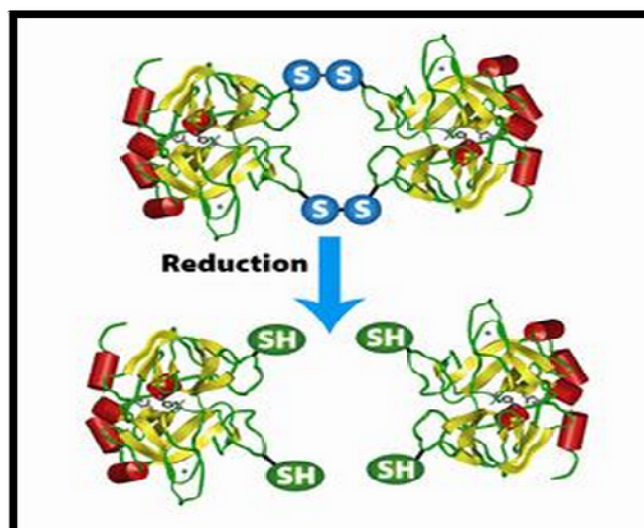


Figure 23: Schematic representation of rupture of disulfide bonds.

Then, the oligonucleotides were purified by using mini quick spin oligo columns to remove unwanted species from the medium. Later on, freshly cleaved thiolated DNA targets were added onto gold substrate (2.0 x 2.0 cm) which was cleaned before using by first diluted ethanol and, and second sterile water respectively.

The attachment of thiolated oligonucleotides onto gold substrate was achieved by adding 250 μ l of 1 M phosphate buffer solution (pH = 7). Following 4 hours incubation at room temperature, unbound targets were removed from the gold surface by washing four times with sterile water. Then, 250 μ l of spacer, 1 mM undecanol dissolved in ethanol, was added onto gold substrate. Later on, SERGen probes dissolved in 150 μ l of 10 mM phosphate buffer (pH = 7), and 75 μ l of 2 M NaCl solutions were added onto the gold surface and waited for 90 min. at room temperature to achieve proper hybridization conditions, Figure 24. Then, the gold substrate was washed with 0.18 M phosphate buffer in a plastic petri dish for 10 minutes, and then washed with sterile water for 5 minutes to remove excess salt amount from the gold surface before recording SERS spectra. Later on,

silver colloids with were added onto the gold substrate, and SERS spectra was recorded.

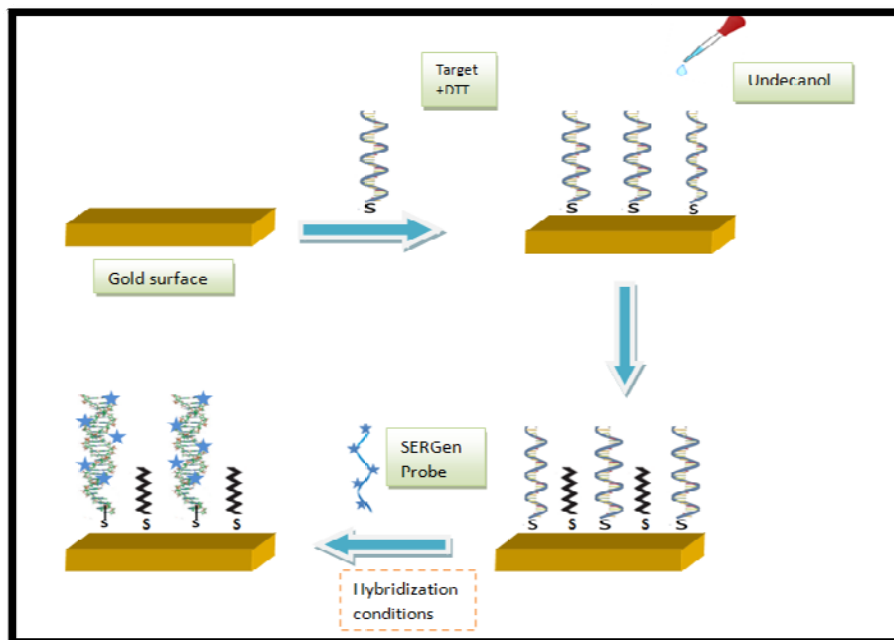


Figure 24: Schematic representation of immobilization of SERGen probes onto gold surface under hybridization conditions.

CHAPTER 3

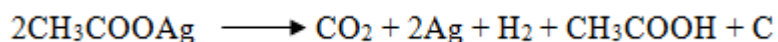
RESULTS AND DISCUSSION

In this study, firstly silver nanoparticles were synthesized by thermal decomposition method, and synthesized nanoparticles then were coated with silica layer via reverse microemulsion. Conditions were optimized thoroughly for both methods and characterization of the particles were done utilizing TEM, SEM and UV-vis Spectrometer. Silver nanoparticles were also synthesized by chemical reduction method, and these nanoparticles were coated with silica layer via modified Stöber method. Comparing the performances of the particles according to these two synthesis routes, it was observed that preparation of raman-dye-labeled nanoparticles probes by using second route, which is synthesis of silver core via chemical reduction method and silica shell via Stöber method, is easier than the first one for DNA studies. For this, SERS nanotags based on this route was studied in. Later on, SERGen probes were prepared via noncovalent labelling with BCB and SERS nano-tags and via covalent labelling with SERS nanotags, and finally hybridization experiments were performed.

3.1. Synthesis of Silver Nanoparticles by Thermal Decomposition Method

Silver nanoparticles can be synthesized with various sizes and shaped depending on the method which is used. In this study, spherical shape silver nanoparticles were preferred. Smaller nanoparticles have surface area:volume ratios that are extremely high. This is the reason of studying small size silver nanoparticles between the range of 4-15 nm in diameter.

Thermal decomposition method provides synthesis of monodisperse silver nanoparticles by using silver acetate in diphenyl ether. According to literature [65], silver acetate undergoes decomposition by heat according to following reaction at 120 °C:



On the other hand, agglomeration of silver nanoparticles as time passes prevented by using oleic acid and oleylamine. Oleylamine weakly adsorbs on silver nanoparticles, so that, uniform size formation for silver nanoparticles is impossible by using only oleylamine. Therefore oleylamine and oleic acid were used together in order to provide self-assembly of silver nanoparticles. In general, size of the nanoparticles can be controlled by adjusting reaction parameters, such as time, temperature, and amount of capping agents, oleic acid and oleylamine. Decreasing time of reaction resulted in the agglomeration of nanoparticles later on. However, five hours reaction time was enough for the synthesis of monodisperse silver nanoparticles, and increasing reaction time more than five hours resulted no change according to absorption spectrum of silver colloid results.

UV-vis measurement of silver colloids has great importance for characterization and understanding the optical properties of these nanostructures. Before thermal decomposition, there is no formation of silver nanoparticles, so that no signal was observed as can be seen in Figure 25-a. However, after thermal decomposition, strong peak at 445 nm was observed showing formation of silver nanoparticles (Figure 25-b).

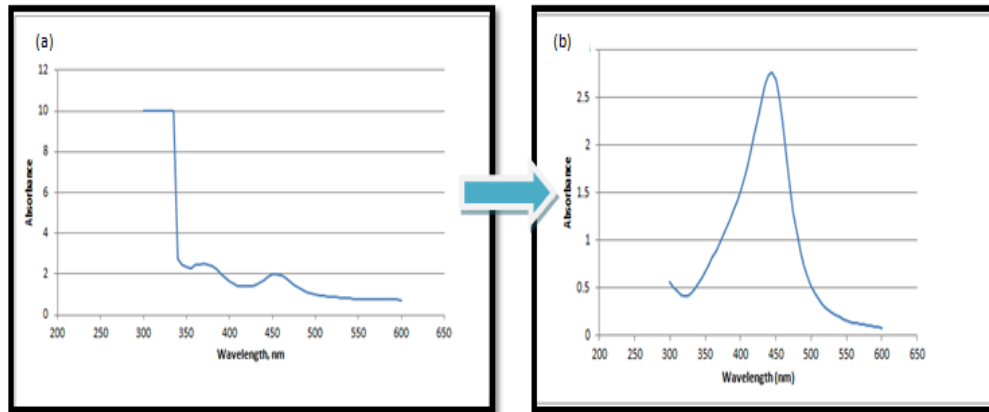


Figure 25: Absorption spectra of nanoparticles (a) before thermal decomposition method (b) after thermal decomposition

Transmission Electron Microscopy (TEM) was used for the characterization of silver nanoparticles in terms of size and shape. TEM image of the particles show that spherical-shaped silver nanoparticles synthesized by this method and one hundred nanoparticles were selected randomly (Figure 26). Number-length (arithmetic) mean size and volume weighted mean size were calculated according to the formulas:

Number - length (arithmetic) mean size:

$$D[1,0] = \frac{\sum diNi}{\sum Ni}$$

Volume weighted mean size:

$$D[4,3] = \frac{\sum di^4 Ni}{\sum di^3 Ni}$$

where 'di' is the diameter of nanoparticles and 'Ni' is the number of nanoparticles. Results of the calculations are given in Table 1.

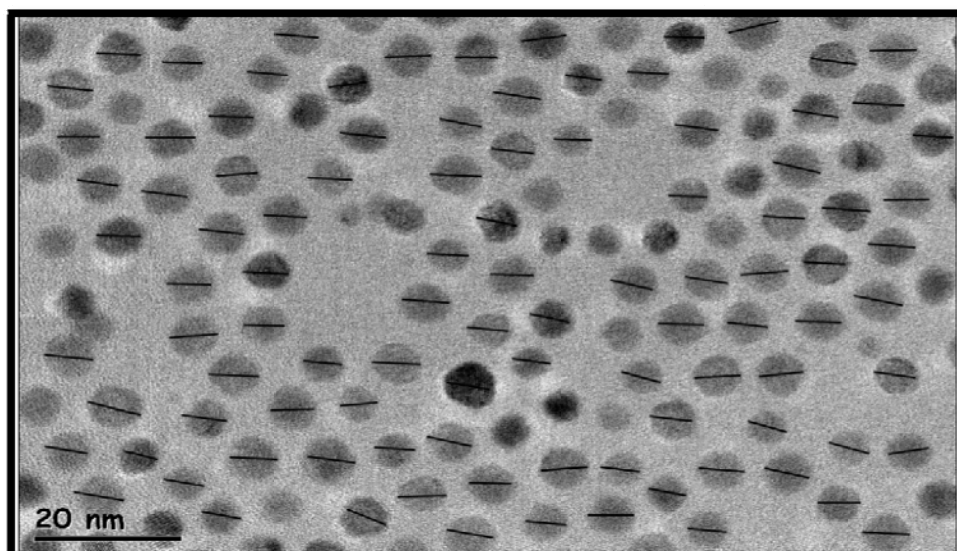


Figure 26: TEM image of silver nanoparticles

Table 1: Size of silver nanoparticles

D [1,0]	D [4,3]	PDI =——	Max. length	SD
4.015 nm	4.15 nm	1.023	4.632 nm	± 0.6 nm, N=100

3.2. Synthesis of Silver Nanoparticles by Chemical Reduction Method

In our research group, citrate reduction method was mainly used for the preparation of silver nanoparticles. However, by this method, the size of the synthesized nanoparticles were quite large, 64 ± 16 nm in diameter [66]. Besides nanostructures were exhibiting nanospheres, together with small amounts of nanorods. Chemical reduction method was also used in this work for the silver nanoparticles synthesis. However instead of citrate, sodium borohydride was used as a reducing agent which provided smaller sphere nanoparticles in 10 nm size range (Figure 27). In this study, the function of sodium citrate was to use as capping agent. Citrate weakly adsorbs onto nanoparticles, and due to being weakly bound capping agent, it is usually used to provide long term stability, and easily displaced by a

range of other molecules such as thiols, amines, polymers, antibodies, and proteins.

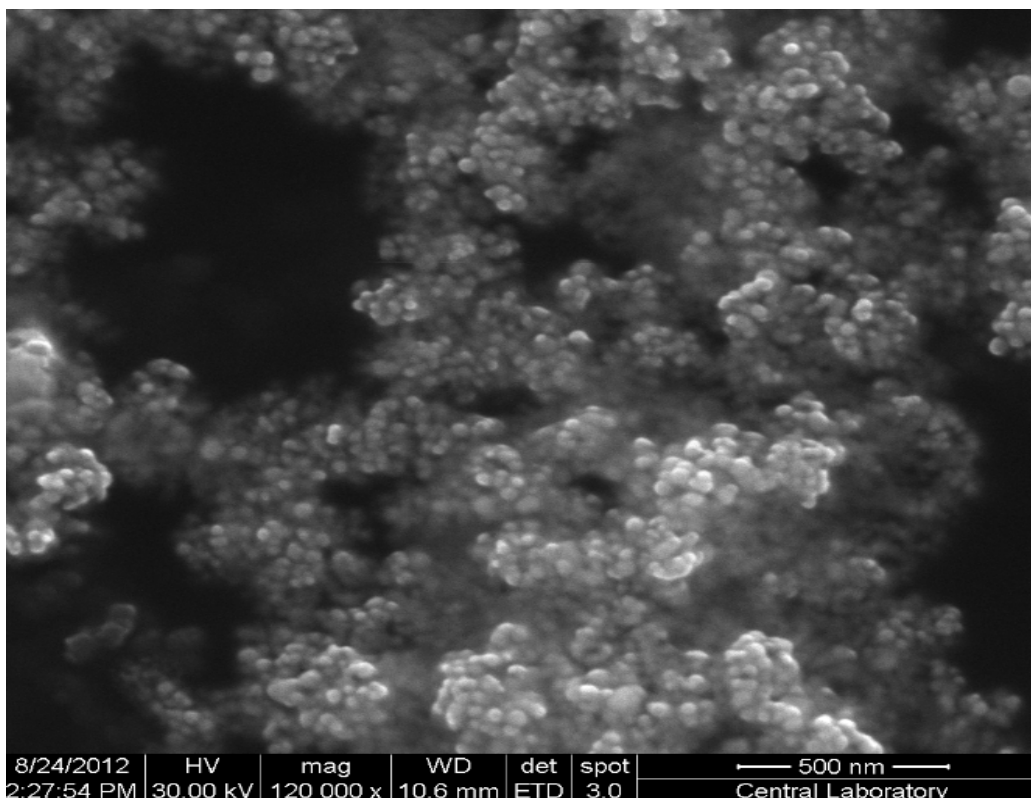


Figure 27: FE-SEM image of silver nanoparticles synthesized by chemical reduction method.

Although chemical reduction method requires less time for synthesis (only one hour) compared to thermal decomposition method (nearly seven hours). This method involves some important considerations. For example, the temperature of the solution during reduction is very critical. Temperature should be kept at 0°C in order to obtain clear silver nanoparticles. Any heat increase during reaction causes the change of the appearance of the colloid solution from clear yellow colour to a blurred yellow and broadening of the plasmon absorption spectrum of the silver colloids, Figure 28. These observations were indicating the change in size distribution of the particles from narrow to wide.



Figure 28 : Effect of temperature on the appearance of silver nanoparticles.

Another important parameter was the addition rate of the silver perchlorate to the mixture of sodium borohydride and sodium citrate solution. For DNA studies, nearly 10 nm size silver nanoparticles are large enough to use. In order to obtain nanoparticles around 10 nm in size, it should be added rapidly. Otherwise larger particles were obtained and this change was followed as red-shifting from 400 nm to 410 nm in absorption spectrum as seen in Figure 29.

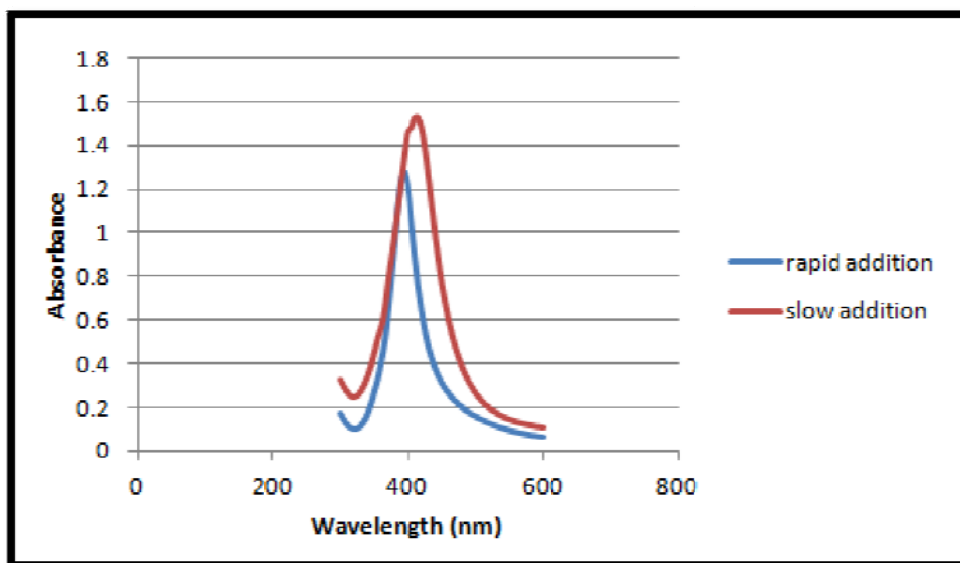


Figure 29: Effect of addition rate of silver perchlorate

Thus prepared solution was stable and no precipitation or change in colour observed for several days.

Figure 30 shows the peak positions of plasmon absorptions of silver nanoparticles prepared by thermal decomposition and chemical reduction methods.

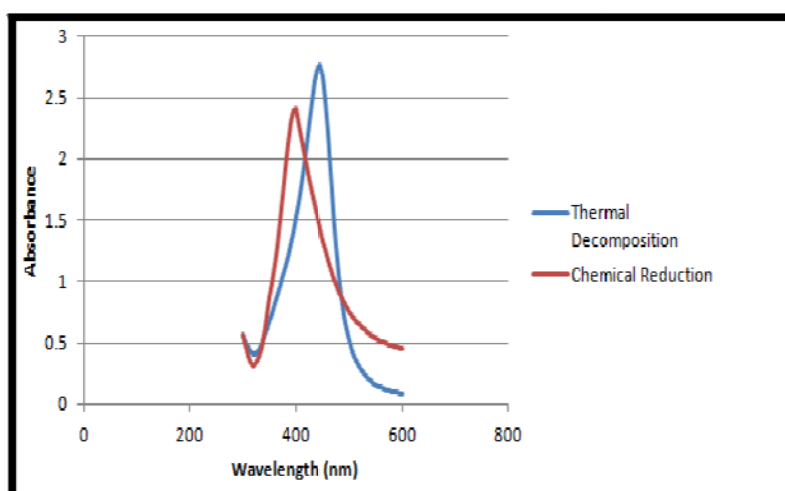


Figure 30: Peak positions of plasmon absorptions of silver nanoparticles prepared by thermal decomposition and chemical reduction methods.

Figure shows 45 nm shift in absorption bands, this was an expected result, because surface plasmon resonance absorption bands in the visible region are very sensitive to particle size, shape, structure, dielectric properties of metal and surrounding medium, because these factors affect electron charge density around the nanostructures. In thermal decomposition method, cyclohexane with refractive index 1.426 and in chemical reduction, water with refractive index of 1.000 were used as solvents. Therefore, the significant shift was arisen due to change in refractive indices of the medium.

The elemental analysis or chemical characterization of the prepared samples were determined by energy dispersive X-ray (EDX) analysis as can be seen in Figure 31. It is mostly used analytical technique with electron microscope techniques. The large aluminium peak comes from the SEM-grids. Synthesized nanoparticles were so small, and we observed embedding of such small particles to the carbon tape, so that, samples for SEM measurements were prepared by dropping onto grids directly without using carbon tape.

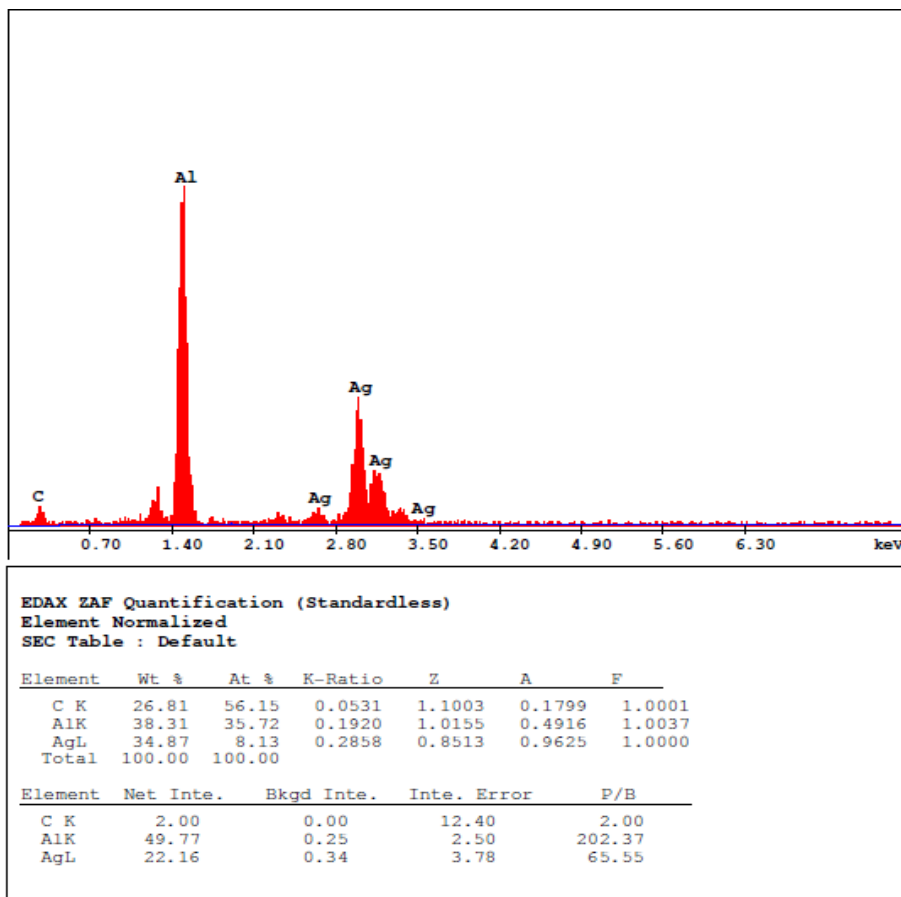


Figure 31: EDX image of silver colloids synthesized by chemical reduction method.

3.3. Preparation of Silica Coated Silver Nanoparticles by Reverse Microemulsion Method

In addition to the use of hydrophilic metal nanoparticles, hydrophobic metal nanoparticles can also be interfaced by silica layer. Via reverse microemulsion method, it is possible to form thin silica layer around the hydrophobic metal nanostructures. Reverse microemulsion method enables to coat small metal nanoparticles, less than 20 nm, and it also can be applied for coating high concentration of nanoparticles which creates problems for other silica coating methods.

In this study, silver nanoparticles synthesized by thermal decomposition method were hydrophobic. In order to be able to use them in aqueous medium, their surfaces were rendered hydrophilic by silica coating through water in cyclohexane reverse microemulsion method. In order to form reverse micelles, both ionic and nonionic surfactants can be used. Nonionic surfactants are relatively insensitive to change in concentration of electrolyte in the medium compared to ionic surfactants. In our study, non-ionic surfactant, Igepal CO-520 was used to form micelles (Figure 32)

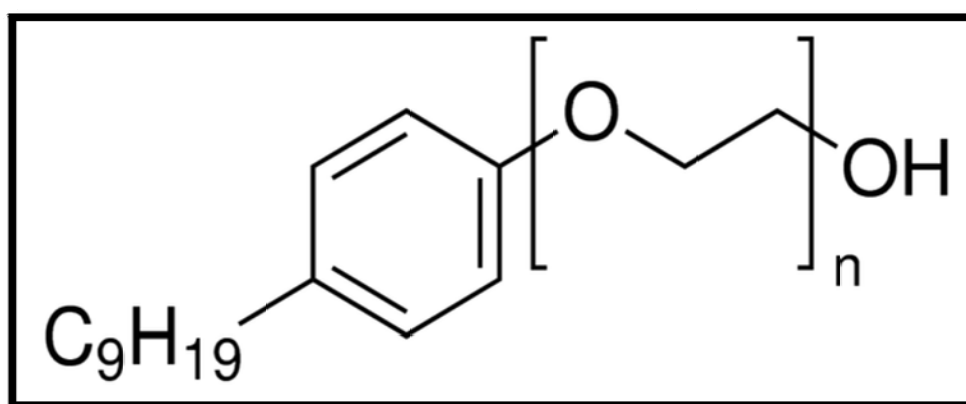


Figure 32: Chemical structure of Igepal CO-520

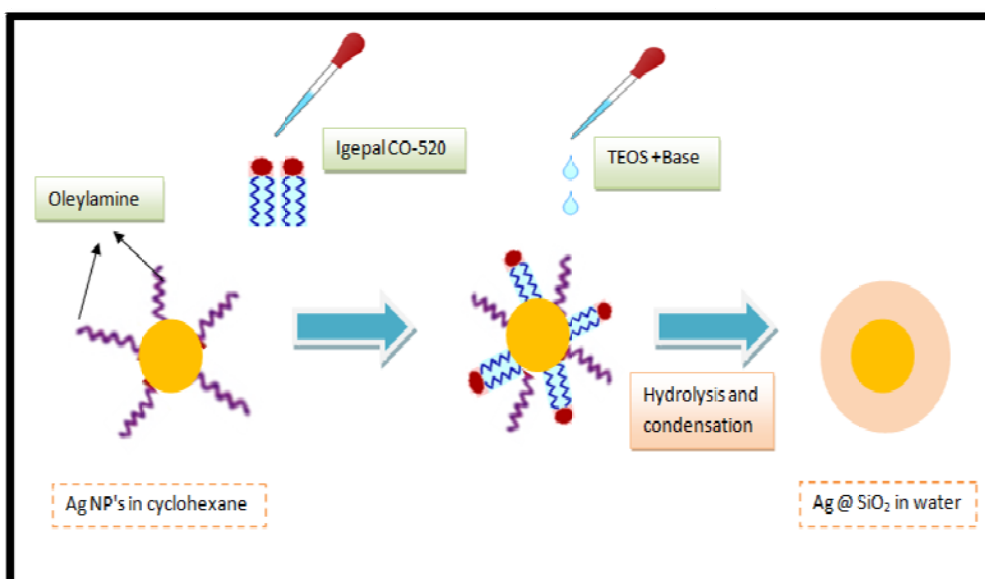


Figure 33: Synthesis of Silica Coated Silver Nanoparticles

Formation of thin silica layer around the silver nanoparticles was achieved by hydrolysis and condensation of tetraethoxysilane (TEOS) in reverse micelles with the addition of base catalysis (Figure 33). TEOS, in chemical structure, includes four ethyl groups attached to SiO_4^{4-} ion, which is called orthosilicate. This chemical has an extraordinary property of converting into silicon dioxide according to reaction:



The final verification of silica coating was done by using TEM measurements. However, before TEM measurements, the performance of the coating was followed by observing the dispersion ability of silica coated nanoparticles in water. The second sign of the silica coating was the colour of solutions. During silica coating process, 500 μl silver nanoparticles prepared through thermal decomposition was used and coated particles were dispersed in 10 μl water. Thus a reference solution was prepared for colour comparison by diluting silver nanoparticles prepared thermal decomposition to the same concentration as the silica coated nanoparticles aqueous dispersion, i.e 500 μl silver nanoparticles were dispersed in 10 ml cyclohexane. Reference solution can be seen in Figure 34.



Figure 34: Reference solution prepared using 500 μl Ag NP's in cyclohexane

The colour matching of stable dispersed silica coated nanoparticles with reference solution was expected to show the proper silica coating around silver surface. Colour matched solutions were selected for TEM characterization.

In the literature ammonia was used as a base for silica coating of nanoparticles, particularly for gold nanoparticles [68] Therefore ammonia was selected as a base in our studies and the parameters such as the amount of base, TEOS, IGEPAL were optimized.

In the optimization of base concentration, various amount of ammonia solution (80 to 150 μ l) was used as catalyst as seen in Table 2.

Table 2: Usage of ammonia solution with different concentration in reverse microemulsion method as catalyst.

Samples	A	B	C	D
Ag NP's	500 μ l	500 μ l	500 μ l	500 μ l
Igepal	1300 μ l	1300 μ l	1300 μ l	1300 μ l
TEOS	100 μ l	100 μ l	100 μ l	100 μ l
NH ₃ . H ₂ O(aq)	80	100 μ l	125 μ l	150 μ l

However, it was observed that nanoparticles were precipitated in water either immediately or in one day time. Besides the colours of the dispersions were totally different than reference solution of silver nanoparticles as shown in Figure 35, which shows the failure of silica coating

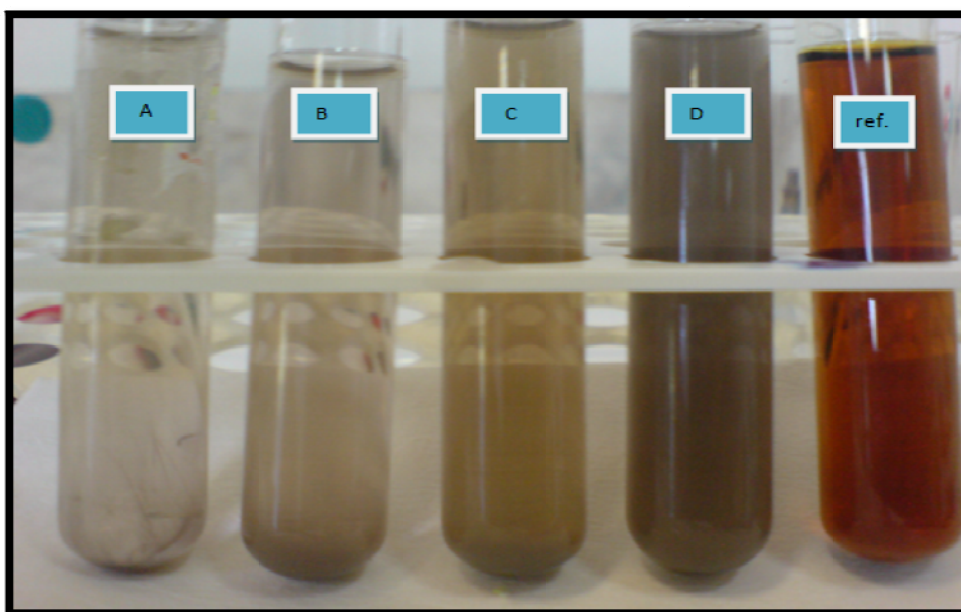


Figure 35: Silver nanoparticles following silica coating process of sample A, B, C, D and ref.

At this point, the amount of surfactant was changed in the range of 1000-1500 μl while keeping the concentration of ammonia constant. Table 3 shows the changing of surfactant concentration during reverse microemulsion method.

Table 3: Changing of surfactant concentration during reverse microemulsion method

Samples	E	F	G	H
Ag NP's	500 μl	500 μl	500 μl	500 μl
Igepal	1000 μl	1200 μl	1300 μl	1500 μl
TEOS	100 μl	100 μl	100 μl	100 μl
NH ₃ (aq)	150 μl	150 μl	150 μl	150 μl

Sample G and H were dispersed in water easily whereas Sample E and F were precipitated. Therefore, it was thought that silica coating was achieved in case of sample G and H, but not for sample E and F as shown in Figure 36.

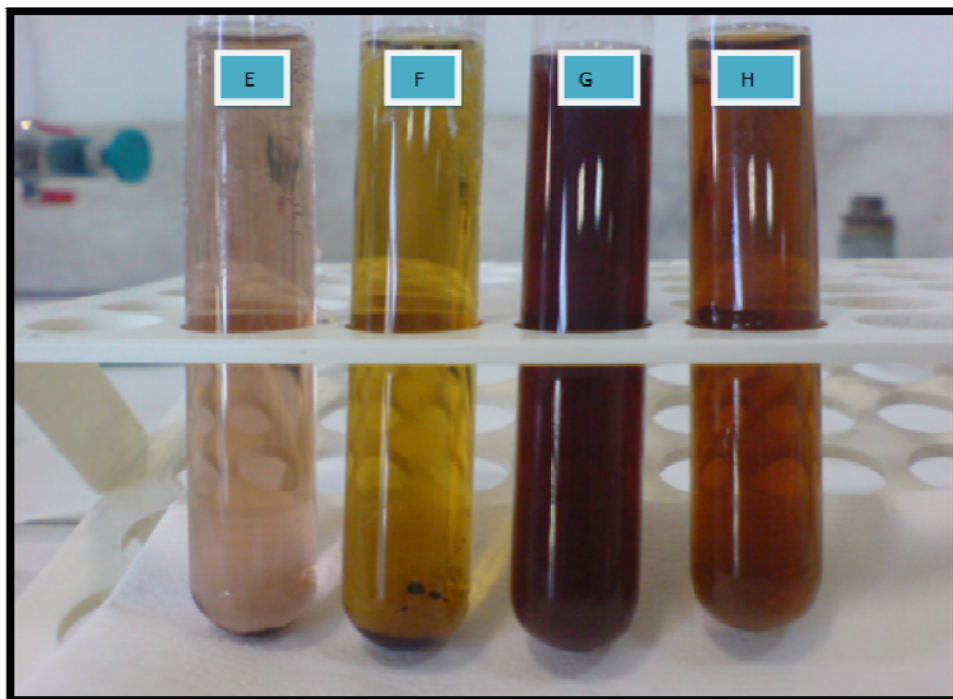


Figure 36: Silver nanoparticles following silica coating process of sample E,F,G and H.

Further characterization was done for sample G and H by using TEM. TEM images of sample G and H are shown in Figure 37 and Figure 38 respectively.

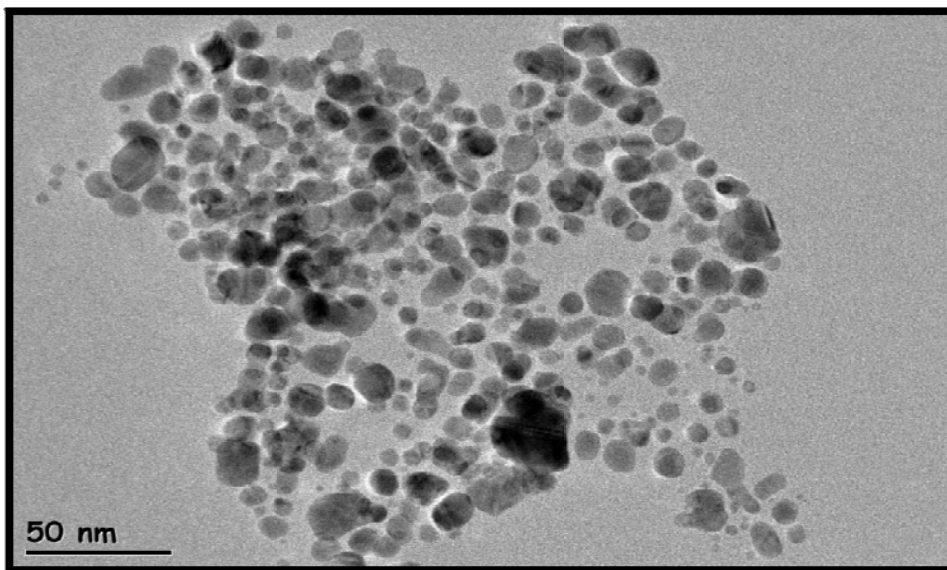


Figure 37: TEM image of Sample G

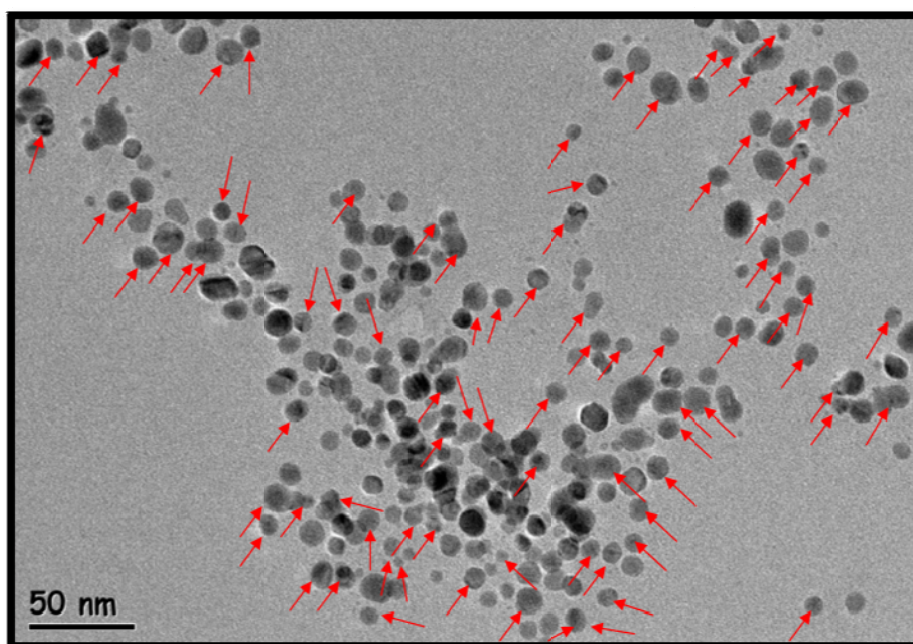
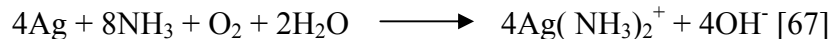


Figure 38: TEM image of sample H.

As expected from their dispersion properties in water, in both case the silver nanoparticles were embedded in silica. However, as can be seen from Figure 37, for sample G, the size and shape of the particles were changed during

coating. Silver nanoparticles were not in the center of these nanostructures and in some places silver particles were accumulated more than the others. In case of sample H (Figure 38) on the other hand, some of these silica particles were formed around silver nanoparticles as desired, although the size of the particles were not uniform, the shapes were not disturbed very much. There were still empty silica shells, agglomerates and accumulation of silver nanoparticles in some areas.

In literature, it was noted that ammonia usage resulted in successful silica coating of gold nanoparticles, however this case is different for silica coating around silver nanoparticles [67]. When the reaction proceeded longer in ammonia solution, silver nanoparticles would be oxidized due to reaction between hydroxide ion. This event results in the formation of AgOH, which easily react with ammonium ions to form $\text{Ag}(\text{NH}_3)_2^+$ complex ions. Oxidation reaction of small silver nanoparticles in ammonia solution is shown as following reaction:



Ying et al was reported the limitation for the silica coating of silver nanoparticles arising from easy oxidizing ability of these nanostructures via reverse microemulsion method. They mentioned that successful silica coating was achieved, but they also reported to short-term stability of silver nanoparticles in ammonia solution [68]. The silver core as they mentioned was 12 nm in size.

Therefore we concluded that the disturbed monodispersity and presence of empty shells according to TEM images might be the related with the deterioration of stability of silver nanoparticles when ammonia solution used as a catalyst and decided to change the catalyst.

Since the coating process was taken place in organic solvent, 1,8-Diazabicycloundec-7-ene (DBU), an organic base was used instead of

ammonia solution. The same experiments were repeated with various concentrations of the new catalyst, DBU, Table 4. As mentioned before, color matching was the first criteria for the success of the coating process. The color of the solutions, having various amount of DBU, were compared with the color of reference solution, Figure 39.

Table 4: Concentration of DBU used throughout reverse microemulsion method.

Samples	S1	S2	S3	S4
Ag NP's	500 μ l	500 μ l	500 μ l	500 μ l
Igepal	1000 μ l	1000 μ l	1000 μ l	1000 μ l
DBU	4 μ l	8 μ l	20 μ L	25 μ l
TEOS	35 μ l	35 μ l	35 μ l	35 μ l
Water	100 μ l	100 μ l	100 μ l	100 μ l

For samples S₁, S₃ and S₄, coating process were resulted in the precipitation of nanoparticles in water, whereas dispersed nanoparticles in water was achieved for sample S₂, in which 8 μ l of catalyst DBU was used, Figure 39. At higher or lower concentration of the catalyst, agglomeration of nanoparticles was observed. However precipitation was taken place at longer time when 4 μ l DBU was used.



Figure 39: Silver nanoparticles following silica coating process of S1,S2, ref., S3 and S4.

TEM image of sample S₁ is shown in Figure 40 . This image had been taken before precipitation of the particles.

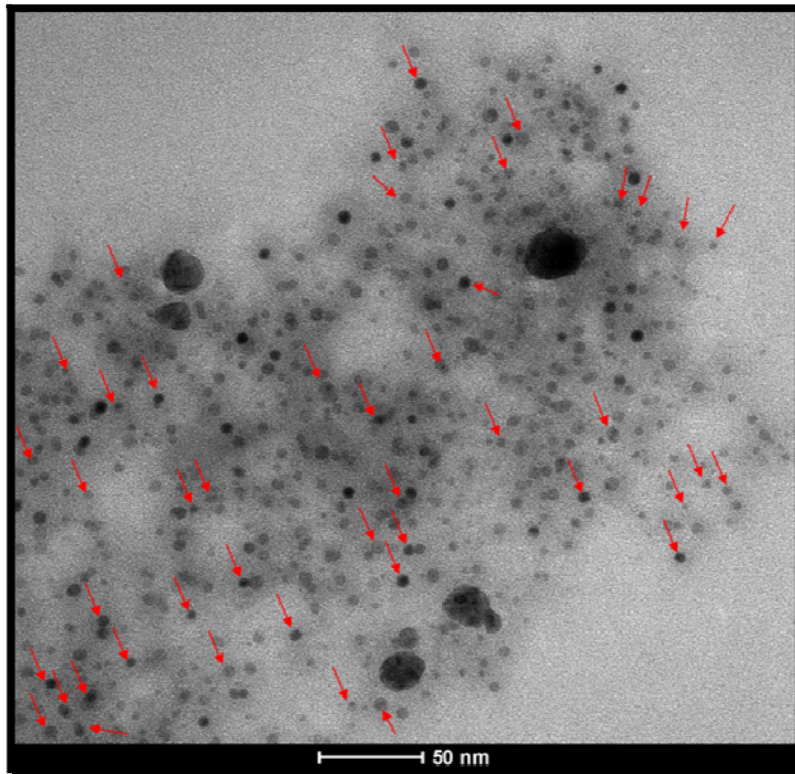


Figure 40: TEM image of silica coating using low amount of catalyst, DBU (Sample S1)

It is difficult to identify the particles in Figure 40. It seems that silica coating around silver particles was achieved (as indicated by small arrow), but all these coated and uncoated silver particles were buried under a silica cloud which was probably causing their precipitation. TEM image of sample S₂ is depicted in Figure 41.

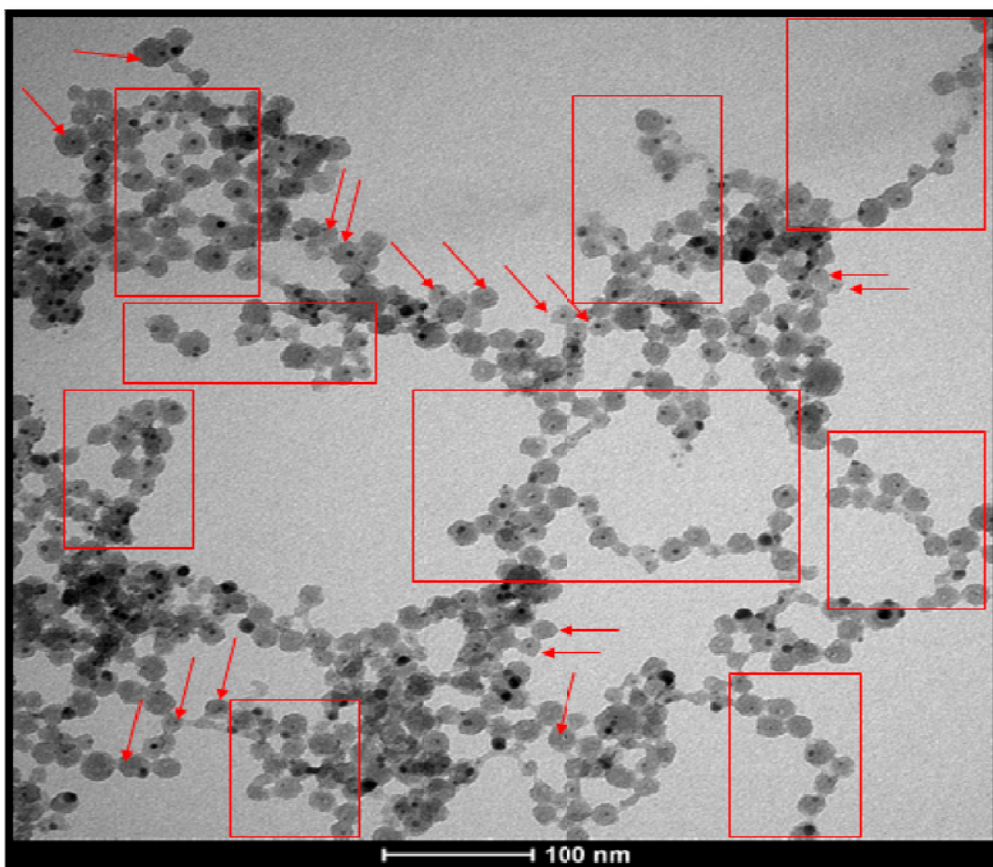


Figure 41: The whole TEM micrograph of silica coated silver nanoparticles prepared in this study (Sample S2)

The TEM image of silica coated silver nanoparticles via reverse microemulsion method (Sample 2) can be seen in Figure 41. TEM image exhibits that most of silver nanoparticles encapsulated by silica layer. The regions corresponding to a proper coating were taken in rectangles.

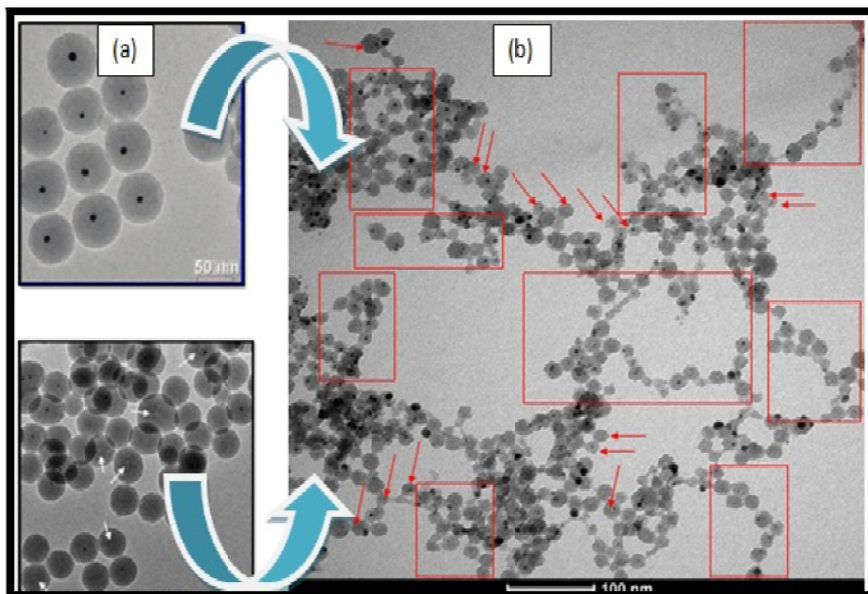


Figure 42: Comparison of TEM micrograph of silica coated silver nanoparticles prepared (a) by Ying et al and (b) in our laboratory

It is difficult to compare our result with the ones given in the literature. Because, the micrographs are not representing the whole image. For example Figure 42-a is representing silica coated silver nanoparticles via reverse microemulsion method. As can be seen, in most parts, particles are overlapping with each other and their sizes show variation. Whereas in literature only a small part of the same or similar micrographs are shown. Therefore TEM images of silica coated silver nanoparticles in this study indicated by arrows and by rectangles, were resembling the silica coated nanoparticles synthesized by Ying et al as seen in Figure 42-b.

Silver nanoparticles synthesized in this study were 4 ± 0.6 nm diameter in size, that is, they were much more smaller than the silver core synthesized by Ying et al, and it was observed that DBU was good candidate as a base catalyst for coating silica through microemulsion .

After addition of TEOS under base catalysis, nanoparticles could easily be dispersed in de-ionized water. This is one of the important evidences of

silica layer formation around silver nanoparticles. After silica coating, UV-vis absorption measurements showed strong peak around 412.5. Shift of absorption spectra (from 440 nm to 412.5 nm) observed was arising from the change in the solvent from organic to inorganic, as seen in Figure 43.

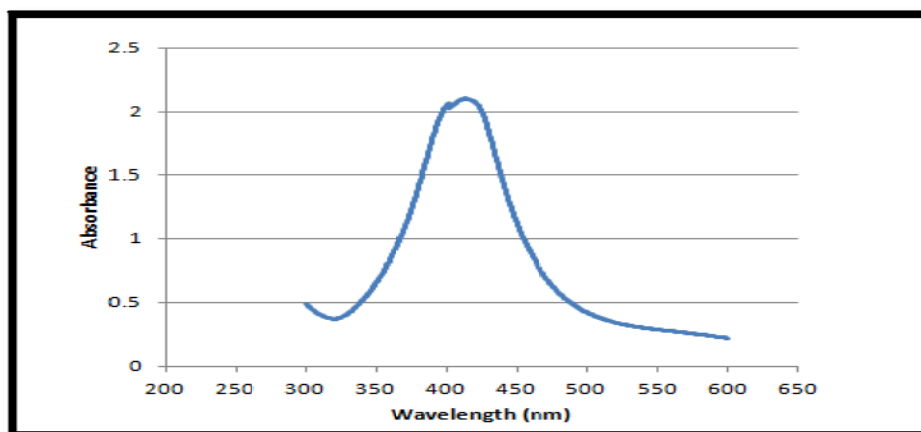


Figure 43: Absorption spectra of silica coated silver nanoparticles via reverse microemulsion method

3.4. Preparation of Silica Coated Silver Nanoparticles by Stöber Method

In literature, it was reported that Stöber method is the only proper method for coating of large nanoparticles with the size of nearly 50 nm in diameter [68]. However, in this study, in contrary to common belief, we observed that silica coating for small nanoparticles is also possible via Stöber method.

For silica coating by Stöber method, silver nanoparticles synthesized by chemical reduction method were used as starting material.

In this study by changing base catalyst to dimethylamine rather than ammonia in a standard Stöber method, it was observed that successful silica coating of silver nanoparticles with TEOS precursor was possible. The

formation of high quality core-shell nanoparticles was illustrated by SEM as can be seen in Figure 44.

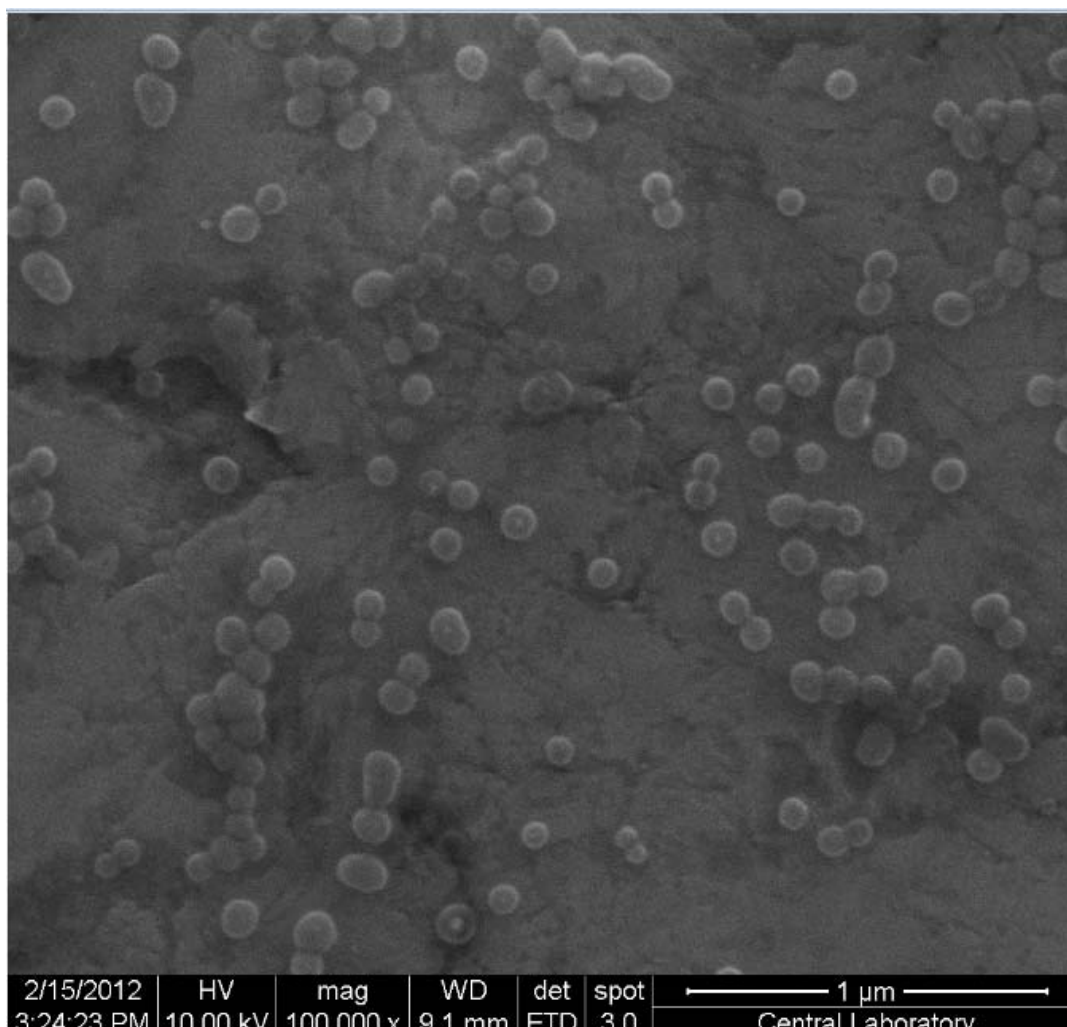


Figure 44: FE-SEM image of resulting silica coated silver nanoparticles by Stöber method

Brighter center part is corresponding to silver and pale part around the silver nanoparticles corresponding to silica layer. FE-SEM image showed a homogenous silica shell around the particles.

For silica coated silver nanoparticles by using Stöber method, a single plasmon band was measured at 414 nm. This red-shift with respect to the

uncoated nanoparticles ($\lambda_{\text{max}} = 400 \text{ nm}$) is due to the increase in local refractive index around nanoparticles and scattering from silica shells after silica coating. Figure 45 shows the red-shift of the localized surface plasmon absorption peak after silica coating.

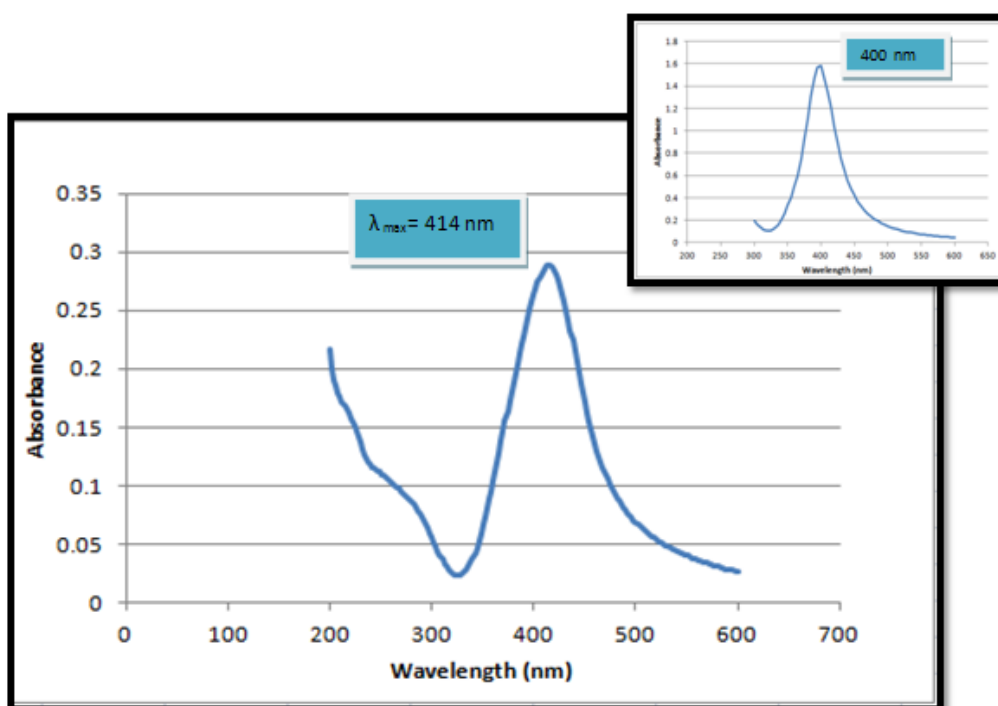


Figure 45: Absorption spectra of silica coated silver nanoparticles via Stöber method

3.5. Preparation of A Raman-Dye- Labeled Nanoparticle Probes

SERS-aided biodetection have come into prominence recently. Thanks to presence of Raman-active reporter molecules, several Raman nanotags can be designed in order to obtain sensitive detection of biological molecules. In this study, to prepare core-shell nanoparticles with an embedded Raman reporter molecule, silver nanoparticles synthesized by chemical reduction method was used as core, and Stöber method for silica coating was applied. Before silica coating, brilliant cresyl blue (BCB) was added to the reaction mixture, which provides embedding of raman reporter into silica shell. BCB

is a positively charged Raman-dye widely used for SERS measurements. BCB has characteristic peak at 580 cm^{-1} due to benzene ring deformation method (Figure 46)

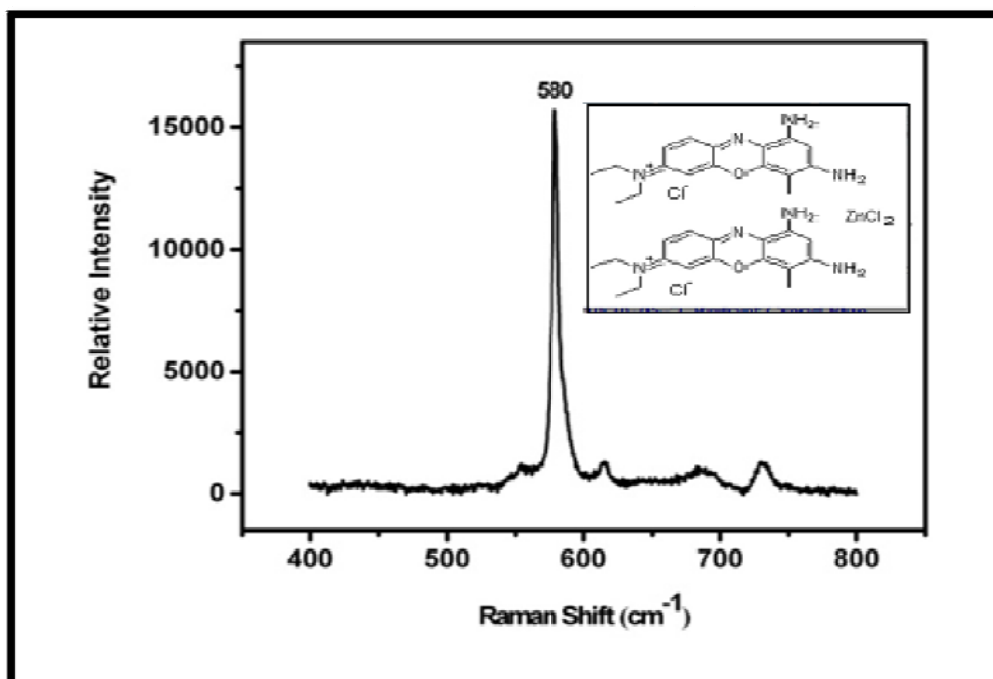


Figure 46: SERS spectrum and chemical structure of BCB

Silver nanoparticles synthesized by chemical reduction method has pH of 9.0. However, it must be considered that, due to positively charged Raman-dye usage, there could not be an electrostatically interaction between the dye and surface of nanoparticles. In the light of these considerations, pH of silver nanoparticles were adjusted to between the range of 6.0 to 7.5 with 0.01 M HCl acid solution slowly. At this point, it was observed that when pH decreases from 7.0 to 6.0, colour change occurred. Colour of silver nanoparticles changed from yellow to gray. This is mostly due to deterioration of silver nanoparticles at low pH, and starting to agglomerate. Figure 47 shows the colour change of nanoparticles when pH changed from 9.0 to 6.0 and in Table 5.

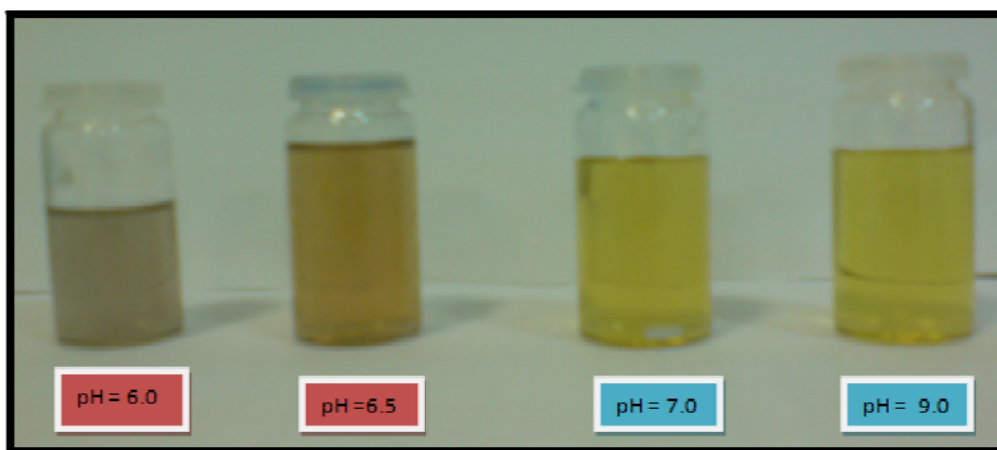


Figure 47: Colour change of silver nanoparticles when the pH changed from 6.0 to 9.0

Table 5: Effect of pH change onto colour of silver nanoparticles

The pH of silver nanoparticles	Colour of silver nanoparticles
pH = 6.0	Firstly, turning to violet and then grayish colour as time passes
pH = 6.5	Turning to violet sol.
pH = 7.0	Clear yellow sol
pH = 9.0	Clear yellow sol

This change was mostly arising from the change in zeta potential of silver nanoparticles which was derived from change in pH. Values of zeta potential exactly gives information about the presence of electric charge around the nanoparticles. For small particles, high negative or positive values of zeta potential provide stabilization of nanoparticles. On the other hand, nanoparticles with low zeta potentials tend to agglomerate. In literature, it is mentioned that to prevent agglomeration of small silver nanoparticles, when the values of zeta potential are fallen in negative sides, stability of nanoparticles increases directly. Table 6 shows the relation

between stability of nanoparticles corresponding to change in zeta potential values [69].

Table 6: Stability Behaviour of the colloid depending on zeta potential ranging from 0 to ± 61 [69]

Zeta Potential	Stability Behavior of The Colloid
From 0 to ± 5	Rapid Coagulation
From ± 10 to ± 30	Incipient instability
From ± 30 to ± 40	Moderate Stability
From ± 40 to ± 60	Good Stability
More than ± 61	Excellent Stability

Table 7: Zeta Potential measurements using silver nanoparticles at different pH ranges [70]

pH	Zeta Potential (mV)
5	-25.5 ± 0.38
7.4	-30.1 ± 0.41
9	-38.3 ± 0.33

For the preparation of SERS nano-tags, although at pH 9, nanoparticles show good stability, due to deterioration of dye at this pH, pH of the solution was set to 7.

Except pH of the solutions, also the concentration of Raman reporter molecule added was one of the crucial parameters. When, 10^{-3} M dye concentration was used, oxidation of silver nanoparticles was observed. This change was examined by the removal of surface plasmon absorption peak of nanoparticles measured with UV-vis spectrometer (in Figure 48), and by the absence of characteristic peak of BCB in SERS measurements (in Figure

49). In order to show effect of concentration of dye on the stability of silver nanoparticles, titration experiments were done with the addition of dye in seconds. Absorption spectra in figure exhibits the decrease in signal intensity.

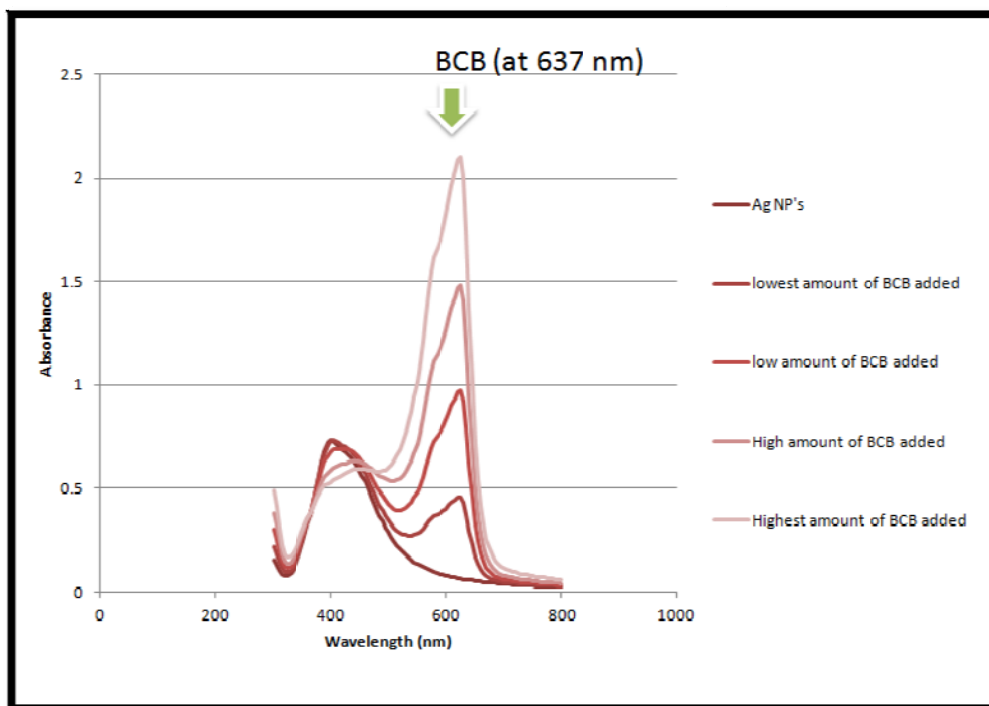


Figure 48: Decrease in signal intensity of silver nanoparticles after 30 minutes reaction period.

After 30 minutes, which is time necessary for the attachment of dye onto silver surface, nearly no absorption spectra was observed as seen in Figure 49 which is one of the clue for the oxidation of silver nanoparticles with high concentration of BCB.

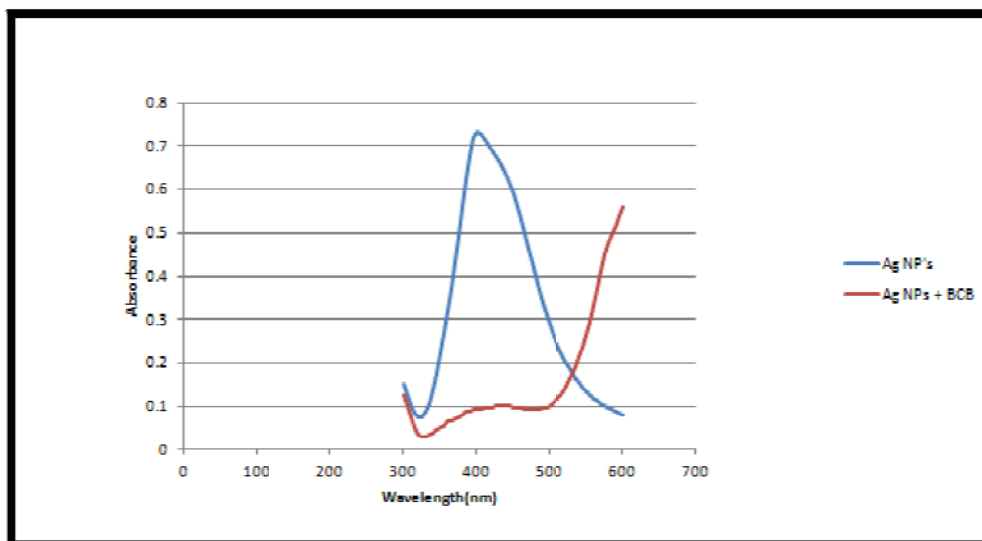


Figure 49: Decrease in signal intensity of silver nanoparticles after 30 minutes reaction period.

Absorption signal seen after 550 nm was arising from the absorption of dye around this range as seen in Figure 49. The drastic decline of the absorption peak was correlated with the convergence of silver nanoparticles to silver ions. During centrifuging steps, instead of 15000 rpm which was the highest rotating speed capacity of the instrument used, very little amount of the nanoparticles could be isolated in eppendorf tubes. Figure 50 shows SERS spectrum of these isolated particles solution. The weak signal obtained was shown that no dye attachment onto the surface of the particles was achieved, following the washing steps, free label was removed and no SERS spectra could be obtained.

These changes in Uv-vis absorption spectra and Raman spectra of SERS nano-tags were correlated to oxidation of silver nanoparticles by Raman dye at the concentration of 10^{-3} M .

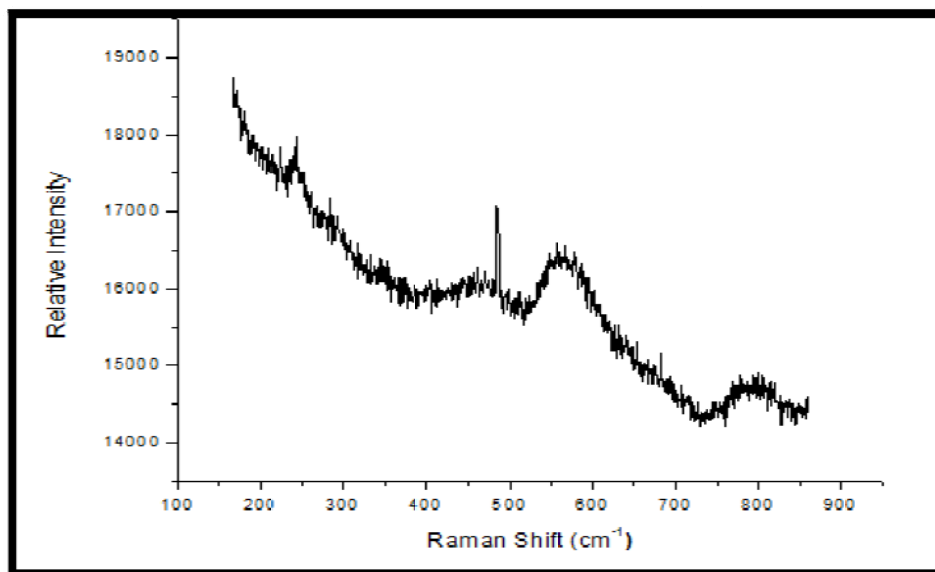


Figure 50: SERS spectrum of BCB adsorbed onto silver nanoparticles surface with high concentration (10^{-3} M)

The signal reproducibility of SERS nanotags were achieved by decreasing dye concentration to 10^{-4} M. The results showed that the Raman intensity of resulting SERS nano-tags, prepared by 10^{-4} M BCB was intense enough to make routine single nanotag detection in Figure 51 and SERS spectrum in Figure 52.

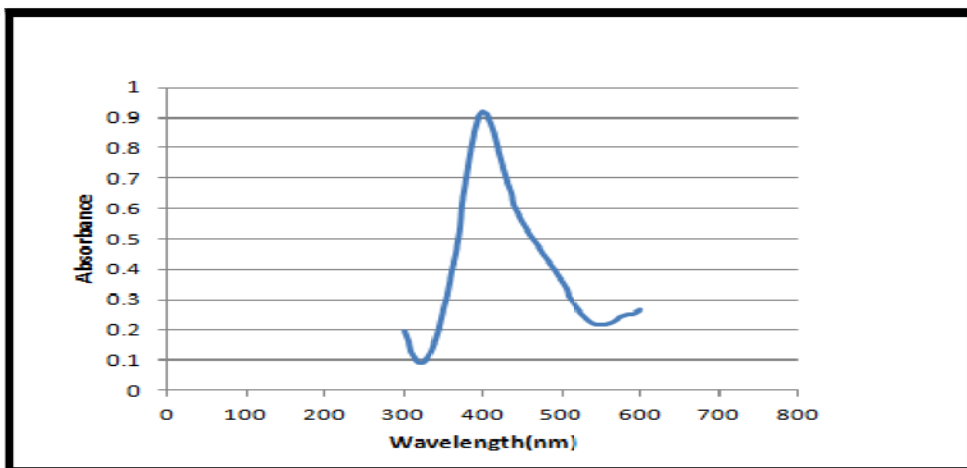


Figure 51: Absorption spectra of BCB adsorbed onto silver nanoparticles surface with low concentration (10^{-4} M)

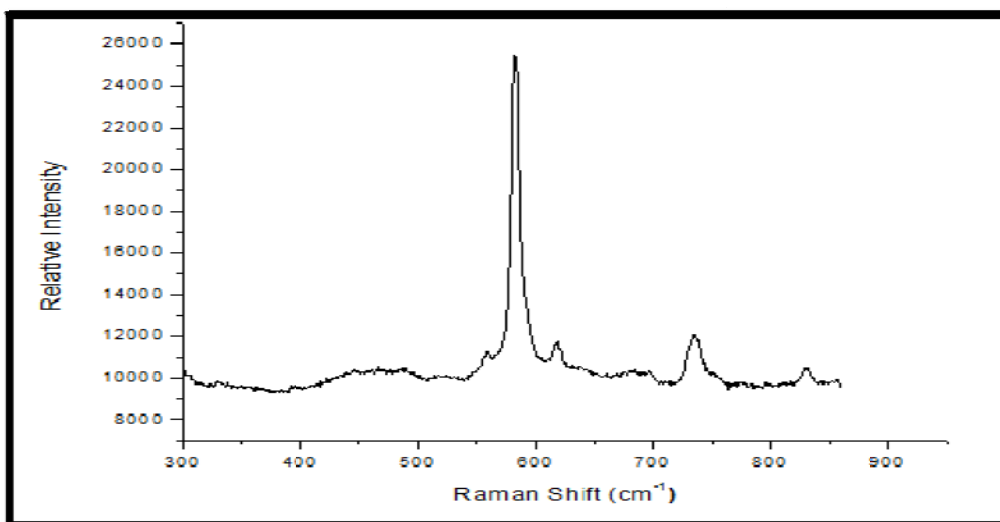


Figure 52: Raman spectra of SERS nanotags prepared using 10^{-4} M BCB

When 10^{-4} M BCB was used, SERS intensity was found nearly 15000 cm^{-1} .

The same titrations with BCB were also done with gold nanoparticles in order to understand whether or not there was deterioration in stability of nanoparticles arising from dye. Yet, Figure 53 shows that there was no

important decrease in absorption spectra when dye molecule was added to the gold colloid solution.

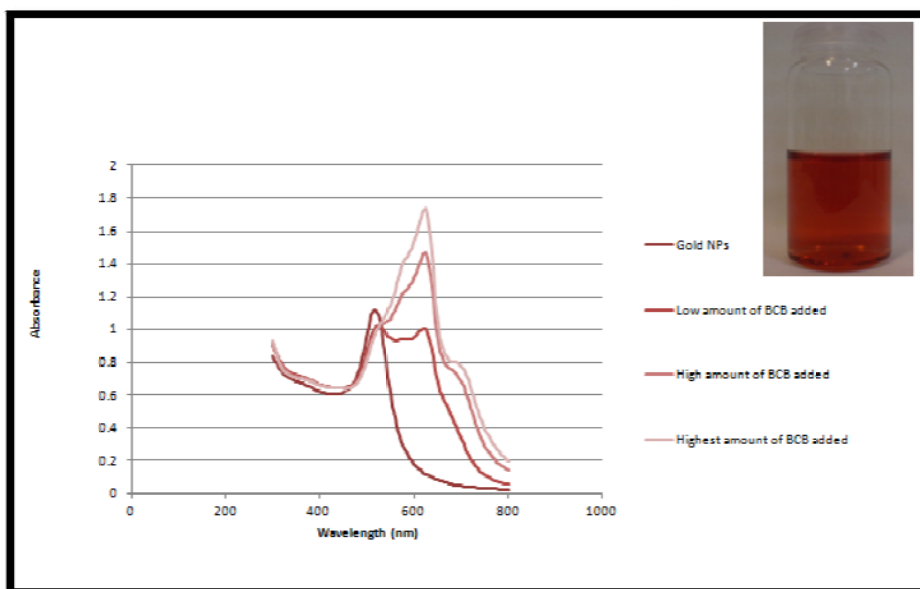


Figure 53 : Absorption spectrum of gold nanoparticles when different amount of BCB was added by titration.

This results obviously show the difficulties for the synthesis of SERS nano-tags when silver core was used instead of gold core. Besides SEM images, FT-IR spectrometer was also used for indication of silica coating on silver nanoparticles. FT-IR spectrum of silica coated silver nanoparticles was shown in Figure 54.

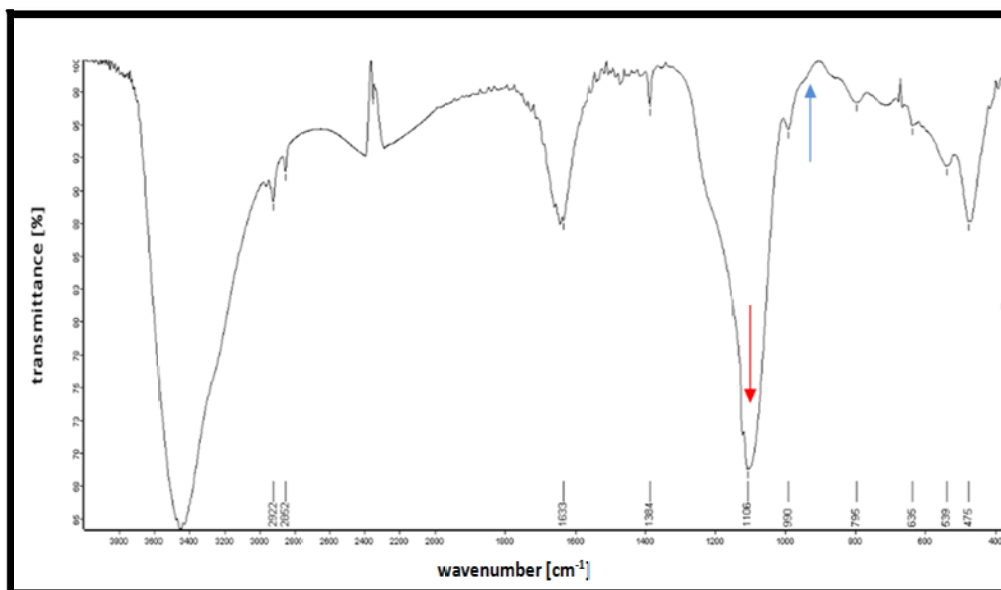


Figure 54: FT-IR spectrum of silica coated silver nanoparticles

As can be seen in the figure, asymmetric stretching of Si-O-Si vibrations was observed at 1079 cm^{-1} (shown with red arrow) and symmetric stretching was observed at 878 cm^{-1} (shown with blue arrow). This is another strong evidence for silica layer around the silver. As well as the presence of silica coating around silver nanoparticles, FT-IR spectrometer was also used to examine the presence of Raman dye BCB onto these particles.

FTIR spectrum of the BCB is shown in Figure 55. Absorption peak coming from N-H wagging was observed clearly near 670 cm^{-1} . Other bands are arising from C-C double bonds stretching in benzene ring appeared at about 1497 cm^{-1} and C-H stretching appears at 3144 cm^{-1} . Both bands are shown with green arrows.

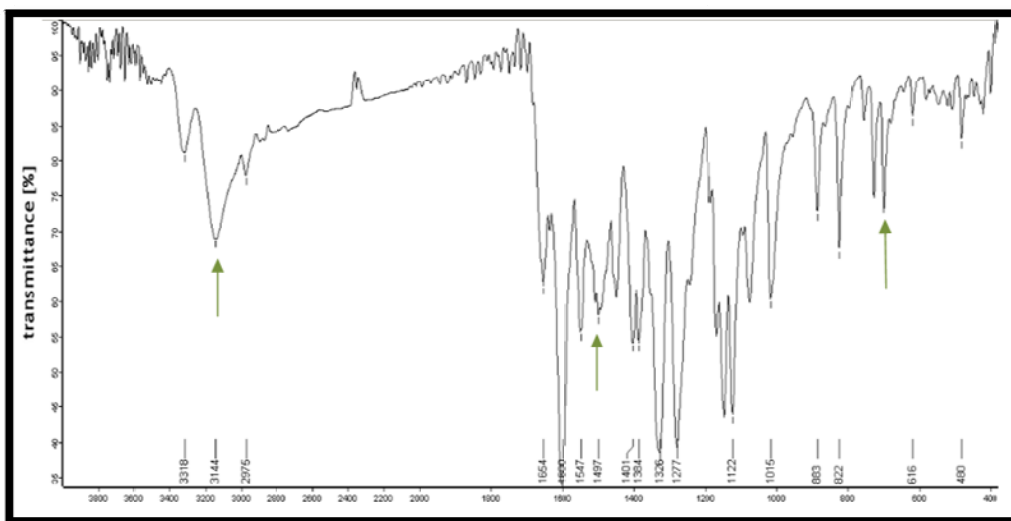


Figure 55: FT-IR spectrum of BCB.

FT-IR spectrum of SERS nano-tags were also taken, Figure 56. In order to investigate the attachment of dye onto silver surface before SERS measurements, FT-IR spectra of silica coated silver nanoparticles, BCB and SERS nano-tags were compared.

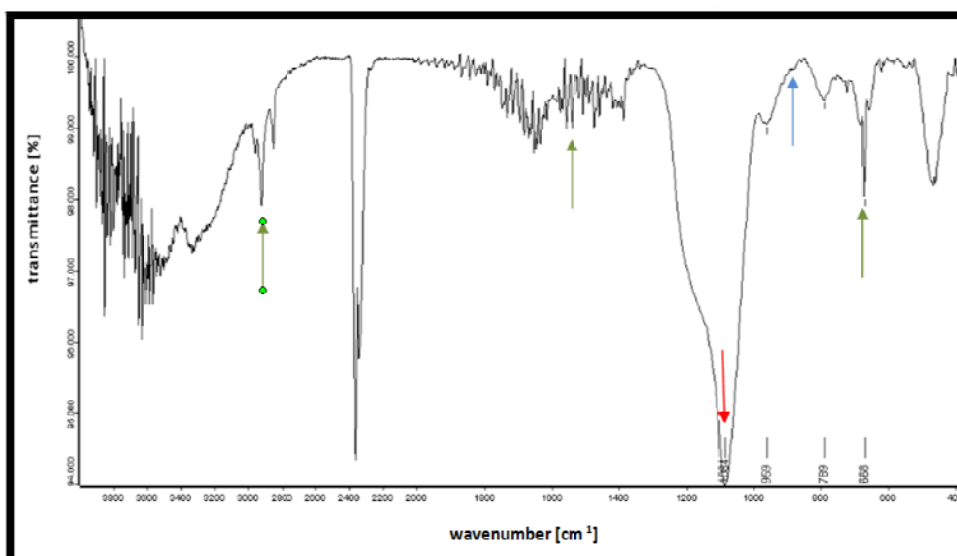


Figure 56: FT-IR spectrum of SERS nano-tags

FT-IR spectrum of SERS nano-tags was the combination of spectra of silica coated silver nanoparticles and BCB. As can be seen in the Figure 56, asymmetric stretching of Si-O-Si vibrations was observed at 1083 cm^{-1} (shown with red arrow) and symmetric stretching was observed at 884 cm^{-1} (shown with blue arrow). Absorption peak coming from N-H wagging was observed clearly at 654 cm^{-1} . Other bands are arising from C-C double bonds stretching in benzene ring appeared at about 1500 cm^{-1} and C-H stretching appears at 2920 cm^{-1} . The presence of absorption bands of BCB in FT-IR spectrum shows the achievement of the SERS nano-tag formation.

3.6. Preparation of SerGEN Probe

In this study, SERGen probes were prepared by noncovalent binding with raman reporter molecule, brilliant cresyl blue (BCB) and with SERS nano-tags, by covalent and noncovalent binding. BCB is a quinone-imide type dye and positively charged in neutral solutions as seen in Figure 57.

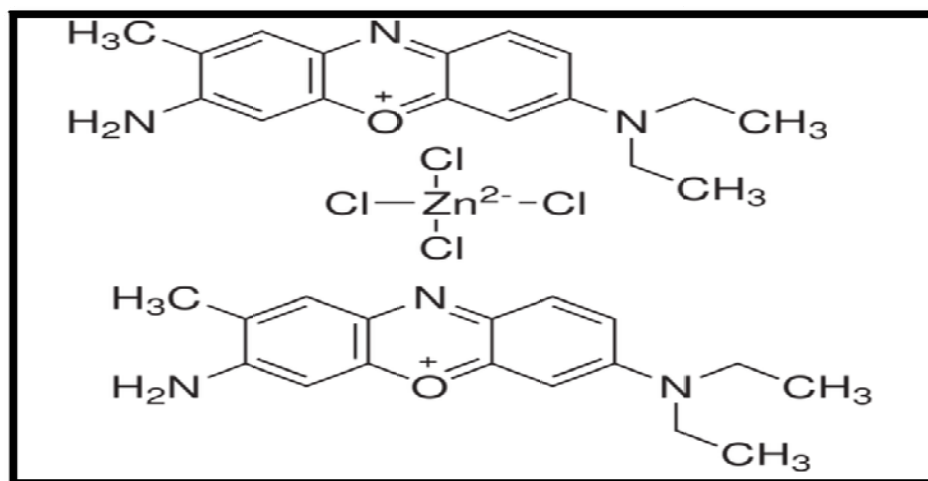


Figure 57: Chemical structure of BCB [70]

The phosphate groups in the DNA backbone have negatively-charged oxygen atoms giving DNA molecule an overall negative charge, and

positively charge BCB Raman dye provides electrostatic attachment easily. For this, labeling was done electrostatically. Electrostatic attachment of Raman dye to the oligonucleotide was achieved as described in section 2.3.6.1.

Preparation of SERGen probes can also be done by covalent labelling of oligonucleotide primers to Raman dye. However, noncovalent labelling is advantageous of being easier, less time consuming and less expensive chemicals needed. For this reasons, noncovalent labelling (also name as electrostatic attachment) was decided to use in the preparation of SERGen probes.

3.7. Immobilization of SERGen Probes onto Gold Surface Under Hybridization Conditions

Thiols are frequently used with noble metal substrates due to strong affinity of sulfur for these metals. Using this information, formation of covalent bonds between the sulfur and gold atoms was applied for the attachment of thiolated oligonucleotides onto gold surface.

In this study, gold substrate was used where hybridization experiments were done. To attach the oligonucleotides onto the gold substrate, 5'-end of thiol modified gene sequence was used as complementary target.

In the presence of oxygen, the formation of disulfide bonds result in not to be tied of oligonucleotides onto gold substrate. The possible formation of disulfide bonds between thiolated oligonucleotides were prevented by using a reducing agent as shown in Figure 58 [71]. In this case it was dithiothreitol (DTT).

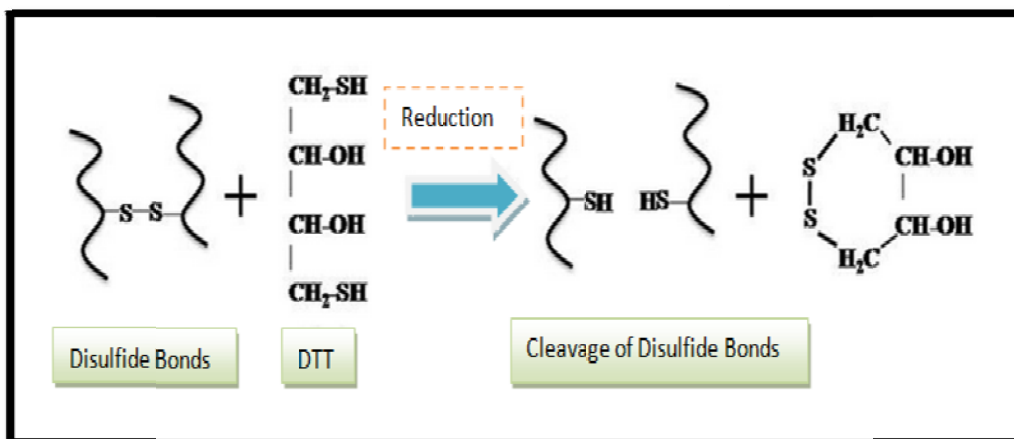


Figure 58: Schematic representation of rupture of disulfide bonds by using DTT

Apart from disulfide bonds, oligonucleotides have several other functional groups, such as amines and carbonyls and negatively charged phosphate backbone. These parts of oligonucleotides have also interaction between gold substrate. These secondary interactions should be prevented in order to achieve hybridization experiments. Various spacers can be used, but in this study we preferred using 11-mercapto-1-undecanol for this function. Figure 59 shows the possible bindings of oligonucleotides onto gold substrate when no spacer is used for hybridization experiments [71].

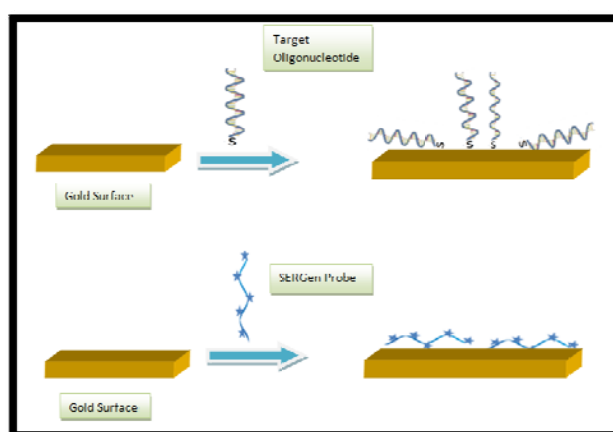


Figure 59: Possible interactions between oligonucleotides and gold surface without spacer

Removal of the spacer in hybridization experiments causes in the convergence of DNA strands to the gold surface and to each other. This event results in the prevention of the binding capability of target oligonucleotide to SERGen probe, thus no hybridization of two oligonucleotides occur.

In this study, the base sequence of oligonucleotides used as target DNA was 5'- SH- TTTTTTTTTT GCA GTG GAT TCT CGG GCC as target gene sequence and the base sequence of nucleic acid probe was 5'- GGC CCG AGA ATC CAC. As can be seen, target and probe sequences are not in the same length. The importance of being long chain of target DNA compared to probe sequence is to decrease steric hindrance of arising from the interaction between SERGen probe and gold surface.

In literature, it was also mentioned that the short sequences of DNA targets which have mainly between 12-40 mer provide hybridization between DNA probes easily [72]. At this point, immobilization of target oligonucleotides onto substrate plays important role to increase sensitivity and selectivity. For this, immobilized biomolecules should maintain stability to minimize nonspecific adsorption and finally nonspecific bindings.

Before recording SERS measurements, silver nanoparticles were added onto gold substrate, and left to dry. It was observed that gold surface, by itself is not enough to generate electromagnetic enhancement. Apart from gold surface, silver colloids should be added onto the surface in order to increase signal intensity. According to SERS spectra as seen in Figure 60, it was concluded that hybridization of thiolated DNA targets and SERGen probes on the gold surface was achieved.

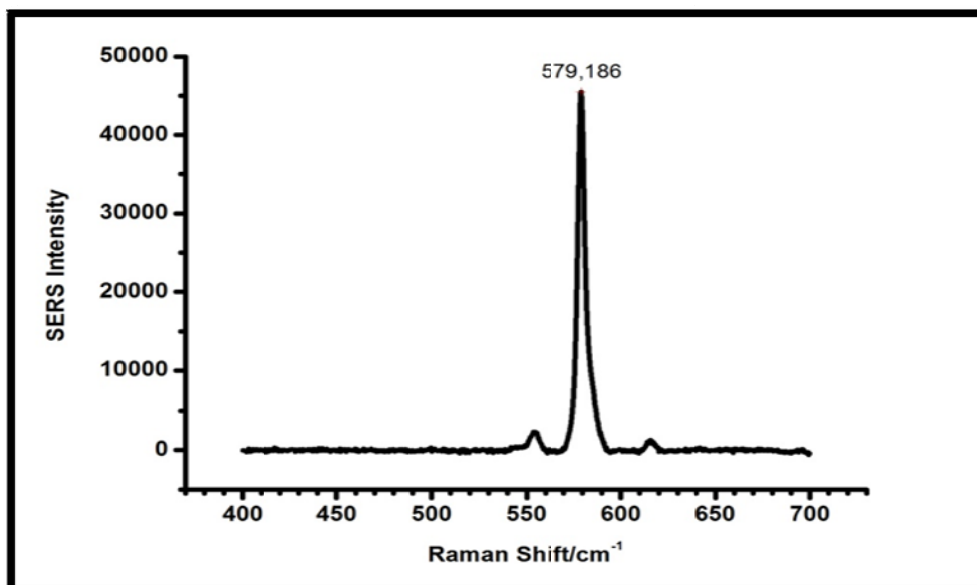


Figure 60: SERS spectra of BCB-labeled DNA after hybridization onto gold surface with silver colloid.

The intense peak at 580 cm^{-1} was totally corresponding to characteristic peak of BCB. All these results show that SERGen probes prepared are appropriate for biological studies, and also the hybridization system with the helping of SERS which has been developed is proper in order to use for clinical samples.

At this point, after the preparation of SERGen probes by noncovalent binding with BCB, SERS nano-tags were tried, as labelling and DNA hybridization experiments were done. With this aim, noncovalent and covalent attachment of SERS nanotags to the probe DNA were performed as seen in Figure 61. After immobilization of target DNA onto gold substrate was achieved, hybridization conditions were supplied to obtain SERS signal. With this aim, SERS nano-tags were functionalized with amine groups using (3-Aminopropyl)triethoxysilane, APTES. Noncovalent attachment of SERS nanotags to the probe DNA includes electrostatic interaction between positively charged amine groups on SERS nanotags and negatively charged DNA molecule. On the other hand, covalent attachment

of SERS nanotags to the probe oligonucleotide was tried by converting 5' phosphate group of oligonucleotide to primary amine containing molecules with the help of EDC and imidazole. By adding directly SERS nano-tags to the probe DNA instead of BCB, we are planning to take advantages of SERS nano-tags including attachment of certain concentration of BCB instead of single dye molecule, less photobleaching of dye molecule due to silica layer, and increase in SERS signal by itself.

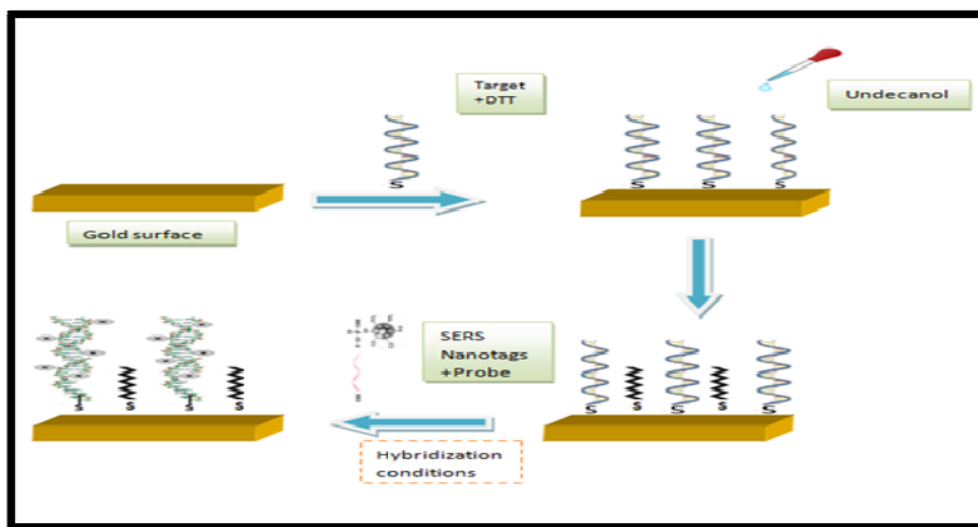


Figure 61: Future Work

However, the results were not as good as we wanted. After washing steps, intensity of SERS signal decreased largely. Figure 62 shows the important decrease in signal intensity. Before amine modification, intensity was around 25000 cm^{-1} . However, after amine modification, signal intensity decreased 500 cm^{-1} . It should be noted that this intensity is not enough for further experiments of DNA hybridization experiments yet.

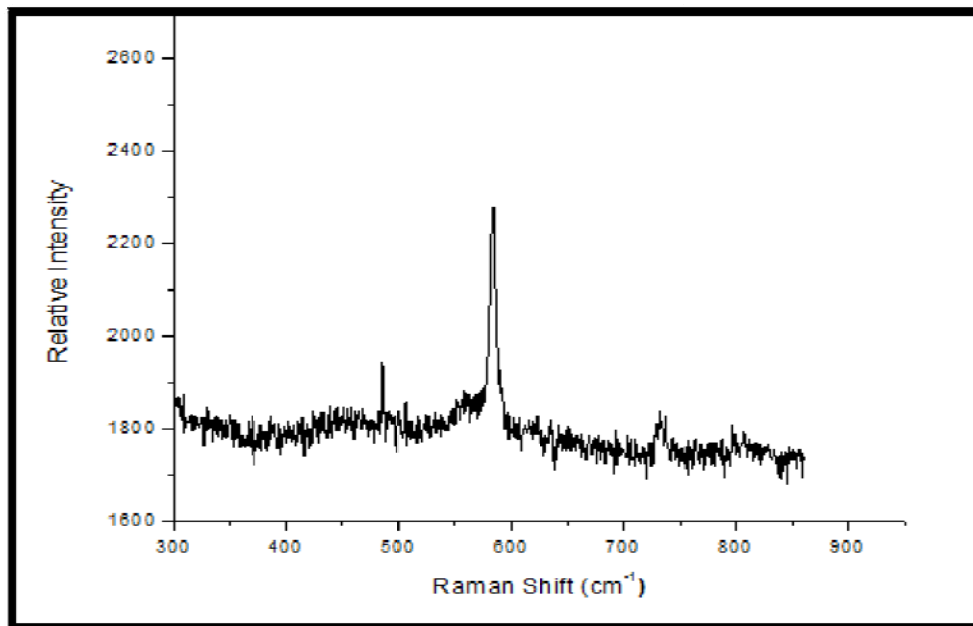


Figure 62: SERS spectra of nano-tags after functionalized with amine groups.

To increase signal intensity, other optimizations will be tried. With this aim, the amount of TEOS will be decreased and finally silica coating and amine modification of SERS nano-tags will be achieved by increasing the amount of APTES which both consists of silica and amine groups in it, and washing steps will be carefully examined. We are in doubt about infiltration of dye during washing steps.

Due to sharp decrease in SERS signal, after amine functionalization, electrostatic and covalent attachment of SERS nanotags to the probe DNA could not be achieved. Characteristic peak of BCB at 580 cm^{-1} could not be observed. Figure 63 and 64 show SERS spectrum of electrostatic and covalent attachment of SERS nanotags to the probe DNA respectively.

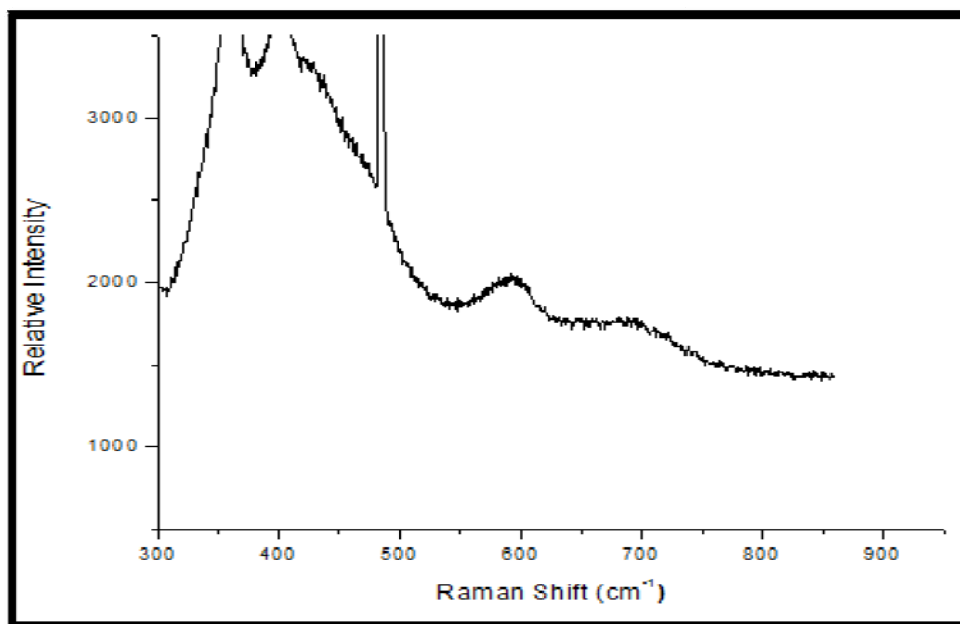


Figure 63: SERS spectra of electrostatic attachment of SERS nanotags to the probe DNA.

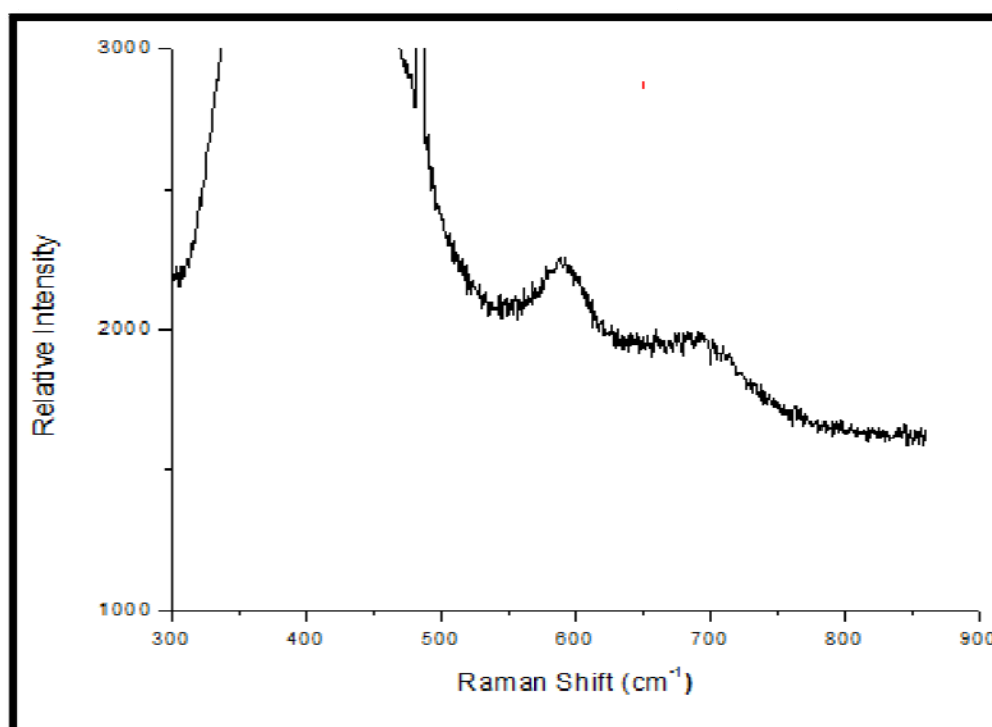


Figure 64: SERS spectra of covalent attachment of SERS nanotags to the probe DNA

CHAPTER 4

CONCLUSION

In this study, SERS nanotags were designed in order to obtain strong Raman signal and to prevent photobleaching of dye by coating with silica layer while detecting biological molecules. SERS nano-tags consist of Raman-active molecule and Raman signal enhancer core encapsulated by protective shell against environmental factor. Silica layer, except protecting ability, also provides surface modification of SERS tags for further experiments. SERS nano-tags that have been developed in this study will be used in order to make multiplex detection of DNA. In the preparation of SERS nano-tags, positively charged brilliant cresyl blue (BCB) was used as Raman reporter molecule. For the attachment of dye onto the silver surface, several parameters were changed, and characterizations were made systematically.

To synthesize silver core, mainly two methods, thermal decomposition and chemical reduction method were used. Silver nanoparticles synthesized by thermal decomposition method, then were coated with silica layer by reverse microemulsion method. On the other hand, silver nanoparticles synthesized by chemical reduction method, were coated with modified Stöber method.

In reverse microemulsion method, a new organic base DBU was proposed as catalyst instead of ammonia solution to remove problems arising from short-term stability of nanoparticles in ammonia solution, and it was observed that preliminary results obtained were comparable with literature values.

In this study, in contrary to common belief, we also observed that silica coating for small nanoparticles at the size of 10 nm is also proper via Stöber method.

Prepared SERS nano-tags have high signal intensity. However, an important decrease in SERS signal was observed after amine group modification onto silica shell. With further studies, we will try to prevent this decrease in the signal.

In this study, we also performed hybridization experiments with DNA. With this aim, immobilization of SERGen probes onto gold platform was achieved. Proper results were obtained in hybridization experiments carried out with SERGen probes prepared with BCB dye. Strong signal of BCB showed the proper attachment of dye onto the oligonucleotide, and success hybridization experiments were done with dye molecule.

Hybridization experiments were also carried out with SERGen probes prepared with SERS nano-tags for labelling by covalent and noncovalent binding. However, after amine functionalization step, large decline in SERS intensity directed us to make further optimizations to increase intensity.

REFERENCES

- [1] Varadan K. V., Chen L., Xie J. (2008). Nanomedicine: Design and Applications of Magnetic Nanomaterials, Nanosensors and Nanosystems
- [2] Gazit, E., (2007). Self-assembled peptide nanostructures: the design of molecular building blocks and their technological utilization. *J. Am. Chem. Soc.* , 36, 1263-1269.
- [3] Stryer L. (1995). *Biochemistry*. Newyork: Freeman
- [4] Fritz, J., Baller K. M., Lang H. P., Rothuizen H., Vettiger P. , Meyer G., Guntherodt H. J., Gerber C., Gimzewski K.J., Translating Biomolecular Recognition into Nanomechanics
- [5]Gault, A. V., Mc Clenaghan, (2009). Understanding Bioanalytical Chemistry, Principles and Applications, UK : John Wiley & Sons.
- [6] Lyon, L. A., Musick D. M., Natan J. M., (1998). Colloidal Au-Enhanced Surface Plasmon Resonance Immunosensing. *J. Am. Chem. Soc.*, 70, 5177-5183.
- [7] Goldman, R. E., Balighian D. E., Mattoussi H., Kuno K. M., Mauro M. J., Tran T. P., Anderson P. G., (2002). Avidin: A Natural Bridge for Quantum Dot-Antibody Conjugates. *J. Am. Chem. Soc.*, 124, 6378-6382.
- [8] Hirsch, R. L., Jackson B. J., Lee A., Halas N., J. ,(2003). A Whole Blood Immunoassay Using Gold Nanoshells., *J. Am. Chem. Soc.*, 75, 2377-2381.

- [9] Ni J. , Lipert J. R., Dawson B. G., Porter D. M. (1999). Immunoassay Readout Method Using Extrinsic Raman Labels Adsorbed on Immunogold Colloids. *J. Anal. Chem.*, 71, 4903-4908.
- [10] Mulvaney P. (1996). Surface Plasmon Spectroscopy of nanosized metal particles. *Langmuir*, 12, 788-800
- [11] Silver Nanoparticles: Physical Properties. Retrieved September 12, 2012, from <http://www.nanocomposix.com/kb/silver/physical-properties>
- [12] Mirkin A. Chad, Letsinger L. R., Music C. R., Storhoff J. J. (1996). A DNA-based method for rationally assembling nanoparticles into macroscopic materials. *Nature*, 382, 607-609
- [13] Schultz A.D. (2003). Plasmon resonant particles for biological detection. *Current Opinion in Biotechnology*, 14, 13-22.
- [14] Chan W. C. W., Nie S., (1998). Quantum Dot Bioconjugates for Ultrasensitive Nonisotopic Detection. *Science*, 281, 2016-2018
- [15] Wolcott A., Gerion D. , Visconte M., Sun J., Schwartzberg A., Chen S., Zhang Z. J. (2006). Silica-Coated CdTe Quantum Dots Functionalized with Thiols for Bioconjugation to IgG Proteins. *J. Phys. Chem. B*, 110, 5779-5789.
- [16] Bruchez M. , Moronne M. Gin P., Shimon W., Alivisatos P. A. (1998). Semiconductor Nanocrystals as Fluorescent Biological Labels. *Science*, 281, 2013-2015.
- [17] Schaefer E. H. (2010). *Nanoscience: The Science of the Small in Physics, Engineering, Chemistry, Biology and Medicine*, Springer.

- [18] Hale G.,D., Jackson J. B., Shmakova E.O., Lee R. T., Halas J. N. (2001). Enhancing the active lifetime of luminescent semiconducting polymers via doping with metal nanoshells. *Appl. Phys. Lett.*, 78, 1502.
- [19] Oldenburg J. S., Westcott L. S., Averitt R. D., Halas J. N. (1999). Surface enhanced Raman scattering in the near infrared using metal nanoshell substrates. *J. Chem. Phys.* , 111, 4729.
- [20] Hirsch L.R., Stafford R.J., Bankson A. J., Sershen R. S., Rivera B., Price E. R., Hazle D. J., Halas J.N., West L. J. (2003). Nanoshell-mediated near-infrared thermal therapy of tumors under magnetic resonance guidance. *PNAS*, 100, 13549-13554.
- [21] Sershen R. S., Westcott L. S., Halas J. N., West L. J. (2000). Temperature -sensitive polymer-nanoshell composites for photothermally modulated drug delivery.
- [22] Cao C. Y. , Jin R., Mirkin A. C. (2002). Nanoparticles with Raman Spectroscopic Fingerprints for DNA and RNA Detection. *Science*, 297, 1536- 1539.
- [23] Liu X., Knauer M., Ivleva P. N., Niessner R. , Haisch C. (2010). Synthesis of Core-Shell Surface Enhanced Raman Tags for Bioimaging. *J. Anal.Chem.* , 82, 441-446.
- [24] Ferraro R. J., Nakamoto K., Brown W. C (2003). *Introductory Raman Spectroscopy*, 2 nd Ed., Elsevier Science (USA)
- [25] Lewis R. I., Edwards M. G. H. (2001) Handbook of Raman Spectroscopy. USA: Taylor & Francis Group, LLC.
- [26] Haynes L. C., Yonzon R. C., Zhang X., Duyne V. P.R., (2005). Surface-Enhanced Raman Sensors: early history and the development of

sensors for quantitative biowarfare agent and glucose detection. *J. Raman Spectrosc.*, 36, 471-484.

[27] Fleischmann M., Hendra J. P., McQuillan J. A., (1974). Raman spectra of pyridine adsorbed at a silver electrode. *Chem Phys. Lett.*, 26, 2, 163- 166.

[28] Chen K., Leona M., Vo-Dinh T., (2007). Surface-enhanced Raman scattering for identification of organic pigments and dyes in works of art and cultural heritage material, *Sensor Review*, 27, 109-120

[29] Kerker M., (1967). The scattering of light and other electromagnetic radiation :London (UK), Academic Press.

[30] Kneipp K., Moskovits M., Kneipp H . (2006). Surface-Enhanced Raman Scattering; Physics and Applications. Germany: Springer.

[31] Siemes C., Bruckbauer A., Goussev A., Otto A., Sinther M., Pucci A. (2001). SERS-active sites on various copper substrates. *J. Raman Spectrosc.*, 32, 231- 239.

[32] Graff M., Bukowska J., Zawada K. (2004). Surface Enhanced Raman Scattering (SERS) of 1-hydroxybenzotriazole Adsorbed on a Copper Electrode Surface. *J. Electroanal. Chem.*, 567, 297-303.

[33] Sabatte G. , Keir R., Lawlor M., Black M., Graham D. , Smith W. Even (2008). Comparison of Surface-Enhanced Resonance Raman Scattering and Fluorescence for Detection of a Labeled Antibody., *J. Anal. Chem.*, 80, 2351, 2356.

[34] Brown O. L., Doorn K. S., (2008). Optimization of the Preparation of Glass-Coated, Dye-Tagged Metal Nanoparticles as SERS Substrates. *Langmuir*, 24, 2178, 2185.

- [35] Ru L. E., Etchegoin P., (2009). Principles of Surface Enhanced Raman Spectroscopy and Related Plasmonic Effects, Elsevier, Amsterdam, The Netherlands.
- [36] Kneipp K., Kneipp H., Itzkan I., Dasari R. R., Feld S. M. (2002). Surface-Enhanced Raman Scattering and Biophysics. *J. Phys.: Condens Matter*, 14, 597-624.
- [37] Han X.X., Zhao B., Ozaki Y. (2009). Surface-Enhanced Raman Scattering for Protein Detection. *J. Anal Bioanal Chem.*, 394, 1719-1727.
- [38] Kneipp K., Kneipp H., (2006). Single Molecule Raman Scattering. *J. Appl. Spect.*, 60, 322A-334 A.
- [39] Peltier K. E., Haynes L. C., Glucksberg R. M., Duyne V. P. R. (2003). Toward a Glucose Biosensor Based on Surface-Enhanced Raman Scattering. *J. Am. Chem. Soc.*, 125, 588- 593.
- [40] Sassolas A., Leca-Bouvier D. B., Blum J. L., (2008). DNA Biosensors and Microarrays. *Chem. Rev.*, 108, 109-139.
- [41] Salata O., (2004). Application of Nanoparticles in Biology and Medicine. *J. Nanobiotech.* 2,3.
- [42] Lewis L. N.,(1993). Chemical Catalysis by Colloids and Clusters. *J. Chem Rev.*, 93, 2693-2730.
- [43] Lee J. H., Jeong H. S. (2005). Bacteriostasis and Skin Innoxiousness of Nanosize Silver Colloids on Textile Fabrics. *J. Textile Res.*, 75, 551-556.
- [44] Niemeyer M. C., (2001). Nanopartifcles, Proteins, and Nucleic Acids: Biotechnology Meets Materials Science. *J. Angew. Chem.* 40, 4128-4158.

- [45] Solov'ev Y. A., Potekhina S. T., Chernova A. I., Basin B. Ya. (2007). Track Membrane with Immobilized Colloid Silver Particles. *J. Appl. Chem.*, 80, 438-442.
- [46] Li Y., Wu Y., Ong B. S. (2004). Facile Synthesis of Silver Nanoparticles Useful for Fabrication of High-Conductivity Elements for Printed Electronics. *J. Am. Chem. Soc.*, 127, 3266, 3267.
- [47] Murphy J. C., Sau K. T., Gole M. A., Orendorff J. C., Gao J., Gou Linfeng, Hunyadi E. S., Li Tan (2005). Anisotropic Metal Nanoparticles: Synthesis, Assembly, and Optical Applications. *J. Phys. Chem. B.*, 109, 13857-13870.
- [48] Bönnemann H., Richards M. R. (2001). Nanoscopic Metal Particles- Synthetic Methods and Potential Applications. *J. Inorg. Chem.*, 2455- 2480.
- [49] Sato S., Mori K., Ariyada O., Atsushi H., Yonezawa T., (2011). Synthesis of nanoparticles of silver and platinum by microwave-induced plasma in liquid. *Surface & Coatings Technology*, 206, 955-958.
- [50] Lee I., Han W. S., Kim Kwan. (2001). Simultaneous preparation of SERS-active metal colloids and plates by laser ablation. *J. Raman Spectrosc.*, 32, 947-952.
- [51] Zhang W., Qiao X., Chen J. (2007). Formation of silver nanoparticles in SDS inverse microemulsions. *J. Mat. Chem. and Phys.*, 109, 411-416.
- [52] Mallick K., Witcomb J.M., Scurrall S. M., (2004). Polymer stabilized silver nanoparticles: A photochemical synthesis route. *J. Mat. Science*, 39, 4459-4463.

- [53] Navaladian S., Viswanathan B., Viswanath R.P., Varadarajan K. T. (2007) Thermal Decomposition as Route for Silver Nanoparticles. *Nanoscale Res. Lett.*, 2, 44-48.
- [54] Halas J. N., (2008). Nanoscience under Glass: The Versatile Chemistry of Silica Nanostructures. *J. Am. Chem. Soc.*, 2, 179-183.
- [55] Vu V. L., Long N. N., Doanh C. S., Trung Q. B., (2009). Preparation of Silver Nanoparticles by Pulse Sonochemical Method and Studying Their Characteristics. *J. Phys.* , 187.
- [56] Li Y., Kim N. Y., Lee J. E., Cai P. W., Cho O. S. (2006). Synthesis of silver nanoparticles by electron irradiation of silver acetate. *Nucl. Instr. and Meth. in Phys. Res.B*, 251, 425-428.
- [57] Wang L., Tan W. (2006). Multicolor FRET Silica Nanoparticles by Single Wavelength Excitation. *Nanoletters*, 6, 84-88.
- [58] Stöber W., Fink A. (1968). Controlled Growth of Monodisperse Silica Spheres in the Micron Size Range, *J. Colloid Inter. Sci.* , 26, 62-69.
- [59] Iler K. R., (1979). New York: John Wiley and Sons.
- [60] Okubo T., Miyamoto T., Umemura K. , Kobayashi K., (2001). Seed Polymerization of Tetraethyl Orthosilicate in the Presence of Colloidal Silica Spheres. *J. Colloid Polym. Sci.*, 279, 1236-1240.
- [61] Yi G-R, Manoharan N. V., Michel E., Elsesser T. M., Yang S-M, Pine D. J. (2004) . Colloidal Clusters of Silica or Polymer Microspheres. *J. Adv Mater.* , 16.

- [62] Zhang H. J., Zhan P., Wang Z. L., Zhang W.Y., Ming B. N.(2003). Preparation of Monodisperse Silica Particles with Controllable Size and Shape, *J. Mater. Res.*, 18, 649-653.
- [63] Bogush H. G., Tracy M.A., Zukoski C. F., (1988). Preparation of Monodisperse Silica Particles: Control of Size and Mass Fraction. *J. Non-Cryst. Solids*, 104, 95-106.
- [64] Park S. K., Kim D. K., Kim T. H. (2002) Preparation of silica nanoparticles: Determination of the Optimal Synthesis Conditions for Small and Uniform Particles, *Colloids and Surfaces A*, 197, 7-17.
- [65] Jeevanandam P., Srikanth K. C., Dixit S., (2010). Synthesis of Monodisperse Silver Nanoparticles and Their Self-Assembly Through Simple Thermal Decomposition Approach. *Mater. Chem and Phys.*, 122, 402-407.
- [66] Kibar S., (December 2010). Preparation and Characterization of Silver SERS Nanotags, Thesis submitted to Chemistry Department of METU.
- [67] Gonzales R.B., Iglesias S. A., Giersig M., Marzan L. L., (2004). AuAg bimetallic nanoparticles: Formation, Silica-coating and Selective Etching. *Faraday Discuss.*, 125, 133-144.
- [68] Han Y., Jiang J., Lee S.S., Ying Y. J. (2008). Reverse Microemulsion-Mediated Synthesis of Silica-Coated Gold and Silver Nanoparticles. *Langmuir*, 24, 5842-5848.
- [69] Zeta Potential. Retrieved September 12, 2012, from http://en.wikipedia.org/wiki/Zeta_potential.

[70] Brilliant Cresyl Blue. Retrieved September 12, 2012, from <http://www.sigmaaldrich.com/catalog/product/sigma/b5388?lang=en®ion=TR>.

[71] Karabiçak S., (2011). Application of Surface- Enhanced Raman Scattering (SERS) Method For Genetic Analysis. Thesis submitted to Chemistry Department of METU.

[72] Sassolas A., Bouvier L. D. B., Blum J. L., (2008). DNA Biosensors and Microarrays. *Chem. Rev.* , 108, 109-139.